CHAPTER 2

Combustion Dynamics and Mechanisms of Combustion Instabilities

Identifying the primary cause, the *mechanism,* is probably the single most important task in understanding combustion instabilities in full-scale systems. The term 'mechanism' refers to that phenomenon or collection of processes forming the chief reason that the instability exists. There may be more than one mechanism, but in any case the ultimate reason for an instability is transfer of energy from the combustion processes, or the mean flow, to unsteady organized motions. Instabilities are commonly observed as nearly periodic oscillations having time-dependent amplitudes. As a practical matter, the chief goal is to reduce the amplitudes to acceptable levels. For that purpose it is essential first to understand the cause, and then to work out the connections with the chamber dynamics. Several of the mechanisms introduced in this chapter will be investigated more thoroughly later in this book.

In the context defined by Figure 1.1, understanding the mechanism of combustion instabilities is equivalent to understanding combustion dynamics. It is essential to keep in mind always that by its very definition, combustion involves chemistry and chemical kinetics within the setting of fluid mechanics. Depending on the mechanism, one or another of those phenomena may dominate. Hence, for example, in some cases involving vortex formation and shedding, we may find that burning is not a central issue. Nevertheless, the presence of the flow field supporting the vortices is itself produced by combustion of reactants. We may therefore justifiably include the phenomenon under the general label 'combustion dynamics', although we are stretching the literal meaning of the term. The main topics covered in this chapter relate largely to the feedback path in Figure 1.1.

The last section (2.7) of this chapter has a character different from the preceding material. It is an analysis of a simple example, the Rijke tube, illustrating the use of a time lag or delay to help interpret a mechanism, in this case heat addition from a wire heater. Familiar in other problems as a factor in causing unstable behavior, the idea of a time delay was introduced as the earliest attempt to explain or interpret the presence of combustion instabilities. The idea of delay as the basis for representing the action of a mechanism remains probably the most common approach to interpreting instabilities. However detailed the calculations may be, conclusions based on the presence of a time delay *per se* must not be confused with 'understanding the mechanism' of a combustion instability. What is required for proper understanding is knowledge of the physical origin of the delay. Only then may we be in a position to modify the system so as to affect the instability in question.

To be definite, practically all discussions of the consequences of time delays are forced, in the absence of deeper information, to assume some sort of *ad hoc* dependence of the delays on parameters defining the physical characteristics of the system at hand. We assume in Section 2.7 that the time delay is constant. The calculations then serve two purposes: to show explicitly the relation between a delay and linear stability; and to work out simple examples of the general analysis developed in the following chapters. Taking the time delay constant—in particular, independent of frequency—is the usual assumption and places a severe restriction on the results. It is well-known, for example, that the effective time lag for solid propellants is a

strong function of frequency. Assuming otherwise produces misleading if not seriously incorrect results for the dynamical behavior of the system in question.

2.1. Mechanisms of Instabilities in Solid Propellant Rocket Motors

In some respects combustion in a solid propellant rocket chamber appears to present a less complicated situation than those existing in any other types of combustor. The burning processes occur almost entirely within a thin region, normally less than one millimeter thick, adjacent to the propellant surface. Although some residual combustion commonly occurs when the propellant contains aluminum or other metallic additives and may affect unsteady global behavior, there is no unambiguous evidence that combustion within the volume contributes significantly as a basic cause of combustion instabilities. We assume that to be the case, leaving surface combustion and purely fluid mechanical processes as the chief origins of possible mechanisms. Figure 2.1 is a composite sketch of the four mechanisms currently regarded as the chief possible causes of instabilities in solid rockets. Of these, the dynamics of surface combustion is by far the most common.

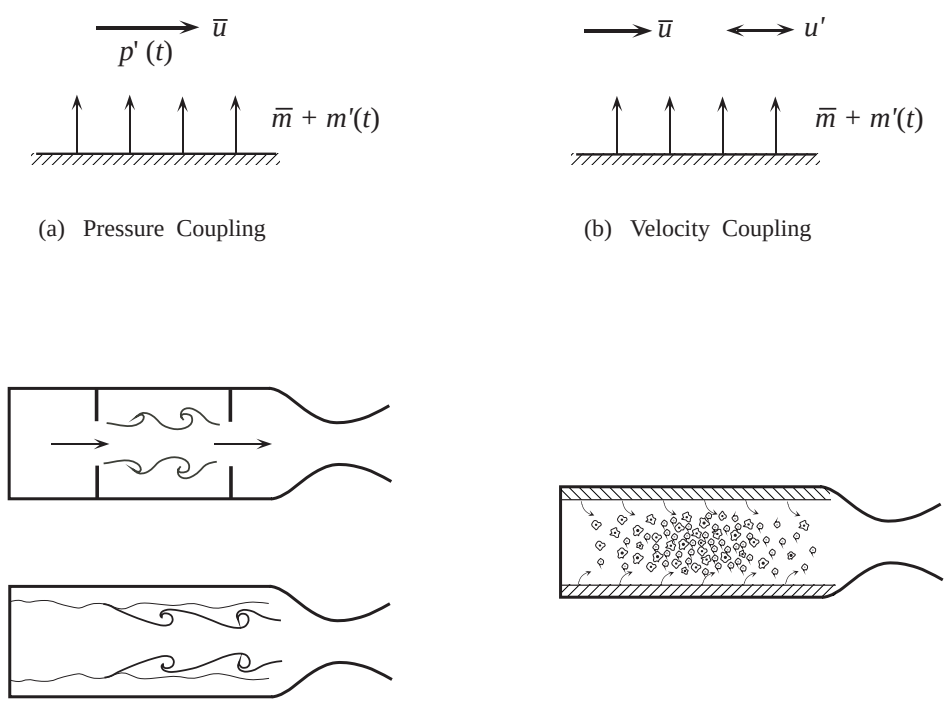

(a) Pressure Coupling

(b) Velocity Coupling

(c) Vortex Shedding

(d) Residual Combustion

FIGURE 2.1. The four possible mechanisms for combustion instabilities in solid propellant rockets.

Vortex shedding from obstacles—as in the Shuttle solid rocket booster—or vortices produced at the lateral surface ('parietal vortex shedding')—as may be the case in the Ariane 5 solid rocket booster—have been identified as mechanisms only in large motors. Excitation of acoustic waves by vortices is of course a well-known phenomenon in a wide variety of wind musical instruments. The idea that vortices might be responsible for oscillations in a solid propellant rocket seems to have been proposed first by Flandro and Jacobs (1974) but it has received particularly intense attention because of the problem in the Shuttle and, during the past decade or so, in connection with the problem of pressure oscillations in the Ariane 5; a particularly good discussion has been given by Vuillot and Casalis (2002).

The dynamics of residual combustion far from the burning surface—most likely associated with aluminum or other metal fuel additives not completely burned at the surface—remains poorly understood. Although some attention has been given to the process (see Section 6.11), analysis of the dynamics is incomplete. No calculations exist assessing quantitatively the possible contributions of residual combustion to linear stability relative to those of surface combustion.

On the other hand, there is no disagreement that the dynamics of surface combustion is the dominant mechanism causing most combustion instabilities in all types and sizes of solid rockets.

2.1.1. Qualitative Interpretation of the Basic Mechanism. The dependence of the burning rate of a solid propellant on the pressure has long been known as a fundamental characteristic. Experiment and theory for the combustion of gases show that the reaction rates vary strongly with both pressure and temperature. It is therefore not surprising that the burning rate of a solid is sensitive to the impressed temperature and pressure. What **is** surprising is that the processes in the gas and condensed phases in the vicinity of the burning surface conspire to produce a dynamical response that exhibits significant dependence on frequency. That dependence on frequency is particularly important because the response is noticeably greater over a rather broad frequency range typically including some of the acoustic resonances of combustion chambers. In that range the combustion processes act to amplify pressure fluctuations. That is, some of the energy released in chemical reactions is transformed to mechanical energy of motions in the combustion products. Hence the dynamics in the feedback path, Figure 1.1, not only provide feedback but as well promote an unstable situation. The burning surface exhibits a sort of resonant behavior but without possessing the spring-like (i.e. restoring) forces associated with a resonant oscillating system such as the simple mass/spring oscillator. Hence the phase relations are different in the two cases.

Since the cavity in a solid rocket possesses its own acoustic resonances, we have a system of two coupled oscillators. If it should happen that the resonant frequencies of the two oscillators are close, then conditions clearly favor an instability. That is the situation commonly occurring in solid rockets and is the simplest direct explanation for the widespread occurrences of instabilities in tactical as well as strategic motors (Price 1961, Blomshield, 2000).

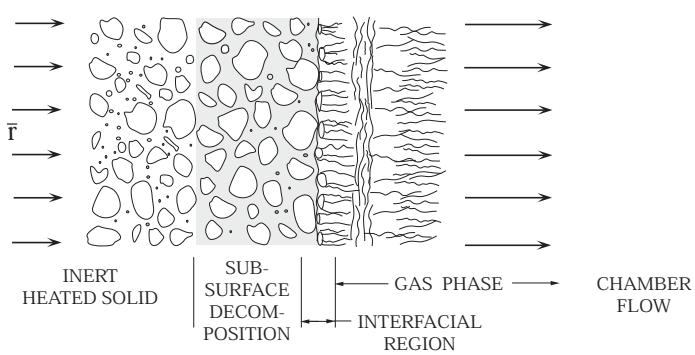

FIGURE 2.2. Sketch of steady combustion of a solid propellant.

The essential features of the combustion processes dominating the behavior just described have long been known. Figure 2.2 is an idealized interpretation showing the main characteristics of a burning composite propellant. The physical character of the materials and the processes involved in their transformation from solid propellant to products of combustion are quite well known. That knowledge has been gained through the efforts of many people and organizations over many years. An excellent summary is the reference volume edited by Davenas (1993). Ultimately it is the fluctuation of the velocity of gases leaving the combustion zone that is the essence of the mechanism. Oscillation of the flow causes the surface to appear locally like

an oscillatory piston or acoustic speaker, a source of acoustic waves. Formally the situation is identical to a planar array of monopoles having zero-average mass flow superposed on the mean flow due to combustion. However, the fluctuation of burning rate is a consequence of fluctuating heat transfer so we can understand the mechanism best by examining the behavior of the temperature profile. In Section 2.2.2 we will treat the propellant as if it were a perfectly homogeneous isotropic material in the condensed phase, and use the one-dimensional approximation throughout, from the cold condensed solid phase to the hot combustion products. Figure 2.3 is one frame from a film of a burning solid taken at the Naval Weapons Center (Price *et al.* 1982), suggesting that any sort of one-dimensional approximation seems unrealistic (See also Price 1984). That is certainly true on the scale of the particle sizes (10s to 100s of microns).

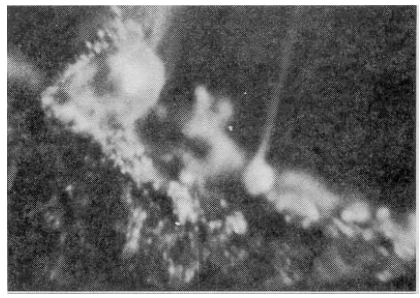

FIGURE 2.3. View of the surface of a burning solid propellant containing aluminum (Price *et al.* 1982).

However, the variations of velocity and pressure in the chamber occur over distances of the order of the chamber dimensions. Hence it is appealing to suppose that for analyzing interactions between the combustion zone and the motions in the chamber, the heterogeneous character propellant can be overlooked in some sense. For example, the linear burning rate of a propellant is measured without special regard for spatial variations on the small scale of compositional inhomogeneities. No instrument is available to do otherwise. That is not to say, of course, that the burn rate and the combustion dynamics do not depend on spatial variations of the condensed material and the gas phase. Rather, we suppose that dependence on such properties as the size distribution of oxidizer particles is accounted for by some sort of averaging procedure. Thus, parameters appearing in the final results, such as A and B in the QSHOD model discussed here, must depend on, for example, an average particle size. No rules exist for the averaging, but recently impressive progress has been made for computed steady burning rates using a "random packing" model (Kochevets, Buckmaster and Jackson 2001). In all of our discussion we adhere to the one-dimensional approximation as far as possible, with no attention paid to the possible errors incurred. In any case it seems a good assumption that if the averaging process is faithful, any errors are likely to be less than uncertainties arising in other parts of the problem, e.g., material properties. We do not address consequences of the statistical nature of the propellant surface which may result in random motions observable as noise in pressure records (e.g., R.L. Glick, Private Communication). Some results for pressure oscillations in the presence of noise are covered in Chapter 7, but possible connections with surface combustion are not investigated.

The mechanism in question here is, broadly speaking, primarily a matter of **combustion** dynamics. It has become customary to represent the mechanism quantitatively as an admittance or response function. We use the latter here, defined generally as the ratio of the fluctuation of the mass flow rate of gases departing the combustion zone, to the imposed fluctuation of either the pressure or the velocity. Thus the response function for pressure fluctuations (commonly referred[1] to as the "response to pressure coupling") is defined in dimensionless form as R_p,

$$R_p = \frac{m'/\overline{m}}{p'/\overline{p}} \tag{2.1}$$

[1]The term 'coupling' in the sense used here is intended to convey the idea that the surface combustion processes are influenced by changes in time of the variable in question, here the pressure. We will be concerned largely with pressure coupling and to a lesser extent with velocity coupling.

where $(\ )'$ means fluctuation and $\overline{(\ )}$ is an average value. The average value $\overline{m}$ represents the average inflow of mass normal to the surface, due to the propellant burning. In almost all applications, the fluctuations may be approximated as steady sinusoidal oscillations, written as

$$\frac{m'}{\overline{m}} = \frac{\hat{m}}{\overline{m}} e^{-i\omega t}$$
$$\frac{p'}{\overline{p}} = \frac{\hat{p}}{\overline{p}} e^{-i\omega t} \qquad (2.2)\text{a,b}$$

and

$$R_p = \frac{\hat{m}/\overline{m}}{\hat{p}/\overline{p}} \qquad (2.3)$$

where $\hat{(\ )}$ denotes the amplitude of the oscillation, including both magnitude and phase. Because generally the oscillations of mass flux rate are not in phase with the pressure oscillations, the function R_p is complex, the real part representing that part of $m'/\overline{m}$ that is in phase with the pressure oscillation.

Although the response function for pressure coupling is most commonly used, there is a second response function, that associated with velocity coupling, which under some practical circumstances is far more important. At this point we confine our remarks to the response function for pressure coupling. We return to velocity coupling in a later discussion (Section 2.2.8).

A simple interpretation of the response function explains its importance to combustion instabilities. According to the definition (2.3), a pressure oscillation having amplitude $\hat{p}/\overline{p}$ produces the oscillation $\hat{m}/\overline{m}$ of mass flow into the chamber

$$\frac{\hat{m}}{\overline{m}} = R_p \frac{\hat{p}}{\overline{p}} \qquad (2.4)$$

Viewed from the chamber, the boundary appears then to oscillate. The apparent motion is entirely analogous to that of a speaker or piston mounted at the boundary emitting waves into a room. Through a complicated sequence of processes whose details are not germane here, those waves coalesce and combine with the original pressure waves causing the fluctuations of mass flux. Whether or not that merging process augments or subtracts from the existing wave system in the chamber depends on the phase between $\hat{m}$ and $\hat{p}$. The part of $\hat{m}$ in phase with $\hat{p}$ increases the amplitude of the wave system and is therefore destabilizing. For a particular motor, the tendency for combustion dynamics to drive instabilities is proportional to the integral of R_p over the entire area of burning surface, but weighted by the distribution of fluctuating pressure at the surface. Hence it is clearly essential to know the response function for the propellant used.

All traditional composite propellants using ammonium perchlorate as oxidizer, as well as advanced propellants using higher energy oxidizers and binder, burn in qualitatively similar fashion. The interface between the condensed and gas phases is fairly well defined, may be dry or wet, and may exhibit local dynamical activity owing to the presence of solid particles and responsive collections of liquid pools or drops. The dynamics of the interfacial region is particularly noticeable in microcinematography when the propellant contains aluminum. The metal collects in molten droplets, mobile and ignitable on the surface; those not fully consumed are carried away by the gaseous products of the interface. The high temperature at the surface is sustained by a balance between heat flow away from the interface, required to heat the cool propellant advancing to the surface; energy required to effect the phase changes at and near the interface; and the heat transfer supplied to the interfacial region from the combustion zone in the gas phase. It's a delicate balance, easily disturbed by changes in the chemical processes in the interfacial region, particularly within the subsurface region in the condensed phase. Figure 2.4 is a sketch of the temperature field for two elementary forms of the distribution of combustion. Note that for this figure we imagine that the temperature exists in a spatially averaged sense. Local variations on the scale of oxidizer particles are smeared out in the averaging procedure and explicit effects of inhomogeneities are absent.

The essentials of the behavior represented macroscopically by response functions can be described as a sequence of elementary steps, described here in simplified form with reference to Figure 2.4:

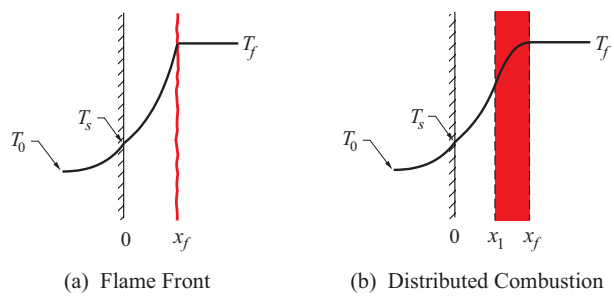

FIGURE 2.4. Representation of the temperature field for a burning solid propellant.

(i) Suppose that for some reason the rate of reactions in the combustion zone increases-perhaps due to a fluctuation of pressure, or temperature, or to increased local mixing associated with greater intensity of turbulence locally in the chamber.

(ii) Increased reaction rates produce a rise in the rate of energy release and an increase of temperature of the combustion zone.

(iii) Due both to radiation and heat conduction, the heat transfer from the combustion zone to the interfacial region increases, having at least two possible consequences: the temperature at the surface is increased; and the rate at which condensed material is converted to gas is also increased.

(iv) Because the temperature in the interfacial region rises, so also does the heat flow to the subsurface region and further into the solid, tending to cool the interface.

(v) If there are subsurface reactions, the heat flow will tend to increase their rate, with consequences depending on the associated energy release (or absorption) rate.

(vi) Exothermic subsurface reactions will act to maintain higher temperature locally, thereby encouraging the conversion of condensed material to gas at the interface, but also tending to increase the heat flow to the cooler solid.

(vii) The net result may be that if the fluctuation of heat flow, and reduction of temperature, at the interface does not happen too quickly, the enhanced reaction rate assumed in Step (i) may produce a fluctuation of mass flow leaving the surface, that is in phase with the initial perturbation. Hence in this event the entire process is destabilizing in the sense that the initial disturbance has the result that the disturbed mass flow into the chamber tends to augment that initial disturbance.

Whether or not the preceding sequence will be destabilizing depends entirely on details of the processes involved. Notably, if sub-surface reactions are endothermic, then the sequence (v)–(vii) leads to the conclusion that the reactions may cause the propellant combustion to be less sensitive to disturbances.

2.1.2. Early Historical Background Leading to the QSHOD Model. In many important respects, problems of combustion instabilities in solid propellant rockets have raised questions, and forced considerations, which are common to practically all combustion systems. The particulars are of course very different, but a large part of the general behavior among the various devices is surprisingly similar. Much is to be gained from understanding broadly the historical background of combustion instabilities in solid rockets.

The problem was first identified in the Soviet Union and analyzed by Zel'dovich (1942) several years before similar work in other countries. Margolin (1999) has given a brief incomplete account. Further developments were for the most part simply not known in the West until twenty years later. To this day we

have sparse knowledge of the field in the USSR, until the 1990s. We will give here a survey to convey an idea of developments in the U.S., with brief references to progress in Western Europe.

In Chapter 1 we have noted some of the early research in the U.S., sponsored during World War II, principally related to the development of tactical rockets. Perhaps the outstanding example is the 2.75 inch rocket.[2] Problems with 'anomalous' or 'rough' burning caused the first uses of resonance rods and other passive 'fixes', such as modifications of the internal configuration. Due to the urgency of development, and crude instrumentation, little was accomplished in respect to discovering the source of the problem. The entire program was moved from Caltech to the Mojave Desert before WWII ended, forming part of the newly established Naval Ordnance Test Station (NOTS). E.W. Price, who had started his career at Caltech, expanded his research on combustion instability. His sponsorship of Grad (1949) produced the first work treating the problem of oscillations in a solid rocket as one of acoustics, a fundamental point of view.[3]

Before Grad's work, although the notion that the unsteady motions were somehow related to acoustical motions had certainly been discussed, it was only one among several ideas. Grad first worked out a quantitative theory based on the assumption that the pressure fluctuations were 'self-excited' and associated initially with small amplitude motions in a compressible medium, the products of combustion. The oscillation then grows if they are unstable, developing into large amplitude motions which were often called 'sonance' or 'sonant burning', terms which have since been dropped. Grad did not propose a particular mechanism for the unstable motions, but introduced a time lag supposed related to unsteadiness in the rate of decomposition of the propellant in its conversion to gaseous products. The work had some definite results but for several reasons—not least, perhaps, that the community was not yet in a state to make use of the analysis—the approach was not developed until later by others.

In fact, despite continuing practical problems with 'anomalous burning', there seem for several reasons to have been no further publications in the open literature until Smith and Sprenger (1952) gave a summary of some of the experimental results obtained at the Aerojet Company.[4] They reported that 'high-frequency' oscillations having large amplitudes were accompanied by large excursions of pressure; the frequencies were close to those of transverse acoustic modes. The general picture was to a considerable extent consistent with that envisioned by Grad, but the paper contains some interesting data taken with laboratory motors. Figure 2.5 is adapted from their Figure 3, showing that the motion was without doubt mainly the first tangential mode of the cylindrical chamber, having frequency proportional to $\bar{a}/R$ where R is the radius of the chamber.

Besides Smith and Sprenger's contribution clarifying the qualitative nature of combustion instabilities in solid rockets, they offered several important basic general observations about the mechanism. They were first to understand that Rayleigh's Criterion (or 'principle') could be extended to become an "explanation of combustion instability phenomena without conflicting with Rayleigh's original intentions . . . . Interpreting the oscillations during sonance as self-excited, the possible sources of energy and causes of damping must be found, and the mechanism for self-excitation described." This correct viewpoint seems to have been barely noticed at the time. Their paper ends with a short description of a mechanism primarily related to fluctuations in the rate of reaction and energy release. The importance of the thermal wave in the solid phase was not yet recognized.

Geckler (1954)a,b, also working at the Aerojet Company, gave two summaries of theory and experiment for the combustion of solid propellants, the second one dealing mainly with unsteady problems. He devoted

[2]The size was set by that of steel pipe readily available during early tests at Caltech. (E.W. Price, Private Communication)

[3]The analysis had actually been formulated initially by J.K.L. MacDonald of NOTS, who died early in the program; his work was continued by Grad. MacDonald perished in an airplane crash, having taken a seat given up by E.W. Price.

[4]As true for many publications of research solid rockets until the 1990s, many details of the experiments, such as compositions and properties of the propellants used, and geometry of the test device, were not given.

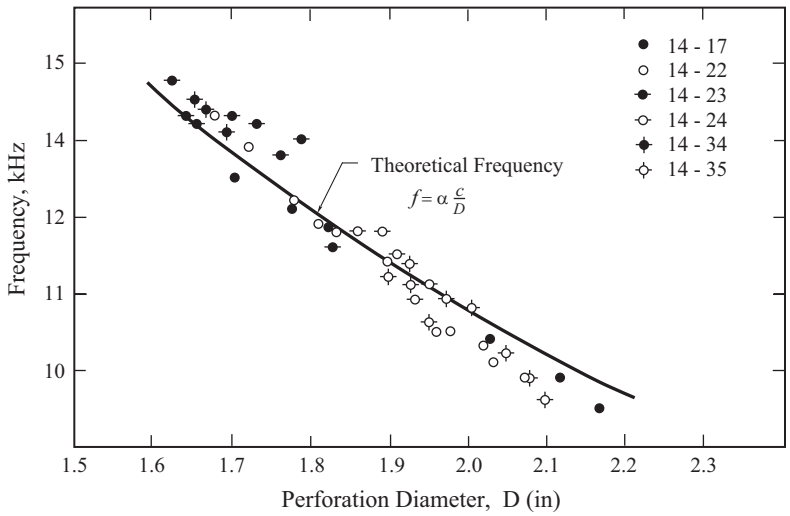

FIGURE 2.5. Measurements showing the presence of the lowest tangential mode during 'sonant' burning (Smith and Sprenger 1952).

much of his discussion to the results found by Smith and Sprenger, the remainder consisting of brief summaries of Grad's model of combustion with a time lag; and Cheng's analysis which involves a more involved (realistic?) model of the conversion of solid material to gaseous products involving a time lag.

During the early 1950s there was more activity in developing analysis of combustion instabilities in liquid rockets than on the corresponding problems in solid rockets. Crocco and Cheng (1952, 1953) had begun their work on one-dimensional notions that would lead to their monograph in 1956. It was reasonable that some of the same ideas should be applied to solid rockets. (Cheng 1952a,b, 1959, 1960, 1962). The results, however, are not applicable because the mechanism proposed is incorrect.

Cheng's main idea is that "primary decomposition" causes the solid propellant to generate at a rate $\dot{m}_i(t)$. Then combustion of those gases produced at time t is assumed to take place instantly and completely at the later time $t + \tau$. The instantaneous rate of burning $\dot{m}_b(t)$ is

$$\dot{m}_b(t) = \left(1 - \frac{d\tau}{dt}\right) \dot{m}_i(t - \tau) \tag{2.5}$$

This result is derived as equation (2.88) here, in the context of liquid rockets. Cheng considers briefly and then discards the possibility that the rate of decomposition, $\dot{m}_i$, depends on the velocity parallel to the surface. As explained later in Section 2.3.2, if the time lag is the period required for completion of unspecified processes in the gas phase, and pressure is the controlling physical variable, then one finds (Cheng's equation 5 in his 1954a paper):

$$\frac{\dot{m}_b(t)}{\overline{\dot{m}}_b} = \frac{p^{n-s}(t)}{[p(t-\tau)]^{n-s}} \tag{2.6}$$

The decomposition rate is assumed to depend on pressure only, $\dot{m}_i(t) \sim p^n(t)$ (Cheng uses n for s), and n has the same meaning here as in equation (2.90). After linearization of (2.6), Cheng found the result for the fluctuation of the flow velocity normal to a burning surface,

$$\frac{v'/\overline{a}}{\rho'/\overline{p}} = -B\overline{v}_b \tag{2.7}$$

and

$$B = 1 - \gamma n + \gamma(n - s)e^{-i\omega\overline{\tau}} \tag{2.8}$$

The ratio (2.7) is, within a constant factor, the admittance function for the surface.

We will not cover Cheng's analysis further. His model of the unsteady burning process has long ago been shown to be wrong. It is interesting only as an example of an attempt to take advantage of an idea (the time lag) which became widely used in analysis of combustion instabilities in liquid rockets. Cheng's treatment of the acoustical motions in the chamber added nothing new and in fact fell short of Grad's results in many respects.

During most of the 1950s there were few published papers on unsteady motions in solid rockets (or any rockets for that matter). That meager production of 'open literature' does not give an accurate picture of the work being done by industry and in government laboratories, in the USSR as well as in the West. As the decade progressed, more pressure was exerted in the US to make the problems better known, and to involve researchers other than the small number directly concerned in the development of hardware.[5] In 1954, Green (1955) wrote a one-page negative critique of Cheng's 1952 work, essentially calling attention to the errors of interpretation of experimental results by Smith and Sprenger, noting particularly that combustion instabilities had been found with 'mesa burning' propellants which have burning rates independent of pressure, for some useful range of pressure. Green's final observation was that limited observations suggested to him that the presence of noise in the appropriate frequency range may precipitate instabilities. It's an idea which has been offered several times since; it has never been shown to be valid. Noise as the origin of substantial oscillations in a combustion chamber is at the present time (2005) being studied in at least one development program.

In the following year, Green (1956) gave a quite good summary of reported observations of instabilities in solid rockets, beginning with early reports by Boys and Schofield (1942) in England, Ferris *et al.* (1945) in the U.S. and the works cited here. Green was evidently concerned largely with "irregular reaction", which meant significant excursions of the mean pressure. He reported no data for oscillations; Figure 2.6 shows an example of some irregular reaction with a composite propellant (composition unspecified).

Green was evidently pre-occupied with his observation that 'irregular reaction' occurred in rockets using propellants having burning rates independent of pressure over substantial ranges. He then reasoned that the basic cause was increasing decomposition rate in the solid phase, with heat transfer due to oscillatory velocity parallel to the surface. Coupling of the temperature and velocity of the gas, near the surface, to the solid material occurs throughout the heat transfer. Consequently the surface temperature of the solid fluctuates, causing variations in the decomposition rate. By implicit assumption, the acoustical motion in the gas phase is supported independently of the decomposition process. It was only a proposal, not supported by a model or calculations.

With his next paper, Green (1958) attempted to work out a quantitative model founded partly on the ideas just summarized. The analysis contains in rudimentary form an idea, the thermal wave, which became part of the description now accepted as the basis for a good first approximation to unsteady combustion of a solid propellant. It's a purely thermal theory, temperature being the sole independent variable. Green's picture for his calculations is the same as Figure 2.4 here; his significant new contribution was inclusion of the thermal wave in the solid material, with no decomposition. Thus Green's calculations rested on solution of the heat conduction equation (2.5) in the solid phase, with no source term. The basic result is a quadratic

[5] Mr. E.W. Price was particularly outspoken and effective in this respect. His efforts were notably influential beginning with the Polaris program. In contrast, the system of classifying information at all levels in the USSR, as the open literature reflects, never relaxed from practices adopted during World War II, continued until the 'fall of the wall'. In the middle 1970s, for example, an academic visitor to Moscow and Novosibirsk, was unable to learn from researchers in the field of combustion of energetic materials that they even knew *of* anybody working on problems related to solid rockets. That extreme secrecy was mainly a continuation of practices followed in World War II continued until the fall of the wall. The situation was different, for example, in the field of gas lasers; the exchange of information was recognized as an important contribution to progress, practically from the beginnings of the field.

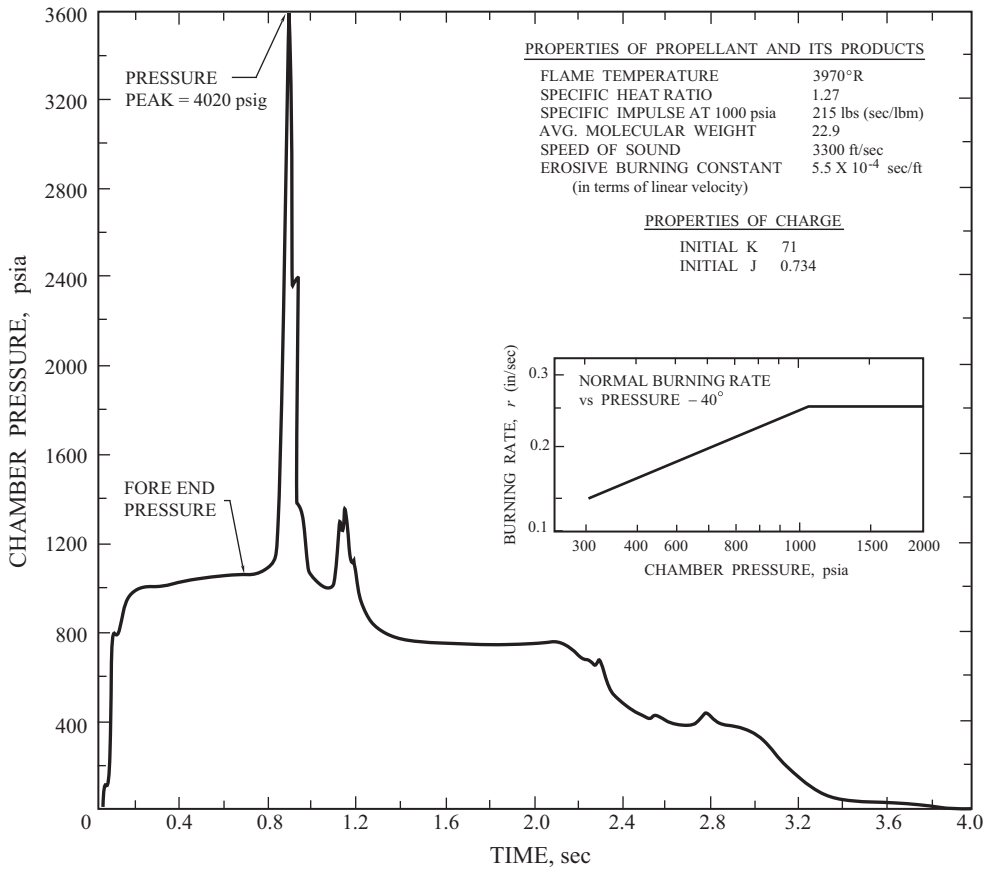

FIGURE 2.6. Mean pressure in a cylindrical motor operating with double-bore propellant (52 inches long, 1 inch initial internal diameter) (Green 1956).

equation for the wavelength of thermal waves, the frequency being set by the oscillatory heat input expressed in terms of a film coefficient.

Because he did not consider the complete problem involving the chamber oscillations—i.e. coupling between motions in the chamber and the thermal waves in the solid was absent—Green was strictly unable to find the conditions for oscillation. He therefore missed the true meaning of his results and tried to force them to produce what he sought, the resonance condition fixing the frequency of oscillations, but without dependence on the properties of the chamber. In doing so he introduced a time lag between the surface temperature and the phase change solid → gas at the surface. As a result, the conclusions are of no use and can be ignored.

The same thermal model was used by Nachbar and Green (1959) in an extended discussion of the 'resonant condition' defined by Green (1958). Thus there are no new ideas in the work. Some of their conclusions are at minimum misleading; while the paper is part of the historical background, if offers little of lasting value.

An interesting and significant note appeared in March 1958, a report of the first tests with an early variant of a new device, the T-burner (Price and Sofferis 1958). Their sketch of the burner using a 'full-length charge' is adapted for Figure 2.7. Various grains were used, including the extending parts way into the chamber from the ends. The experimental program at the U.S. Naval Ordnance Test Station

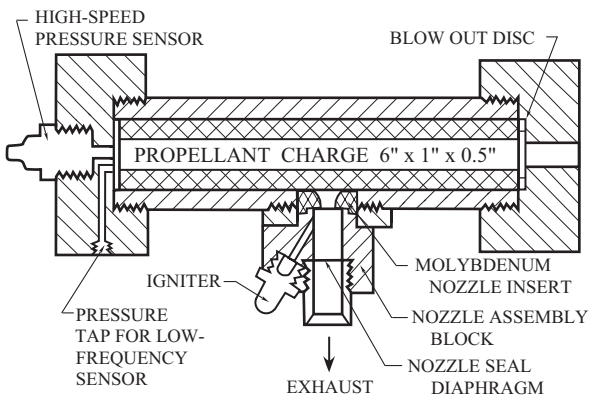

FIGURE 2.7. Sketch of the first test device having the form of a T-burner (adapted from Price and Sofferis 1958).

was especially important for its emphasis on research directed to understanding the basic properties and causes of combustion instabilities in solid rockets, as opposed to performing tests directed primarily to solving a particular problem encountered in a development program. This work was conducted to help clarify the "mechanism of excitation of instability"; and to study the influence of oscillatory behavior on the average burning rate of propellant. Already many tests had established, albeit indirectly, that the burning rate ($\bar{r}$) increases, sometimes substantially, when the pressure oscillates. The burner shown in Figure 2.7 was specially designed to exhibit unstable longitudinal modes having frequencies comparable with those of tangential modes in motors. Note that the oscillatory velocity would correctly be parallel to the burning surface of the propellant shown in Figure 2.7, so the device provides a good approximation to the motions in a tangential mode. In this sense the work constituted a significant departure from previous experiments by providing a simulation rather than a re-creation of the actual problem.

The bulk of the short paper was devoted to using test results obtained with the new burner to check the truth of five 'contentions' identified in the works of Grad; Smith and Sprenger; Cheng; Geckler; and Green. One result concerns the mode excited—longitudinal, in contrast to the tangential modes observed in the works cited. The remaining four were:

(i) the chamber oscillations were excited by pressure, not velocity oscillations;
(ii) the noise in the device (lower than in previous equipment) was not a "conspicuous factor in exciting combustion instability";
(iii) the average burning rate decreased at low chamber pressures (500–1700 psi) and increased at higher pressures;
(iv) the average burning rate was apparently unaffected by the low mean gas velocities present in the tests.

Subsequent work in many laboratories have shown that (i), (iii) and (iv) are not generally true. Item (ii) remains not generally settled; it is this author's belief that while noise modifies some features of instabilities, it is not a fundamental cause or mechanism of instabilities, or of increased amplitudes of modes.

Price (1958) gave a thorough, balanced review of combustion instabilities in solid rockets at the IXth IAF Congress, a short time before a great deal of recent work became publicly available—i.e. was declassified.[6] It's a readable qualitative discussion of the field, containing a number of succinct observations still valid. Perhaps

[6]The papers by Grad (1949) and Cheng (1956) seem to be the first works in universities on combustion instabilities. Not until 1960 did Brownlee publish the next account (Brownlee and Marble 1960) of work done at Caltech's Jet Propulsion Laboratory. At about the same time, Horton completed his Ph.D. thesis at the University of Utah (Horton 1961).

the only real fault with the discussion is a short treatment of the 'time lag' assumed to be a crucial item in the excitation process. While the notion of time lag as an important matter in discussions of combustion instabilities in liquid rockets as recently as the late 1980s and 1990s, it was soon rendered obsolete in respect to solid rockets by a well-grounded (albeit approximate) theory of the combustion response function for solid propellants.[7].

The entire field in the U.S. began to undergo significant changes of emphasis and even, one might argue, direction, with the participation of F.T. McClure and his colleagues at the Johns Hopkins Applied Physics Laboratory, beginning in early 1959. McClure enlisted the cooperation of the leading investigators, almost all of whom were experimentalists working in government or industrial laboratories. Although the Technical Panel on Solid Propellant Instability of Combustion existed for only a bit more than three years, its work had a lasting influence. Its main publication is a useful collection of papers released in 1964, *Technical Panel on Solid Propellant Instability of Combustion—Scientific Papers 1960–1963.* The effectiveness of the Technical Panel was made possible by a decision taken at high levels within the Defense Department to allow open publication of as much information as possible, a decision not to be underrated.

In 1959 Hart and McClure (1959) published the first work by the group at the Applied Physics Laboratory. The work set a tone strongly influenced by the authors' background as physicists. They tried to extract the main attributes of the phenomena studied, and grounded them in basic principles; often observational details are recognized but gracefully ignored, in seemingly arbitrary fashion, to favor clarification and simplification of the theory at hand. Hart and McClure settled on the interaction (or "coupling") between acoustic waves and the burning surface as *the* principal cause of combustion instabilities. Further, they chose to ignore the effects of erosivity in their first approximation to the coupling process. After estimates of characteristic times for gas phase reactions; heat conduction in the solid and gas; mass transfer; and reactions in the solid phase, they formulated a model which is essentially the same as the QSHOD model discussed in Section 2.2. Figure 2.8(a) is an adaptation of Hart and McClure's sketch of their model; Figure 2.8(b) shows a result for the real part of the admittance function. The details of the analysis have been much simplified in later work (see Section 2.2) and need not be covered here.

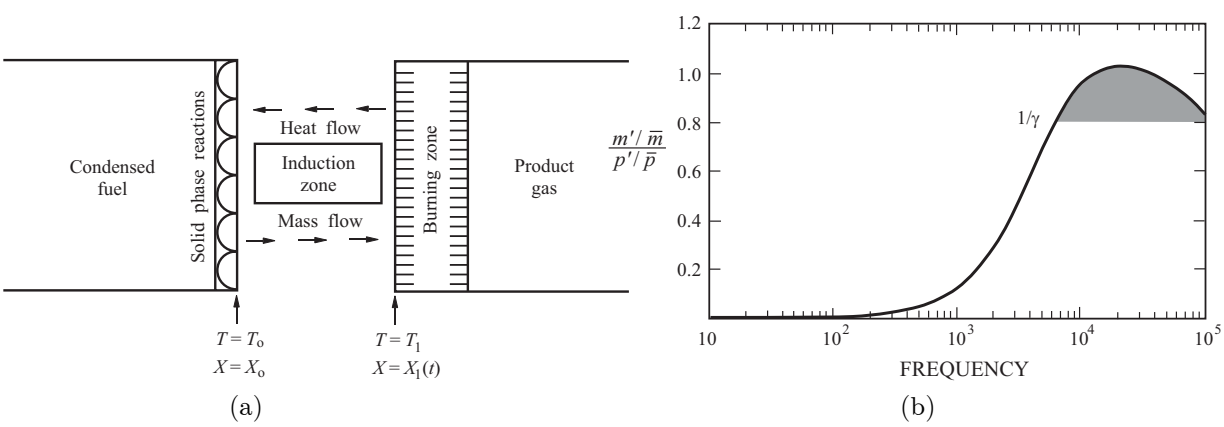

FIGURE 2.8. Adapted from Hart and McClure (1959). Part (a): a sketch of their model of surface combustion; Part (b) a result for the quantity proportional to the real part of the admittance function.

[7]The main shortcoming of a time lag representation is the unknown and important dependence on frequency. Thus the assumption is commonly made that the lag is independent of frequency, a serious error for solid propellants and possibly for liquid propellants as well

In the following year, McClure, Hart and Bird (1960)a began a series of papers dealing with various aspects of combustion instabilities in solid propellant rockets, not all of which had been treated, or even recognized, previously. They treated oscillations in a cylindrical motor with the unsteady combustion processes represented in the manner formulated in the 1959 paper. The principal important new feature, original with this work, was accounting for oscillations of the solid material. Combustion response to pressure oscillations only was accounted for, but in a short section of the paper, the authors examined possible consequences of erosive burning.

It is fairly evident that the normal modes of oscillation in a cavity containing a significant amount of solid material may differ from those in a cavity filled with gas. That result was shown by McClure, Hart and Bird. For applications there are in the first instance two questions to answer: How much material is required to be "significant"?; and What are the actual properties of the material? In other words, roughly, how compressible is the propellant, and how effectively does it dissipate mechanical motions? Subsequent work over the following 10-15 years showed that motions of the solid could be ignored, so far as combustion instabilities are concerned, except in certain large motors. The first question asked above can be answered only for the particular cases one must deal with. Determining material properties under unsteady conditions remains a difficult experimental matter usually carrying large uncertainty.

There are at least two important consequences of unsteady flow parallel to a burning surface: the steady burning rate may be affected, a fairly direct extension of the familiar phenomenon of 'erosive burning'; and there can be a truly time-dependent process affecting unsteady changes in the burning rate, analogous to the unsteady behavior accompanying rapid pressure fluctuations. It is the second type of 'erosive burning' which is of particular interest in the present context for it contains the possibility of coupling acoustic waves to the combustion processes. In their first paper on the possible effects of unsteady erosive burning, Hart, Bird and McClure (1960)a avoided the problem of formulating a theory of the process, but tried to construct a general description which would fit into their structure for computing the acoustics of a chamber. Their beginning point was the linearized representation of the burning rate expressed as the mean flow leaving the surface in the normal direction,

$$m_b(p, v_e; t) = \overline{m}_b(\overline{p}) + \left(\frac{\partial m_b}{\partial p}\right)_0 p' + \left(\frac{\partial m_b}{\partial p_t}\right)_0 \frac{\partial p'}{\partial t} + \left(\frac{\partial m_b}{\partial |\mathbf{u}'|}\right)_0 |\mathbf{u}'| + \left(\frac{\partial m_b}{\partial |\mathbf{u}'|_t}\right)_0 \frac{\partial |\mathbf{u}'|}{\partial t} \tag{2.9}$$

where $\mathbf{u}'$ is the unsteady (acoustic) velocity parallel to the burning surface. In this form, $\left(\frac{\partial m}{\partial |\mathbf{u}'|}\right)_0$ contains the usual erosion constant k for steady burning,

$$\left(\frac{\partial m}{\partial |\mathbf{u}'|}\right)_0 = \overline{m}_0 k \tag{2.10}$$

The terms proportional to p' and $\partial p'/\partial t$ can be re-written using the definition of the admittance function.

We will not consider any further the analysis[8] by McClure, Hart and Bird, which consists mainly in examining the possible effects of erosion in a cylindrical chamber. Probably the lasting value of the work lies in the formulation of the boundary condition (2.9) which, perhaps in modified forms, has subsequently been used by many others. The manner of incorporating the basic phenomenon of rectification has lasting influence. On the basis of their incomplete calculations, the authors concluded that for reasonably large values of $k|\overline{\mathbf{u}}|$, with $k > 0$, the erosive effect of the mean flow is stabilizing. The real importance of the paper is probably the influence it had, calling the attention of others to the subject. However, the matter of the effects of erosion—any sort—on stability remains to a large extent an unsolved problem.

By 1960 there was no dissension that the simple basic model of the combustion response of a burning solid captured part of the observed behavior, qualitatively at least. To what extent quantitatively could not

[8] It is difficult to follow, contains typographical errors and does not account for all influences of the mean flow, even for a cylindrical chamber.

truly be assessed until more extensive and more accurate data became available. McClure, Hart and Bird (1960) summarized the situation in a page-and-a-half note. In the following year, the same authors (1961) added a few comments concerning the dependence of the propellant response (and, presumably, instabilities) on a few properties: e.g. instabilities are more severe if the rate of heat release is higher, and the chamber pressure is lower. Such conclusions should be regarded with caution, because the actual behavior depends as well on the chamber geometry, flow field and properties of the particular propellant used. The authors also attribute the known result of aluminum to suppress instabilities to its tendency (maybe) to reduce the response function, by affecting surface combustion processes; or to its effect on losses (unspecified) in the system. It would be several years before 'particle damping' would be generally accepted as the dominant process.

Much of the work in the immediate future consisted in working out some of the consequences of ideas introduced in the period c.1959–c.1963. McClure, Bird and Hart (1962) discussed in greater detail their formulation of the influence of erosion on axial modes. Their discussion contains their basic ideas but the development is brief and really doesn't do justice to the importance of the material. It is important to realize that 'erosion' as treated by McClure *et al.*, by Price, and others is really a matter of *kinematics,* not dynamics. Further, despite many speculations and a modest amount of data, which sometimes has questionable relevance, there is no physical theory of the unsteady 'erosion mechanism', now commonly referred to as 'velocity coupling. Two important features of velocity coupling were recognized in the early 1960s: the kinematic nonlinearity; and the dependence on the magnitude of the sum of the local mean and unsteady gas velocities, causes the coupling of the surface combustion to the gas dynamics to vary with position on the surface. The second property means that any 'response function for velocity coupling' will necessarily depend on position, unlike the case for pressure coupling, for example R_p defined by (2.3). We will discuss velocity coupling further in Section 2.2.8.

The literature in this period was (and to some extent this is still true!) a mixture of classified and unclassified documents. Even if available in principle, the latter may be difficult to locate and obtain. An example is an excellent review by Price (1961) describing the fundamentals of the subject then understood (much of the discussion remains valid) and summarizing in considerable detail virtually all practical examples then known.

The group at APL was quite active in 1960–63, examining several problems which were central to understanding practical aspects of combustion instabilities in solid rockets. With their previous papers cited above, they had constructed a framework which gave the field generally a cohesiveness previously absent, and helped identify the problems that demanded attention. A natural result was the division of processes into 'gains' or 'losses'. Thus two papers, Hart and Cantrell (1963), and Cantrell, McClure and Hart (1963) dealt with an important source, acoustic damping or attenuation. The second was an attempt to compute, by using a variational method, the acoustic losses on the side walls in an end-burning rocket, intended to approximate conditions in some test devices. No further use of the method has been made. While the first of these papers contains some interesting observations, it too has had no lasting consequences.

Extensive observations of unstable tangential modes had first been reported by Brownlee and Marble (1960) and described in detail by Brownlee (1961). That form of instability had been a common problem in tactical solid rockets, but hadn't been subject to interpretation grounded in fundamental ideas until the discussion by Bird, McClure and Hart (1963). The paper is directed mainly to consequences of varying geometrical parameters, all the tests having been done with cylindrical motors. Following their previous work, the authors organize their discussion explicitly around the balance of gains and losses of acoustic energy. At the time, quantitative information was not available for most of the processes; the work is interesting mainly as a measure of the state of the field—there are no specific results. The authors discuss but discard erosive effects except for possible changes in the burning rate. Thus, gains of acoustic energy are ascribed entirely to pressure coupling which could not be assigned a value with confidence.

Of the possible losses—essentially viscous or viscoelastic in the solid or gas—only gas-particle interactions were found to provide (roughly) the correct behavior. The propellant did not contain aluminum and it is questionable (even doubtful) that the combustion products contained the material (1% by mass of 0.5μ particles) postulated to account for the observed stability boundary. Consequently, neither the gains nor the losses seem to have been satisfactorily explained or provided ideas more generally useful. However unsuccessful it was, the paper remains as the first attempt to interpret observed stability boundaries, see Section 6.7.3 for commentary based on later work.

Perhaps motivated partly by the serious lack of certain relevant information, Bird and Hart (1963) gave an interesting survey of the difficulties associated with scaling. The authors recognized that, in a sense, scaling steady combustion instability cannot be done: It is simply not possible to determine the stability of a motor from the stability characteristics of a smaller, geometrically similar model: There are too many processes having diverse dependencies on frequency. Nevertheless, people concerned with problems of stability of small amplitude disturbances in full-scale motors may gain much from understanding the rules governing scaling of the basic processes. It would be a mistake to expect formulation of concise, strict scaling laws such as one finds, for example, in the field of aerodynamics. A fundamental reason is that combustion instabilities necessarily mix time- and space-dependent physical behavior—e.g. wave propagation in complicated geometries—and the physical properties of chemically active solids and gases. Hence useful scaling laws are generally valid only over narrow ranges of the important parameters.

Except for a review, apparently the last paper from APL was essentially an effort by Cantrell and Hart (1964) to derive a formula for the growth constant of unstable oscillations in a general form applicable to any geometry. Although not stated in the account, a motivation was surely increasing concern with combustion instabilities that could not readily be related to the modes of oscillation in a circular cylindrical chamber. The authors' central idea was to begin with the definition of the growth constant as one-half of the time rate-of-change of time-averaged acoustic energy in a chamber,

$$\alpha = \frac{1}{2}\frac{1}{\mathcal{E}}\frac{d\mathcal{E}}{dt} \tag{2.11}$$

The analysis may appear at first acquaintance to be related to the variational method referred to above but it is not. Moreover there is no theoretical connection with the method of least residuals developed by Powell (1971) and Powell and Zinn (1971) or with the spatial averaging first used by Culick (1961) and which were developed to become central to much of this book. The differences arise with definitions of the rates of change of $\mathcal{E}$ in terms of processes at the boundary of the volume treated. We discuss the point in Section 6.9.

Equation 2.11 is a *definition* following from linear theory. Consequently it offers no beginning for extension to nonlinear behavior. Furthermore, because practically no further use is made of the equation of motion, this approach contains no hints for computation of the field variables $(\mathbf{u}, T, p)$ or the terms of their orderly expansion in the Mach number of the mean flow. Thus the value of the work lies mainly with some qualitative discussion of stability in T-burners and cylindrical rockets.

Hart and McClure (1965) brought the program on combustion instability at the Johns Hopkins Applied Physics Laboratory to an end with a review paper covering mainly the state of theory in mid-1965. It's a summary of the field at that time, containing no ideas that had not previously appeared. They devote a short section to comments on nonlinear behavior but, because the APL analytical work seems to be almost irretrievably restricted to linear problems, the discussion does not initiate or suggest novel developments in that direction.

The leadership and significant positive influence exerted by McClure and his colleagues at APL far exceeded the value of their specific technical contributions. Their work on theory gave the field of combustion

instabilities in solid rockets a flavor and a thrust which were new and permanent.[9] In addition to initiating several lines of analytical work, the APL formulation of the basic acoustics problem greatly encouraged continuation and expansion of the program to measure the response of surface combustion at NOTS under E.W. Price. A thesis (Horton 1961) and three papers (Horton 1961, 1962; and Horton and Price 1961) began the international activity of measuring the admittance function of propellant samples mounted in an 'end-burner', generically called the T-burner.[10] (Figure 1.21.)

In his thesis, Horton (1961) reported the first measurements of an admittance function. Figure 2.9(a) shows his results which were given in his second paper (Horton 1962).[11] The picture in Figure 2.9(b) is a record (taken with an 'oscillograph' which no longer exists!) of a particularly good T-burner firing (Horton and Price 1962). Apparently Price had suggested to Horton during the latter's thesis program that the initial (final) periods would ideally show exponential growth (decay), i.e. the envelope of the oscillations has the form $e^{\pm\alpha t}$; and that the information could be used in principle to compute the admittance function for the burning surface. For linear behavior, equation (2.10) applies. For an acoustic field one can write approximately $\varepsilon \sim |p'|^2$ (see Section 5.4) and from the envelope of the pressure trace one can compute

$$\alpha = \frac{1}{|p'|}\frac{d|p'|}{dt} \tag{2.12}$$

Let α_g be the value for the growth period and α_d for the decay. If the losses are the same during the growth and decay, and α_c is due to the combustion driving only, then $\alpha_g = \alpha_c + \alpha_d$, so

$$\alpha_c = \alpha_g - \alpha_d \tag{2.13}$$

Thus with (2.12) and (2.13) one can in principle find α_c. In practice there are serious difficulties obtaining accurate reproducible results, particularly for propellants containing aluminum; see the "T-burner manuals" (Culick 1969, 1974).

It is an interesting aspect of Horton's work that he worked out a simple method for using experimental data to infer both the real *and* the imaginary parts of the response function. That is correctly the information one should obtain from T-burner tests. Owing to experimental difficulties (apparently) it seems that Horton's is the only report for both parts of the response function. See the discussion in Section 6.7.

T-burner tests to characterize fully the dynamics of a propellant over ranges of pressure and frequency are expensive. Moreover, the results generally carry significant experimental errors. Hence the T-burner is best used to detect changes in dynamics, or generally for comparing propellants. Although hopes for improvement may have been held high, the nature of results from T-burner testing has not changed greatly in forty years. Nevertheless, there is still no better test apparatus and for qualitative purposes the T-burner has not been superceded. Indeed, even with the measurement errors always present, no other method has yet been proven more useful for obtaining qualitative data.

After McClure's working group had been established, and more information became publicly available, research on combustion instabilities in solid rockets attracted increasing attention. Brownlee, who had begun work on the problem in Canada, carried out the first systematic measurements of stability boundaries (Brownlee and Marble 1960); Smith (1960) and Shinnar and Dishon (1960) in the same AIAA volume published papers on the response of a burning surface to changes in the environment. While both works treated unsteady temperature profiles in the solid phase, neither emphasized the thermal wave. They could not, therefore, find the very special and important contributions of the thermal wave to the surface admittance function.

[9] For example, the early 1959 and 1960 papers attracted this author's responsive attention at the end of his Ph.D. research program. He subsequently was introduced to the solid rocket community by Mr. W.A. Berl, assistant to Dr. McClure.

[10] A center-vented symmetrical burner was first used by Price and Sofferis (1958) but the name T-burner was coined by Dr. H.M. Schuey in honor, it seems, of the piece of plumbing he chose in 1963 to serve as the center vent.

[11] We should note particularly that Horton inferred both the real and imaginary parts of the admittance function. Most reports of results obtained with T-burners show only the real part.

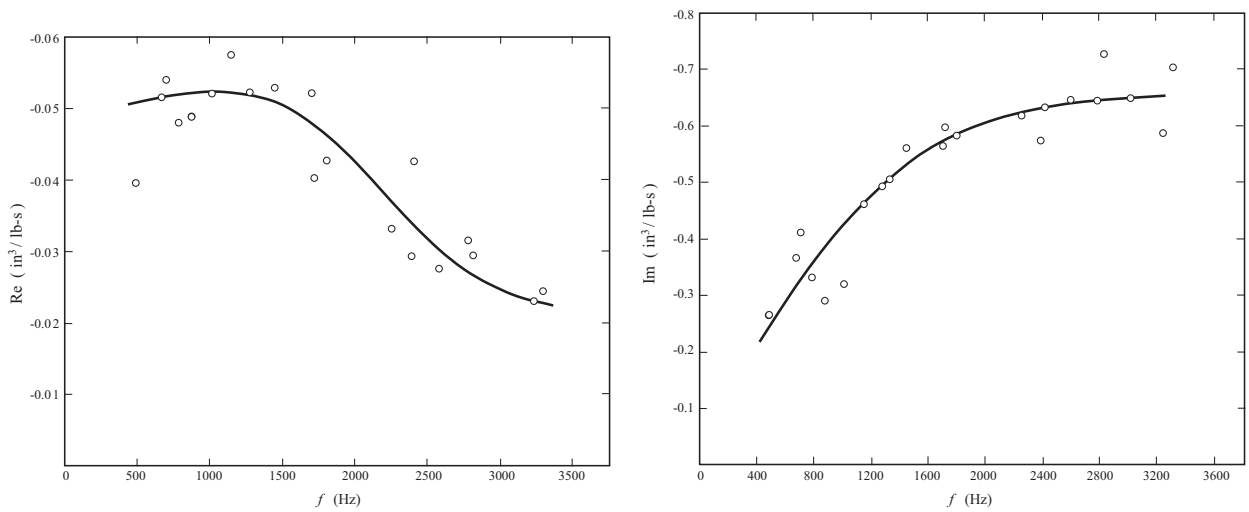

(a)

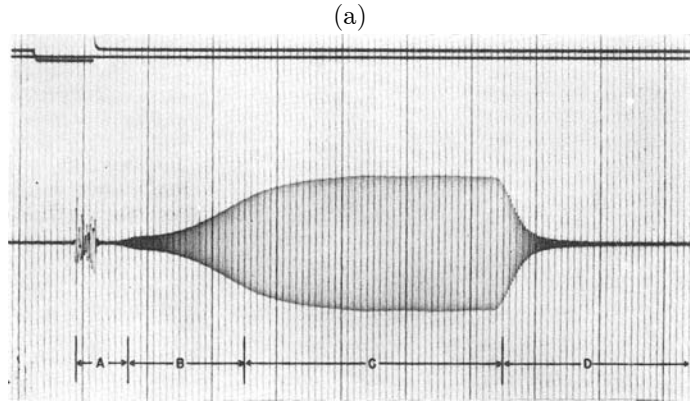

(b)

FIGURE 2.9. The first reported values of the real and imaginary parts of the admittance function for a burning surface. (a) experimental results inferred with the real and imaginary parts of equation (5), Horton (1961); (b) pressure record for a T-burner firing (Horton and Price 1962).

In the early 1960s attempts to measure the admittance function were made by more organizations—or perhaps their efforts were finally made public. Watermeier (1961) at the Army Ballistic Research Laboratories reported motion pictures of the burning surface (of a double-base propellant) exposed to the output of a siren. Only qualitative observations were made. Two years later, Watermeier *et al.* (1963) and Strittmater *et al.* (1963) discussed experimental investigations with modified forms of the T-burner, also using double-base propellants. One interesting observation concerned the agglomeration of molten aluminum on the surface, a "probable" cause for reduction of the admittance at low frequencies. Other features of the behavior of molten aluminum in the vicinity of the burning surface were noted, but without quantitative measurements no conclusions can be drawn. Wood (1963) also made measurements in a T-burner with propellant similar to that described by Price and Sofferis. Although he tried to make direct connection between compositional properties and the admittance function defined by McClure *et al.*, Wood's data and observations were too crude to allow definite conclusions. The work marks a transitional step to more realistic representations involving dynamical thermal behavior of the solid phase.

Denison and Baum (1961) produced a work which not only represented (in retrospect!) the culmination and joining of several ideas but, because it is firmly based on fundamental behavior, has had lasting influence

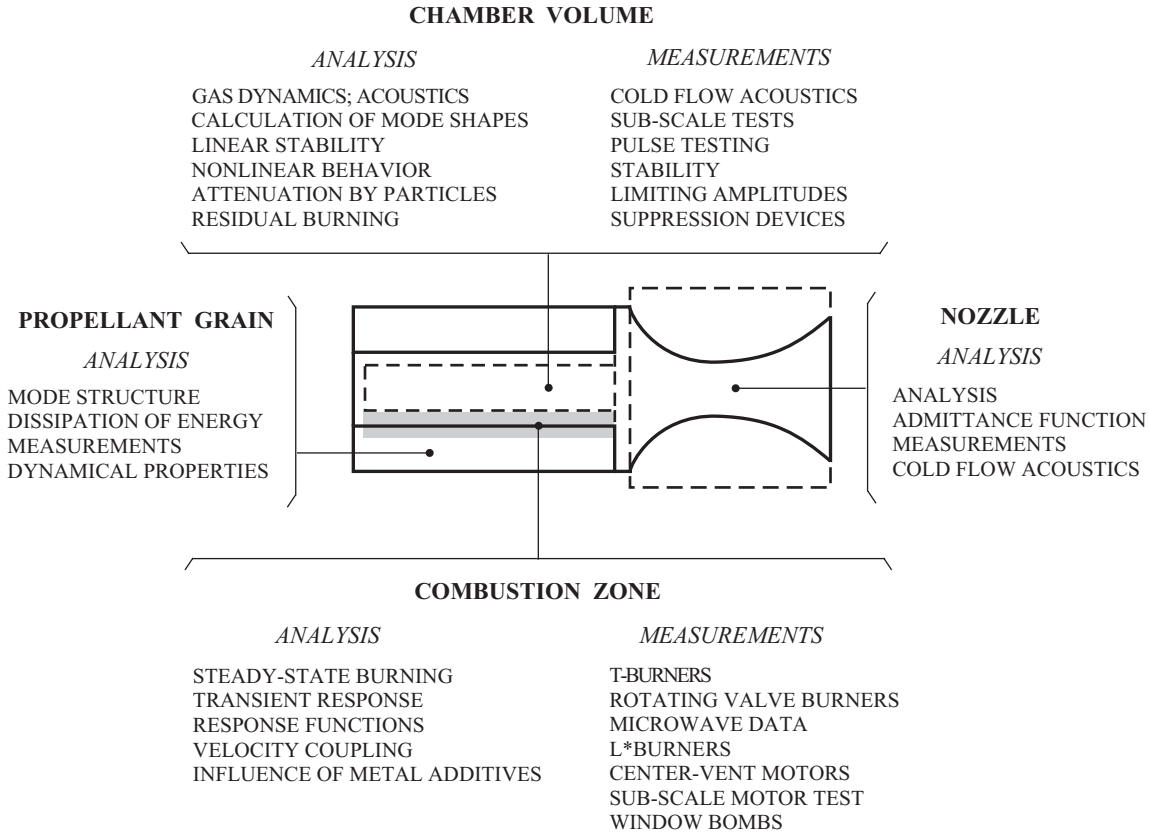

FIGURE 2.10. A summary of the instability problems for solid propellant rockets in 1970 (Culick 1970).

on theoretical treatments of burning. At the time, the paper did not instantly attract widespread attention, but its importance was gradually recognized.[12] When Denison and Baum's analysis appeared, its general applicability was not immediately apparent. In 1968, Culick (1968) showed that at that time ten analyses were equivalent to that of Denison and Baum in the sense that if parameters are given appropriate values in each case, then the response function (2.3) is the same function of frequency. That recognition has had important influence on experimental and theoretical work. Departures from the QSHOD model are important, difficult to treat and are still a subject of research; Sections 2.2.5 to 2.2.8 contain examples.

Figure 2.10 is a complete summary of the various kinds of work proceeding on combustion instabilities in solid propellant rockets, c. 1970.

2.2. Analysis of the QSHOD Model

The model we will analyze here is the simplest possible capturing a dominant contribution to the combustion dynamics. Only unsteady heat transfer in the condensed phase causes true dynamical behavior, i.e. dependence of the response to pressure coupling. That process must in any case be present. This problem

[12]In fact, the model defined by Denison and Baum was in a sense really an unnecessarily detailed special case of that proposed twenty years earlier by Zel'dovich (1942) and developed by Novozhilov (1965). The first was unknown in the West and the second was not recognized properly until the late 1960s. In simplest terms, an imperfect model of the gas phase in Denison and Baum's analysis is replaced by two sorts of experimental data in the Zel'dovich-Novozhilov model.

(model) is therefore the reference always used to assess the possible influences of other dynamical processes, in particular those in the gas phase and decomposition in the condensed phase. The substance of the model is defined by the following assumptions:

(i) **q**uasi-**s**teady behavior of all processes except unsteady conductive heat transfer in the condensed phase;
(ii) **h**omogeneous and constant material properties, non-reacting condensed phase;
(iii) **o**ne-**d**imensional variations in space;
(iv) conversion of condensed material to the gas phase at an infinitesimally thin interface.

The acronym QSHOD for this model derives from the five bold letters in assumptions (i)–(iii).

During the early years of this subject, from the mid-1950s to the mid-1960s, roughly ten analyses of the response function were published in the Western literature, giving apparently distinct results. Culick (1968) showed that, due to the fact that all of the models were based in the same set of assumptions (i)–(iv), the results were dynamically identical. That is, all had the same dependence on frequency and, with appropriate values for the various parameters involved, give coincident numerical values. Hence the term QSHOD is a useful term referring to a class of models. Differences between the models are associated with different detailed models of the steady processes, notably the flame structure in the gas phase.

A different approach to compute the combustion response was taken by Zel'dovich (1942) in Russia and elaborated in great depth by Novozhilov (1965, 1973, 1996). The result has come to be known as the Z-N model. That representation of the response has certain distinct advantages, most importantly giving convenient connections between the parameters in the response function and quantities characterizing and measurable in steady combustion. The idea is explained briefly in Section 2.2.4. However, an important point often overlooked is that the dynamics contained in the basic Z-N model are the same as those in the flame models treated within the general QSHOD model.

Analysis of the model sketched in Figure 2.1 amounts to quantitative representation of the sequence (i)–(iv). Even in the simplest form described here, the problem is too complicated for a closed form solution. Apart from recent results obtained numerically for the entire region, covering the cold solid to the hot combustion products, the usual procedure familiar in many problems of this sort is based on solutions found for the separate regions defined above; the results are then matched at the interfaces. The solutions and the matching conditions are based on the one-dimensional equations of motion. In the reference frame selected here, the origin is fixed to the average position of the burning surface, and under unsteady conditions all interfaces move, a feature that must be correctly incorporated in the analysis.

2.2.1. Estimates of Some Characteristic Lengths and Times. It is helpful to have a qualitative idea of the sizes of a few important variables. That information provides a context for understanding the physical problem and a basis for making realistic approximations to simplify analyses. One way to view the situation is shown in Figure 2.11, based on Figure 1 of Culick (2000). The four levels of dynamics—chemical dynamics, combust**ion** dynamics, combust**or** dynamics and motor (engine) dynamics—are each characterized by different lengths and times. A typical size of a rocket, for example, is also the length scale for engine and combust**or** dynamics, say one meter, to tens of meters. The burning zone for a solid propellant is a millimeter or less. Hence the ratio of those lengths may vary from 10^3 to 10^6. Chemical dynamics evolve on a scale 10^{-3} to 10^{-6} smaller. Thus it is fairly clear that the details of phenomena associated with the three different scales can, to a very good approximation, be treated separately, although they are ultimately coupled. Averaging of processes on the smaller scale produces consequences that matter on the larger scale. In this book we are concerned largely with unsteady motions on the scale of the device in question. But those motions are commonly driven, e.g., at the boundaries, by forces and energy flow which originate at a smaller scales.

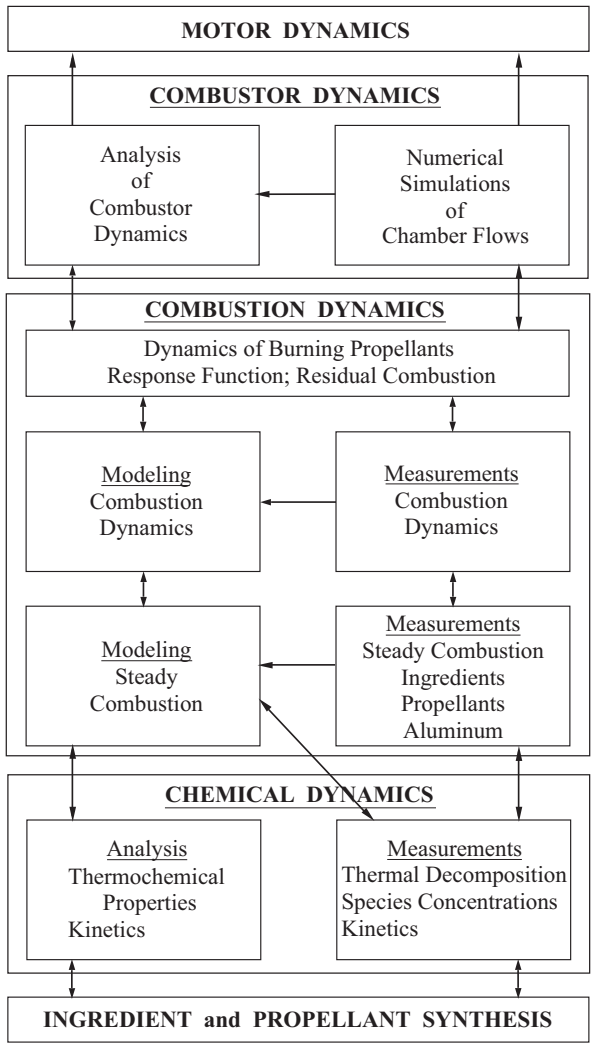

FIGURE 2.11. A view of the areas of research and their connections in solid propellant rockets (Culick 2000).

Often, the *mechanics* of the unsteady motions require descriptions on a much smaller scale. The unsteady response of a burning surface is a good example of that fact. We assume for present purposes that the combustion processes generate a zone like that sketched in Figure 2.2, and make a few estimates of its characteristics. Several discussions of approximate representations exist (e.g. Hart and McClure 1959); we base our remarks on Culick and Dehority (1969) who computed the burning rate assuming a finite region of uniform combustion. The flame thickness is roughly 0.5μ–500μ for the thermal conductivity of the gas varying from 2×10^{-5} to 2000×10^{-5} cal/s-cm-°K, the pressure less than 900 atmospheres and reasonable values for other parameters (temperatures, heat of reaction, etc.); Table 2.1 is a list of the properties used in the following remarks. We take 250μ as a conservative estimate; as a rough guide, the thicker is a flame, the greater is its tendency to behave dynamically, in contrast to quasi-staticallly.

Table 2.1 contains values of the properties we need for the following estimates. The characteristic time for the chemical reaction process in the gas phase is the flame thickness divided by the average speed, $\tau_f \sim \delta_f/\bar{u}_g$ where $\delta_f \approx 250\mu$. Thus τ_f is the time for a particle to pass through the flame. We estimate the gas speed from continuity, $\bar{u}_g = \rho_p \bar{r}_b/\bar{\rho}_g$ and taking values from Table 2.1, $\bar{u}_g \sim (1766)(0.01145)/(7.97) \approx 2.5\,\mathrm{m/s}$.

Then the characteristic time for the steady reaction process is

$$\tau_f \sim \frac{\delta_f}{\bar{u}_g} \sim \frac{250\mu}{2.5\,\mathrm{m/s}} \sim \frac{(250)(10^{-6})}{2.5\,\mathrm{m/s}}\mathrm{m} \sim 10^{-4} \tag{2.14}$$

for a rather thick flame zone, $250\mu \equiv 0.25\,\mathrm{mm}$.

The period of an oscillation is the reciprocal of the frequency, $\tau_a = 1/f = 2\pi/\omega_a$. For the chemical activity in the gas phase to be treated as 'quasi-static', chemical changes must be fast relative to the acoustic period, which implies

$$\frac{\tau_f}{\tau_a} \ll 1 \qquad \text{(quasi-static chemical reaction)} \tag{2.15}$$

With the estimate just quoted, $10^{-4} f_a$ should be small for quasi-static reactions. This implies $f_a < 10,000$ Hz. We conclude that while the chemistry in a solid propellant flame can probably be assumed to respond quasi-statically over a useful frequency range, something less than 10,000 Hz, the approximation should probably be examined more closely for higher frequencies.

TABLE 2.1. Typical Values of Combustion and Physical Properties.

mean pressure	$\bar{p} = 1.06 \times 10^7$ Pa
linear burning rate	$\bar{r}_b = 0.0078[\bar{p}/(3.0 \times 10^6)]^{0.3} = 0.01145\,\mathrm{m/s}$
chamber temperature	$\bar{T} = 3539\,\mathrm{K}$
Prandtl number	$Pr = 0.8$
thermal conductivity of combustion gases	$\lambda_g = 0.0838$ J/K-m-s
thermal conductivity of solid propellant	$\lambda_p = 0.126$ J/K-m-s
thermal diffusivity of gases	$\kappa_g = 3.97 \times 10^{-4}\,\mathrm{m^2/s}$
thermal diffusivity of propellant	$\kappa_p = 1.0 \times 10^{-7}\,\mathrm{m^2/s}$
specific heat of gas	$C_p = 2020$ J/kg K
specific heat of condensed material	$C = 0.68C_p$
propellant density	$\rho_p = 1,766\,\mathrm{kg/m^3}$
gas density	$\bar{\rho}_g = 7.97\,\mathrm{kg/m^3}$
γ (gas only)	$\gamma = 1.23$
gas constant	$R = (\gamma - 1)C_p/\gamma = 377.72$ J/kg K
speed of sound	$\bar{a} = \sqrt{\gamma R T} = 1282\,\mathrm{m/s}$
speed of combustion products at the burning surface	$\bar{v}_b = (\rho_p/\rho)\bar{r}_b = 1.86\,\mathrm{m/s}$
Mach number at the burning surface	$\bar{M}_b = 0.00173$

For much of our needs, some sort of thermal theory serves quite well to describe both steady and unsteady behavior of a burning propellant surface. The governing equation is then the energy equation which will have a different form in each of the regions (solid, interfacial, gas, ...). An important question is: How quickly does the flow respond to changes of conditions? A very fast response of the flow means that the distribution of temperature in a region will be the same as it would be in steady state for the same boundary (or end) conditions and values of energy sources. If, on the other hand, the state of the flow is not instantaneously responsive, the temperature differs significantly from its steady form due to the presence of waves. A measure of the departure from the 'quasi-steady' form is the ratio of the net flow of energy, into a fluid element, by heat conduction to the rate of change of energy in the element,

$$N_c = \frac{\partial}{\partial x}\left(\lambda_g \frac{\partial T}{\partial x}\right) \Bigg/ \bar{\rho} C_v \frac{\partial T}{\partial t} \tag{2.16}$$

where x is measured normal to the burning surface, in the direction of greatest variations.

Suppose (cf. Figure 2.13) that the temperature changes by ΔT in distance Δx and time Δt so we can estimate N_c as

$$N_c = \frac{\lambda_g \Delta T}{(\Delta x)^2} \Bigg/ \frac{\bar{\rho} C_v \Delta T}{\Delta t} = \frac{\lambda_g \Delta t}{\bar{\rho}_g C_v (\Delta x)^2} \tag{2.17}$$

where $\bar{\rho}$ is a representative density (gas or solid), C_v is the specific heat and Δx, Δt are the intervals of space and time in question. For a wave motion, the period $\tau = 1/f$ is a measure of the characteristic time. Spatial variations occur over the flame thickness, $\Delta x \sim \delta_f$, so

$$N_c = \frac{\lambda_g}{\bar{\rho}_g C_v \delta_f^2 f} = \frac{\kappa_g}{\delta_f^2 f} \tag{2.18}$$

where κ_g is the thermal diffusivity. For N_c large, the rate of heat transfer to a layer dominates the rate of change of energy within the layer having thickness δ_f; then the term $\bar{\rho} C_v \partial T/\partial t$ can be neglected in the energy equation and the temperature field changes in quasi-static fashion. For the properties given in Table 2.1,

$$N_c = \frac{3.97 \times 10^{-4}}{(250 \times 10^{-6})^2 f} = \frac{6352}{f} \tag{2.19}$$

According to this result, the assumption of quasi-static behavior is not valid for frequencies above, say 1000–1500 Hz, perhaps higher. In any case, the analysis is so much simpler when this assumption is made, that it must be used in the initial stage, as a 'first try'.

2.2.2. Calculation of the Response Function. The following remarks are based on the review cited above, Culick (1968). Since that time much work has been done to determine the consequences of relaxing the assumptions on which the following analysis (the QSHOD model) is based. We will later examine some of those ideas. In this section we assume that the combustion proceeds as transformation of a condensed phase at a single flat surface adjacent to the gas phase, requiring that solutions be matched at only one interface. We choose a reference system with origin ($x = 0$) fixed[13] to the average position of the interface. Hence the cold unreacted solid material progresses inward from the left. Figure 2.12 shows this definition and the matching conditions that must be satisfied at the interface. Note that the velocity $\dot{x}_s$ of the interface appears explicitly in these conditions and is to be determined as part of the solution to the complete problem.

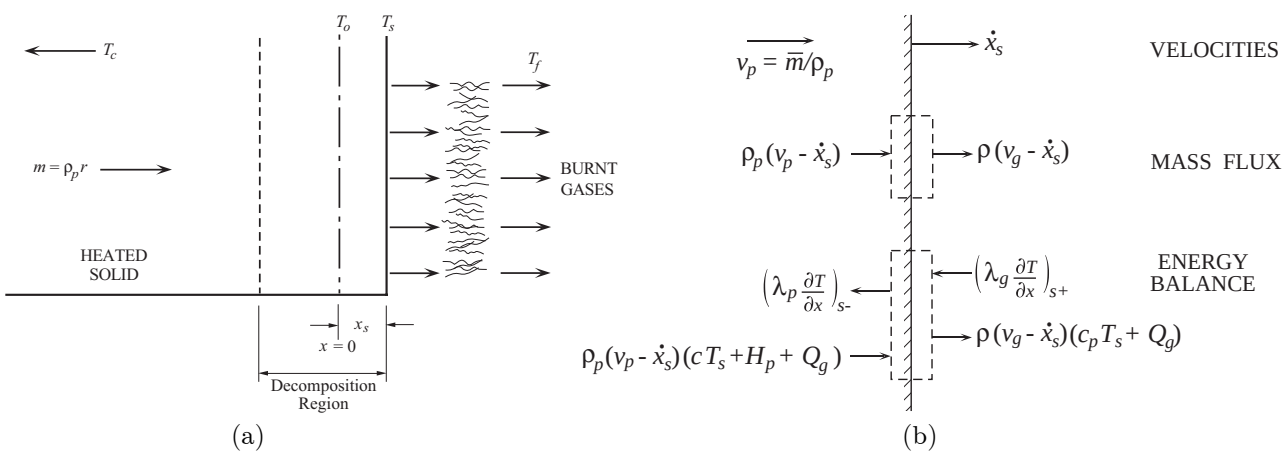

FIGURE 2.12. (a) reference system and (b) matching conditions for the QSHOD Model.

For the simple model used here, the analysis involves only three steps: solution for the temperature field in the solid phase; solution for the temperature field in the gas phase; and matching the two solutions at the interface. Because the temperature field is central to the analysis, the final results should correctly be

[13]Alternatively, the reference frame may be fixed to the instantaneous position of the surface; it is therefore not an inertial frame for the unsteady problem. For the linear problem, it is easy to show the equivalence of the results obtained with the two choices of reference systems. If more than three regions are treated—e.g., when an additional decomposition zone is included in the condensed phase—it may be more convenient to take $x_s = 0$ for the reference frame, and account for the motions of all interfaces relative to that plane, which is the time-averaged location of the solid-gas interface.

regarded as a thermal theory of steady and unsteady combustion of a solid propellant. No diffusive processes are accounted for and the pressure is uniform throughout the region considered: changes of the momentum of the flow do not enter the problem.

(a) *Solid Phase.* The energy equation for the temperature in the solid phase assumed to have uniform and constant properties, is

$$\lambda_p \frac{\partial^2 T}{\partial x^2} - \overline{m} c \frac{\partial T}{\partial x} - \rho_p c \frac{\partial T}{\partial t} = -\dot{Q}_d \tag{2.20}$$

where $\overline{(\ )}$ means time-averaged value; $(\ )_p$ denotes propellant; c is the specific heat of the solid; $\overline{m} = \rho_p \overline{r}$ is the average mass flux in the reference system defined in Figure 2.12; and $\dot{Q}_d$ is the rate at which energy is released per unit volume due to decomposition of the solid ($\dot{Q}_d > 0$ for exothermic decomposition). We assume $\dot{Q}_d = 0$ here, an assumption to be relaxed in Sections 2.2.5 and 2.2.6. It is convenient to use the dimensionless variables

$$\xi_p = \frac{\overline{r}}{\kappa_p} x \ ; \quad \tau = \frac{T}{\overline{T}_s} \tag{2.21}$$

where values at the interface are identified by subscript s and $\kappa_p = \lambda_p / \rho_p c$ is the thermal diffusivity of the propellant. Equation (2.20) becomes

$$\frac{\partial^2 \tau}{\partial \xi^2} - \frac{\partial \tau}{\partial \xi_p} - \frac{\lambda_p \rho_p}{\overline{m}^2 c} \frac{\partial \tau}{\partial t} = 0 \tag{2.22}$$

Solution to (2.22) with the time derivative dropped gives the formula for the normalized mean temperature

$$\overline{\tau} = \overline{\tau}_c + (1 - \overline{\tau}_c) e^{\xi_p} \tag{2.23}$$

satisfying the conditions $\overline{\tau} = \overline{\tau}_s = 1$ at the surface and $\overline{\tau}_c = \overline{T}_c / \overline{T}_s$ far upstream ($\overline{T} = \overline{T}_c$) in the cold propellant.

For harmonic motions, set $\tau = \overline{\tau} + \tau'$ and[14] $\tau' = \hat{\tau} e^{-i\omega t}$, $\hat{\tau}$ being the amplitude, a complex function of position in the solid material. Substitution in (2.22) leads to the equation for $\hat{\tau}(\xi_p)$, easily solved to give

$$\tau' = \hat{\tau}_0 e^{\lambda \xi_p} e^{-i\omega t} \tag{2.24}$$

where λ satisfies the relation

$$\lambda(\lambda - 1) = -i\Omega \tag{2.25}$$

and Ω is the important dimensionless frequency,

$$\Omega = \frac{\lambda_p \rho_p}{\overline{m}^2 c} \omega = \frac{\kappa_p}{\overline{r}^2} \omega \tag{2.26}$$

For the numbers given in Table 2.1, $\Omega \approx 20 f$. In order that $\tau' \to 0$ for $x \to -\infty$, the solution of (2.25) with positive real part must be used; $\lambda = \lambda_r - i\lambda_r$ and

$$\begin{aligned} \lambda_r &= \frac{1}{2} \left\{ 1 + \frac{1}{\sqrt{2}} \left[(1 + 16\Omega^2)^{1/2} + 1 \right]^{1/2} \right\} \\ \lambda_i &= \frac{1}{2\sqrt{2}} \left[(1 + 16\Omega^2)^{1/2} - 1 \right] \end{aligned} \tag{2.27a,b}$$

Due to the choice of reference system, $\hat{\tau}_0$ in (2.24) is the fluctuation of temperature at the average position of the interface ($\xi_p = 0$). However, matching conditions at the interface requires values and derivatives of the temperature at the interface itself, having position x_s and velocity $\dot{x}_s$. Values at the interface are calculated

[14]Note that consistently throughout this book we use the negative exponential, $\exp(-i\omega t)$. In some of the literature the positive exponential is used, so care must be taken when making comparisons of results.

with Taylor series expansions about $x = 0$; only the first order terms are retained for the linear problem, and on the solid side of the interface[15]:

$$\begin{aligned} \overline{T}_s(x_s) &= \overline{T}(0) + x_s \left(\frac{d\overline{T}}{dx}\right)_{0-} \quad ; \quad \left(\frac{d\overline{T}}{dx}\right)_{s-} = \left(\frac{d\overline{T}}{dx}\right)_{0-} + x_s \left(\frac{d^2\overline{T}}{dx^2}\right)_{0-} \\ T'_s(x_s) &= T'_{0-}(0) + x_s \left(\frac{\partial\overline{T}}{dx}\right)_{0-} \quad ; \quad \left(\frac{\partial T'}{\partial x}\right)_{s-} = \left(\frac{\partial T'}{\partial x}\right)_{0-} + x_s \left(\frac{\partial^2 T'}{\partial x^2}\right)_{0-} \end{aligned} \tag{2.28}$$

Hence the required results for the upstream side of the interface cannot be completed until the interfacial region is analyzed.

(b) *Interfacial Region.* Three relations govern the behavior at the interface: conservation of mass and energy, and the law for conversion of solid to gas. The first two are established by considering a small control volume placed about the true burning surface, as sketched in Figure 2.12. The volume is then collapsed to give "jump" conditions associated with the total unsteady mass and energy transfer in the upstream ($s-$) and downstream ($s+$) sides of the interface:

$$\begin{aligned} \frac{\rho_p \dot{x}_s}{\overline{m}} &= -\left[1 - \frac{\overline{\rho}_{gs}}{\rho_{ps}}\right] \frac{m'_s}{\overline{m}} \approx -\frac{m'_s}{\overline{m}} \\ \left[\lambda_g \frac{\partial T}{\partial x}\right]_{s+} &= \left[\lambda_p \frac{\partial T}{\partial x}\right]_{s-} + \overline{m}\left[1 - \frac{\overline{\rho}_p \dot{x}_s}{\overline{m}}\right](L_s) \end{aligned} \tag{2.29)a,b}$$

The mean gas density $\overline{\rho}$ near the surface is much smaller than the density of the condensed phase, for cases of current interest, so the term $\overline{\rho}/\rho_p \ll 1$ will hereafter be dropped. For an exothermic surface reaction, the change $L_s = h_{s+} - h_{s-}$ of the thermal enthalpy is positive and may be viewed as a 'latent heat'. The heat fluxes $[\lambda_p \partial T/\partial x]_{s-}$ and $[\lambda_g \partial T/\partial x]_{s+}$ are respectively flows of heat *from* the interface to the condensed phase and *to* the interface *from* the gas phase; note that (2.29)b has not yet been split into mean and fluctuating parts.

An Arrhenius law has commonly been assumed for the conversion of solid to gas, giving the total surface mass flux

$$m_s = Bp^{n_s} e^{-E_s/R_0 T_s} \tag{2.30}$$

To first order in small quantities, the perturbed form of (2.30) is

$$\frac{m'_s}{\overline{m}} = E e^{i\omega\tau_1} \tau'_s + n_s e^{i\omega\tau_2} \frac{p'}{\overline{p}} \tag{2.31}$$

where $E = E_s/R_0 T_s$ is the dimensionless activation energy for the surface reaction. Time delays or lags τ_1 and τ_2 are included in (2.31), but presently there is no way to compute them; hence they will largely be ignored here except for some results given in Section 2.2.6.

For steady combustion, the energy balance (2.29)b, with (2.23) substituted for $d\overline{T}/dx$, becomes

$$\left(\lambda_g \frac{d\overline{T}}{dx}\right)_{s+} = \overline{m}\left[c\left(\overline{T}_s - T_c\right) + L_s\right] \tag{2.32}$$

The linear unsteady part of (2.29)b is

$$\left(\lambda_g \frac{\partial T}{\partial x}\right)'_{s+} = \left(\lambda_p \frac{\partial T}{\partial x}\right)'_{s-} + m'_s \overline{L}_s + \overline{m}(c_p - c) T'_s \tag{2.33}$$

[15]The temperature is continuous at the interface, but on $x = 0$, the fluctuations T'_{0-} and T'_{0+} computed from the solutions for the solid and gas phase need not be continuous.

Combination of (2.23) and (2.24) and the appropriate parts of (2.28) gives the formula for the heat transfer into the condensed phase from the interface:

$$\left(\lambda_p \frac{\partial T}{\partial x}\right)'_{s-} = \overline{m}c\left[\lambda T'_s + \frac{1}{\lambda}\left(\overline{T}_s - T_c\right)\frac{m'_s}{\overline{m}}\right] \tag{2.34}$$

In this result, the approximation in (2.29)a has been used. Substitution of (2.34) in (2.33) leads to the boundary condition to be set on the unsteady heat transfer at the downstream side of the interface:

$$\left(\lambda_g \frac{\partial T}{\partial x}\right)'_{s+} = \overline{m}c\left[\lambda T'_s + \left(\frac{c_p}{c} - 1\right)T'_s + \left\{\frac{1}{\lambda}\left(\overline{T}_s - T_c\right) + \frac{L_s}{c}\right\}\frac{m'_s}{\overline{m}}\right] \tag{2.35}$$

This result contains two assumptions:

(i) $\overline{\rho}_g/\overline{\rho}_p \ll 1$ $(x = x_s)$
(ii) nonreacting condensed phase having constant and uniform properties

Normally, the first assumption is reasonable. However, the second is restrictive, possibly seriously so according to some analyses; see Section 2.2.5. The important point is that (2.35) explicitly contains the transient behavior (the dynamics) associated with unsteady heat transfer in a benign solid material. If no further dynamics is attributed to the processes at the interface or in the gas phase, then the response function found with this analysis reflects only the dynamics of unsteady heat transfer in the single homogeneous condensed phase. That is the basic QSHOD result. Hence it is apparent that the form of the dependence of the response function in frequency *will necessarily in this case be independent of the model chosen for the quasi-static behavior of the gas phase.* The details of the model selected will affect *only* the particular values of parameters appearing in the formula for the response function. The conclusion is true for the basic Z-N model as well as for all flame models assumed to behave quasi-statically.

(c) *Gas Phase.* To complete the analysis, it is best at this stage to choose the simplest possible model for the gas phase. We assume that the thermal conductivity is uniform in the gas phase and that the combustion processes (i.e. the rate of energy release per unit volume) are also uniform in a region beginning some distance from the interface and extending downstream, ending at a location that is, by definition, the edge of the flame zone. This is a useful model containing two simple limits: uniform combustion beginning at the interface; and a flame sheet, obtained by letting the thickness of the combustion zone become infinitesimally thin. Figure 2.13 is a sketch of the model. Analysis of the model for steady burning was given by Culick (1969) with the following results.

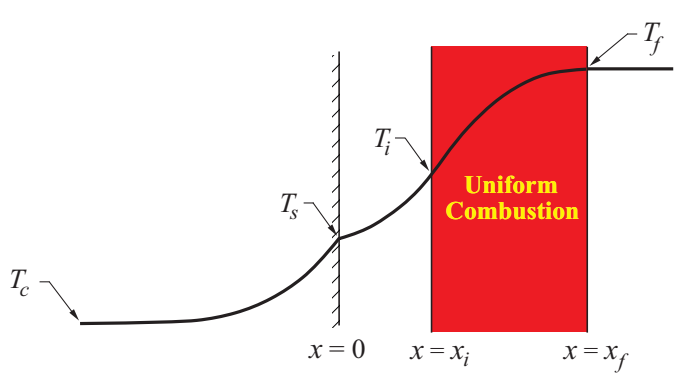

FIGURE 2.13. Sketch of the model of a solid propellant burning with uniform combustion in the gas phase.

The governing equation for this thermal theory is

$$mc_p \frac{d\overline{T}}{dx} - \frac{d}{dx}\left(\lambda_g \frac{d\overline{T}}{dx}\right) = \rho_g Q_f \dot{\epsilon} \tag{2.36}$$

where Q_f is the energy released per unit mass of reactant mixture (assumed to be constant), ρ_g is the local gas density and $\dot{\epsilon}$ is the local rate of reaction. At the downstream edge of the combustion zone, the boundary conditions are

$$\overline{T} = \overline{T}_f \ ; \quad \frac{d\overline{T}}{dx} = 0 \quad (x = x_f) \tag{2.37)a,b}$$

where $\overline{T}_f$ is the adiabatic flame temperature. On the interface,

$$\overline{T} = \overline{T}_s \tag{2.38}$$

and the energy balance at the interface gives

$$\left(\lambda_g \frac{d\overline{T}}{dx}\right)_{s+} = m\left[c\left(\overline{T}_s - T_c\right) + L_s\right] \tag{2.39}$$

For steady combustion, consideration of the energy flow across the gas phase gives

$$\overline{\left(\lambda_g \frac{dT}{dx}\right)}_{s+} = \overline{m}\left[Q_f - c_p\left(\overline{T}_f - \overline{T}_s\right)\right] \tag{2.40}$$

On the other hand, integration of (2.36) across the combustion zone, and application of the boundary conditions (2.37)a,b and (2.38) leads to

$$\left(\lambda_g \frac{d\overline{T}}{dx}\right)_{s+} = \int_0^\infty \rho_g Q_f \dot{\epsilon} dx - mc_p\left(\overline{T}_f - \overline{T}_s\right) \tag{2.41}$$

Because Q_f is constant, comparison of (2.40) and (2.41) leads to the requirement on the overall reaction rate

$$\int_0^\infty \rho_g \dot{\epsilon} dx = m \tag{2.42}$$

We assume λ_g constant (an assumption that is easily relaxed) and transform from x to the dimensionless variable ζ:

$$\zeta = \frac{mc_p}{\lambda_g} x \tag{2.43}$$

The energy equation (2.36) becomes

$$-\zeta^2 \frac{d^2\overline{T}}{d\zeta^2} = \Lambda^2 \tag{2.44}$$

where the eigenvalue Λ^2 is

$$\Lambda^2 = \frac{\lambda_g Q_f \overline{w}}{m^2 c_p^2 \overline{T}_s} \tag{2.45}$$

and

$$w = \rho_g \dot{\epsilon} \tag{2.46}$$

Generally, of course, $\dot{\epsilon}$ and hence w and therefore Λ^2 are dependent at least on temperature, so Λ^2 is implicitly a function of ζ. However, we assume Λ^2 independent of ζ, defining the condition of uniform combustion.

Then with ζ_i the value of ζ at the beginning of the combustion zone (where ignition is assumed to occur) and ζ_f the value at the downstream edge of the flame, the first integral of (2.44) gives

$$\left(\frac{d\overline{T}}{d\zeta}\right)_{s+} = \left(\frac{\zeta_f - \zeta_i}{\zeta_f \zeta_i}\right)\Lambda^2 \tag{2.47}$$

Thus

$$\left(\lambda_g \frac{d\overline{T}}{dx}\right)_{s+} = \frac{\lambda_g Q_f}{c_p}\left(\frac{1}{\zeta_i} - \frac{1}{\zeta_f}\right)\frac{w}{m} \tag{2.48}$$

For $\zeta_f \gg \zeta_i$, and in the limit of combustion beginning at the solid/gas interface so $\zeta_i = 1$,

$$\left(\lambda_g \frac{d\overline{T}}{dx}\right)_{s+} = \frac{\lambda_g Q_f}{c_p}\frac{w}{m} \tag{2.49}$$

The assumption of quasi-steady behavior implies that the fluctuation of heat transfer at the surface is given simply by the linearized form of (2.49):

$$\left(\lambda_g \frac{dT}{dx}\right)'_{s+} = \overline{m} c_p \overline{T}_s \Lambda^2 \left(\frac{w'}{\overline{w}} - \frac{m'}{\overline{m}}\right) \tag{2.50}$$

We also find as the linearized form of (2.40):

$$\left(\lambda_g \frac{dT}{dx}\right)'_{s+} = m'\left[Q_f - c_p\left(\overline{T}_f - \overline{T}_s\right)\right] - \overline{m} c_p \left(T'_f - T'_s\right) \tag{2.51}$$

This equation gives a formula for the fluctuation of flame temperature,

$$T'_f = T'_s + \frac{m'}{\overline{m}}\left[\frac{Q_f}{c_p} - \left(\overline{T}_f - \overline{T}_s\right)\right] - \frac{1}{\overline{m} c_p}\left(\lambda_g \frac{dT}{dx}\right)'_{s+} \tag{2.52}$$

Substitution of (2.50) for the last term gives the formula for computing T'_f when the combustion is uniform. In general, T'_f is not equal to the local fluctuation of temperature due to acoustical motions in the gas phase, the difference appearing the temperature fluctuation associated with an entropy wave carried by the mean flow departing the combustion zone.

By letting $\zeta_i \to \zeta_f$, the corresponding results can be obtained for a flame sheet; see Culick (1969; 2002). We will consider here only the case of a combustion zone having finite thickness; the response functions found for the two cases differ only in small details.

To progress further, we must specify the form of $w = \rho_g \dot{\epsilon}$; the reaction rate per unit volume. For the quasi-steady part of the processes, we assume that the mass flow provided by the surface is well-approximated by the Arrhenius law (2.30) and its fluctuation is (2.31) with zero time delays,

$$\frac{m'}{\overline{m}} = E\frac{T'_s}{\overline{T}_s} + n_s \frac{p'}{\overline{p}} \tag{2.53}$$

Due to the assumption of quasi-steady behavior, this formula represents the fluctuation of mass flow throughout the gas phase.

Finally, we need an explicit form for w as a function of the flow variables. To construct a consistent formula for the reaction rate in the gas phase, we equate the two results for heat transfer to the interface during steady burning: (2.39), the energy balance for steady combustion, generally valid at the interface; and (2.49) found for the special case of steady uniform combustion. For quasi-steady behavior in the gas phase, we replace average by instantaneous values of the temperatures, giving the expression for w:

$$w = \frac{c_p}{\lambda_g Q_f} m^2 \left[c\left(T_s - T_c\right) + L_s\right] \tag{2.54}$$

We assume that the right-hand side can be written as a function of pressure only by approximating the pyrolysis law $m = a(T_s)p^n$ as

$$m = ap^n = b(T_s - T_c)^s p^{n_s} \tag{2.55}$$

so

$$T_s - T_c = \left(\frac{a}{b}p^{n-n_s}\right)^{\frac{1}{s}} \tag{2.56}$$

Then (2.54) becomes

$$w = \frac{c_p}{\lambda_g Q_f}(ap^n)^2\left[c\left(\frac{a}{b}p^{n-n_s}\right)^{\frac{1}{s}} + L_s\right] \tag{2.57}$$

The fluctuation w' of the reaction rate is then

$$\frac{w'}{\overline{w}} = \frac{\left(1 - \frac{T_c}{\overline{T}_s}\right)}{\Lambda^2}\frac{c}{c_p}w\frac{p'}{\overline{p}} \tag{2.58}$$

where Λ^2 is given by (2.45) written for the steady problem,

$$\Lambda^2 = \frac{\lambda_g Q_f \overline{w}}{\overline{m}^2 c_p^2 \overline{T}_s} \tag{2.59}$$

and

$$\begin{aligned} \overline{w} &= \left[2(1+H) + \frac{c_p}{c}\frac{1-\frac{n_s}{n}}{c}\right] \\ H &= -\frac{L_s}{c(\overline{T}_s - T_c)} \end{aligned} \tag{2.60)a,b}$$

Instead of the calculations leading from (2.49) to (2.58) one could as well simply assume $w' \sim p'$. The only purpose of these remarks is to give an example of relating fluctuations of the reaction rate to the pressure for a well-defined model of combustion in the gas phase.

(d) *Construction of the Response Function.* We find the formula for the response function in the following way:

(i) Substitute the pyrolysis law (2.53) in (2.35) which combines the interfacial conditions for energy and mass transfer:

$$\frac{1}{\overline{m}c\overline{T}_s}\left(\lambda_g\frac{\partial T}{\partial x}\right)'_{s+} = \left(\lambda + \frac{A}{\lambda}\right)\frac{T'_s}{\overline{T}_s} + \left(\frac{c_p}{c} - 1 + \frac{LA}{1-\frac{T_c}{\overline{T}_s}}\right)\frac{T'_s}{\overline{T}_s} + n_s\left(L + \frac{1-\frac{T_c}{\overline{T}_s}}{\lambda}\right)\frac{p'}{\overline{p}} \tag{2.61}$$

where

$$\begin{aligned} L &= \frac{L_s}{c\overline{T}_s} \\ A &= (1 - \frac{T_c}{\overline{T}_s})(\alpha_s + \frac{E_s}{R_0\overline{T}_s}) \end{aligned} \tag{2.62)a,b}$$

(ii) Substitute the reaction rate (2.58) into the expression (2.50) for the heat loss from the gas phase to the interface:

$$\frac{1}{\overline{m}c\overline{T}_s}\left(\lambda_g\frac{\partial T}{\partial x}\right)'_{st} = \left(1 - \frac{T_c}{\overline{T}_s}\right)w\frac{p'}{\overline{p}} - \frac{c_p}{c}\Lambda^2\frac{m'}{\overline{m}} \tag{2.63}$$

(iii) Equate (2.61) and (2.63) and use the pyrolysis law (2.53) to eliminate $T_s'/\overline{T}_s$; this step leaves an equation which can be rearranged to give the ratio defined to be the response function for pressure coupling:

$$R_p = \frac{m'/\overline{m}}{p'/\overline{p}} = \frac{\left(AW + \frac{c_p}{c}n_s\right) + n_s(\lambda - 1)}{\lambda + \frac{A}{\lambda} + \left[\frac{c_p}{c}E\Lambda^2 - HA + \frac{c_p}{c} - 1\right]} \tag{2.64}$$

(iv) Write (2.64) in the form

$$R_p = \frac{c_1 + n_s(\lambda - 1)}{\lambda + \frac{A}{\lambda} + c_2} \tag{2.65}$$

For the assumed steady burning rate law, $m = ap^n$, the fluctuation can be written for quasi-steady (infinitely slow) changes of pressure and hence burn rate:

$$R_p = \frac{m'/\overline{m}}{p'/\overline{p}} = n \tag{2.66}$$

Thus in the limit of zero frequency ($\lambda = 1$), the right-hand side of (2.65) must equal n, giving the condition

$$\frac{c_1}{1 + A + c_2} = n$$

Define B and A with

$$c_1 = nB$$

and

$$c_2 = B - (1 + A)$$

Hence (2.65) becomes

$$\boxed{R_p = \frac{nB + n_s(\lambda - 1)}{\lambda + \frac{A}{\lambda} - (1 + A) + B}} \tag{2.67}$$

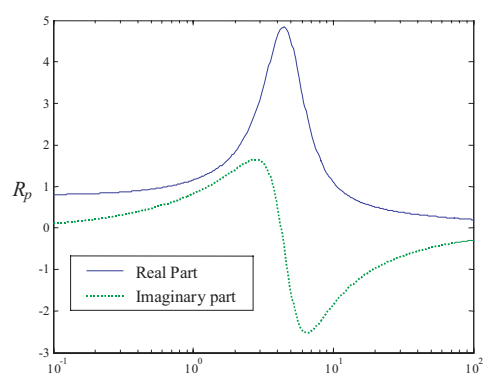

FIGURE 2.14. Real and imaginary parts of a QSHOD response function computed with equation 2.67: $n_s = 0$, $A = 6.0$, $B = 0.60$.

Figure 2.14 shows typical results for the real and imaginary parts of this formulas when $n_s = 0$. Experimental results given in the following section have long established that the QSHOD model captures a major contribution to the dynamical behavior, due to unsteady heat transfer in the condensed phase. Thus it is important to understand the preceding analysis. However, even with the large experimental errors associated with all current experimental methods, it seems there is little doubt that other dynamical processes cannot be ignored for many propellants, especially in the range of frequencies above that where the broad peak of the real part of R_p appears.

An important reason for retaining pressure dependence in the pyrolysis law for the transformation solid→gas (cf. equation 2.30) is that $R_p \neq 0$ if $n_s \neq 0$ even though $n = 0$, so the steady burning rate is independent of pressure. The experimentally observed presence of pressure coupling for 'mesa' propellants has long been an ill-explained feature of unsteady surface combustion still not well understood. More generally, n should be taken as a function of pressure, a behavior reported in several of the references cited but not covered here. See especially reports by the group at NWC (later NWAC).

A second deficiency of the QSHOD model of surface combustion response is that it contains no dependence of the mean burning rate on oscillatory pressure. This effect had been reported already in some of the earliest works on oscillations in solid rockets (for some measurements see Crump and Price 1961 and Eisel 1964). Figure 2.15 shows two examples. The observed changes of mean burning rate and mean pressure with oscillatory conditions in a chamber is indeed a complicated and by no means well-understood matter. In a motor, the oscillatory pressures and velocity ('velocity coupling') may both affect the mean burning rate and pressure in ways which are quite likely to depend on the distributions of those quantities along the burning surface. Consequently, the internal configuration of the propellant grain may be a significant factor. Thus it is evident that a single response function defined for oscillatory pressures is only part of the story.

2.2.3. Measurements of the Response Function; Comparison of Experimental Results and the QSHOD Model. For more than forty years, measurement of the response function has been the most important basic task in research on combustion instabilities in solid rockets. That problem still exists. Without accurate data, the truth of theoretical results cannot be assessed; predictions and interpretations of instabilities in motors are uncertain; and the ability to screen propellants for optional behavior is seriously compromised. Unfortunately, no entirely satisfactory method exists for accurate measurements of the combustion response over practical range of operating conditions, irrespective of cost. Two recent final reports of extended programs (Culick (editor), 2002, Caltech MURI; and Krier and Hafenrichter (editors), 2002, UIUC MURI) have led to this conclusion after five years' investigation of the five main existing methods:

(i) T-burner
(ii) ultrasonic apparatus
(iii) laser recoil method
(iv) magnetohydrodynamic method
(v) microwave technique

A sixth method based on using a burner (e.g., an L* burner) in which bulk oscillations are excited, was not investigated, partly because it is intrinsically limited to relatively low frequencies.

It is not our purpose here to review these methods; see the two MURI reports, Cauty (1999), and references contained in those works for discussions of all but the last method. The microwave technique was introduced in the 1970s (Strand *et al.* 1974, 1980) and has been continually improved, but the accuracy of the data remains inadequate, particularly for metallized propellants for which the method is useless under some conditions. The last work with the device was done in the late 1990s by a group in Russia and reported by Zarko (1998).

(a) *Examples of Early Data.* The ultimate question for modeling and theory is: how good is the agreement between predicted and measured values? It appears that the first extensive comparison for this purpose were carried out many years ago (Beckstead and Culick, 1971) soon after the recognition that all the available models/analyses were equivalent to the QSHOD (A,B) model. With only two parameters available to adjust the theoretical results to fit data, the task of comparing theory and experiment became manageable. At that time, only T-burner and limited L^*-burner data were available. Figures 2.16 and 2.17 show two results.

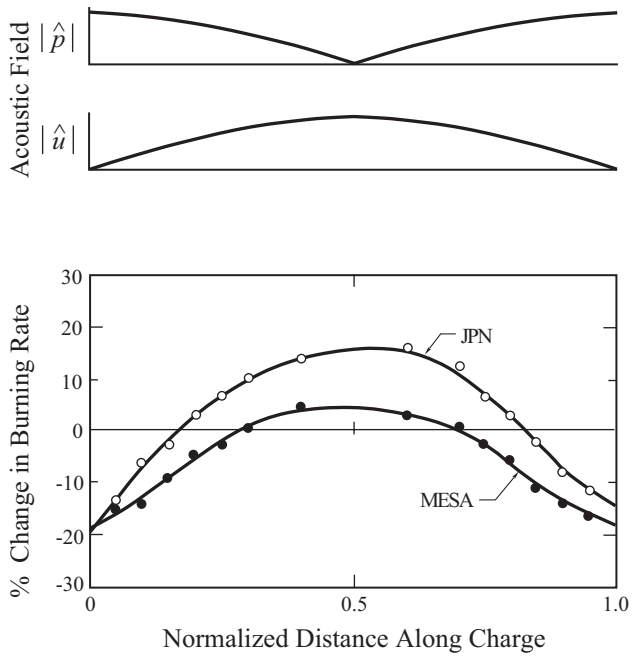

FIGURE 2.15. Experimental results for the change of burning rate of two double-base propellants (Crump and Price 1961).

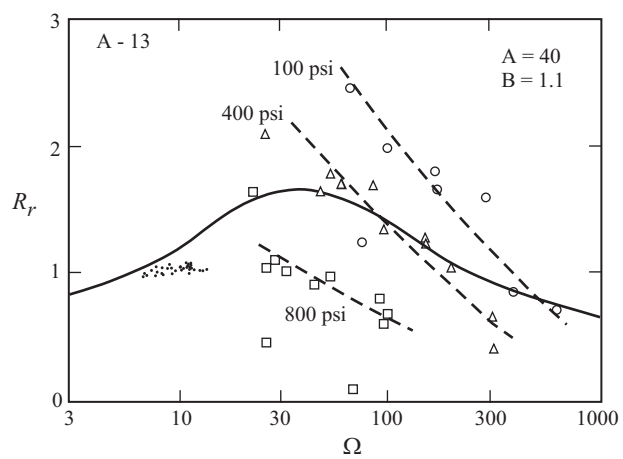

FIGURE 2.16. The real part of the response function vs. the non-dimensional frequency, $\alpha_t\omega/r^2$ for A-13 propellant: the solid curve is calculated from the QSHOD formula for the values of A and B shown; the dashed curves represent the T-burner data at the indicated pressures (Beckstead and Culick 1971).

One purpose of the report by Beckstead and Culick was to combine the formula for the QSHOD response function with results obtained from analyses of the T-burner and the L*-burner to obtain formulas for the parameters A and B in terms of measurable quantities. The main conclusion was that unique values of A and B could not be obtained for a given propellant tested at a chosen value of operating pressure. Consequently, large differences existed between the data and curves of the sort shown in Figure 2.16 and 2.17.

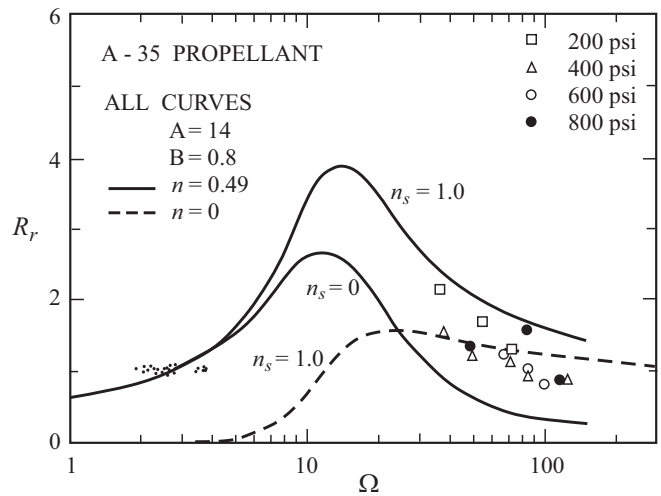

FIGURE 2.17. The real part of the response function vs. the non-dimensional frequency for A-35 propellant; the curves were calculated from the QSHOD formula (Beckstead and Culick 1971).

Since that time, many examples of using the A, B model to fit data have been given. Most, if not all, approach the matter as a two-parameter (A and B) curve fitted to data for the real part of the response function only. Strictly, that tactic is incorrect and could produce misleading results. The proper approach requires that the two-parameter representation be used to fit *simultaneously* the real and imaginary parts of the response function. There are also cases in which investigators have failed to respect the distinction between the response function $R_p \sim m'/p'$ and the admittance function $A_p \sim u'/p'$ defined for velocity fluctuations. That error arises due to failure to recognize which quantity a particular method actually measures. For example, T-burners give R_p directly, but the magnetohydrodynamic method provides data for A_p because it measures the unsteady velocity of the combustion products near the burning surface.

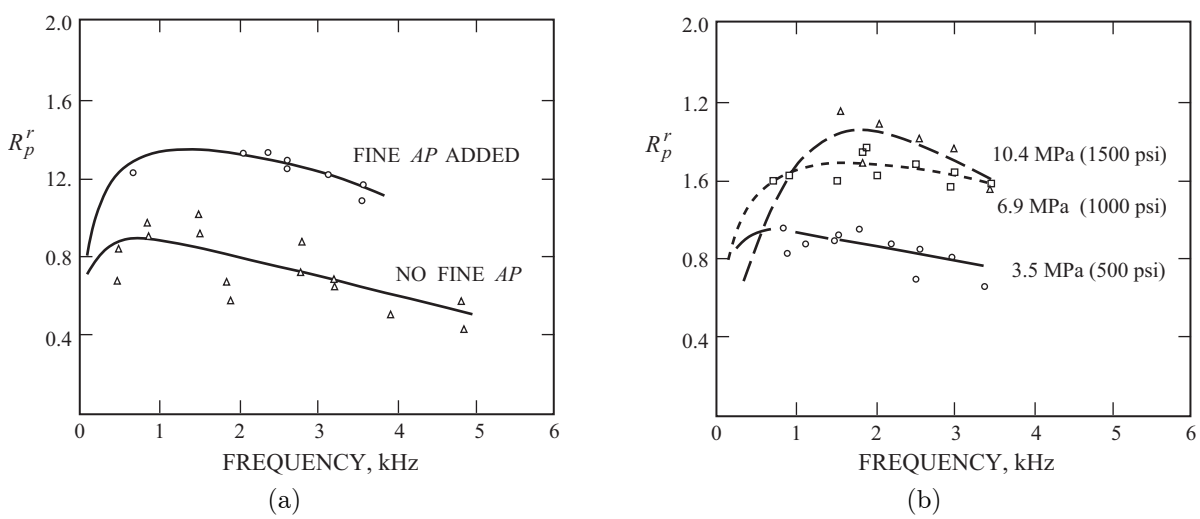

FIGURE 2.18. Real part of the response function measured with T-burners (Price 1984).

The apparent reduction of the real part of the response function when the mean pressure is reduced, more clearly shown by the latter data plotted in Figure 2.16, seems to be a common trend. Fifteen years later,

Price (1984) reported similar results plotted in Figure 2.18. Although the pressure dependence of the surface reaction ($n_s \neq 0$) does seem to explain some of the trend, there still is no incontrovertible explanation. It's just one of many incomplete topics on the subject.

Without attention paid to those points, any comparisons between data and a model are suspect. Even accounting for those common deficiencies, there is no doubt that the QSHOD model cannot and does not accurately represent the dynamics of actual propellants. One would anticipate without experimental results that the assumption of quasi-steady behavior in the gas phase must fail at high frequencies, commonly believed to be around 1000 Hertz and higher. Moreover, observations of steady combustion have shown that important decomposition processes take place in the sub-surface zone near the interface of most propellants. Hence at least two improvements of the QSHOD model should be made.

(b) *Some Results from the MURI Program.* During the past 40–45 years an immense amount of data has been collected for the combustion dynamics of solid propellants. Some are accessible; much is not. It is inappropriate here to try to give a thorough survey; it seems best in this limited space to quote a few results from the most recent publications, covering work carried out in the period 1996–2001 in the Caltech and UIUC MURI programs cited above. The research spanned the broadest possible range of activities from basic propellant chemistry and synthesis to motor dynamics. Work in the research groups included a complete range of experimental methods; modeling; theory and analysis; and numerical simulations, all for both steady and unsteady combustion of propellants.

Three classes of propellants were tested, to determine their burning rate laws and their dynamical behavior. Table 2.2 summarizes the main characteristics distinguishing the propellants in the three groups referred to as Phase I, Phase II and Phase III. Further details and the chief motivations for selecting those propellants are included in Attachment A of the Caltech MURI Final Report. All propellants were provided to all research groups measuring response functions.

TABLE 2.2. Principal Characteristics of the MURI Propellants.

	Manufacturer	**Oxidizers**	**Binders**	**Remarks**
PHASE I	Thiokol, Inc.	AP	HTPB	• plateau and biplateau propellants • 11 formulations including reduced smoke and smokeless
PHASE IIA	Thiokol, Inc.	AP	BAMMO/AMMO with GAP	• two formulations reduced smoke and smokeless
PHASE IIB	CSD, Inc.	AP/HMX	HTPB/GAP	• five aluminized formulations, one with some AP replaced by HMX and one with GAP replacing HTPB • AP size distributions varied
PHASE III	Alliant Techsystems, Inc.	AP	Nitrato-type energetic binders	• seven formulations including four aluminized and three smokeless

2.2.4. The Zel'dovich-Novozhilov (Z-N) Model. Zel'dovich (1942) was first to consider true combustion dynamics for solid propellants. He was concerned with problems of transient burning—i.e. what happens to combustion of a propellant when the impressed pressure is changed rapidly—but not explicitly with the response function. Novozhilov (1965) later used Zel'dovich's basic ideas to find a formula for the response of a burning propellant to sinusoidal oscillations of pressure. The result has exactly the same dependence on frequency as the QSHOD model, i.e. it is identical with the formula obtained by Denison and Baum (1961) four years earlier.

The basic Z-N model incorporates quasi-steady behavior of the burning in a clever and instructive fashion. Moreover, the parameters—there are, of course, two corresponding to A and B in the QSHOD model—are so defined as to be assigned values from measurements of steady combustion of the propellant in question. Hence there is no need to become enmeshed in the details of modeling the combustion processes in the gas phase. If the measurements could be done accurately, it would be possible to obtain good predictions of the combustion response for propellants, subject of course to all the assumptions built into the QSHOD model. Unfortunately, the required quantities are difficult to measure accurately. Confirmation of the results still requires measurements of both the real and imaginary parts of the response function and comparison with the predictions of the model.

The condensed phase and interfacial region are treated as described in Section 2.2 for the QSHOD model. Instead of detailed analysis of the gas phase, that is, construction of a "flame model", the assumption of quasi-steady behavior is applied by using relations among the properties of steady combustion, the burning rate and the surface temperature as functions of the initial temperature of the cold propellant and the operating pressure:

$$\begin{aligned} m &= m(T_c, p) \\ T_s &= T_s(T_c, p) \end{aligned} \qquad (2.68)\text{a,b}$$

The assumption is also made that these functions are known sufficiently accurately that their derivatives can also be formed, introducing the four parameters

$$\begin{aligned} \nu &= \left(\frac{\partial \ln \overline{m}}{\partial \ln \overline{p}}\right)_{T_c} \\ \mu &= \frac{1}{\overline{T}_s - T_c}\left(\frac{\partial \overline{T}_s}{\partial \ln \overline{p}}\right)_{T_c} \\ k &= (\overline{T}_s - T_c)\left(\frac{\partial \ln \overline{m}}{\partial T_c}\right)_{\overline{p}} \\ r_{ZN} &= \left(\frac{\partial \overline{T}_s}{\partial T_c}\right)_{\overline{p}} \end{aligned} \qquad (2.69)\text{a,b,c,d}$$

Subscript ZN is attached to r to distinguish it from the linear burning rate. It is not apparent from the remarks here why the four parameters (2.69)a–d are significant in this theory; see the works of Novozhilov (1965 and later).

Recall that in Section 2.2 the sole reason for analyzing a model of combustion in the gas phase was to produce a formula for the heat feedback, $\lambda_g(\partial T/\partial x)_{s+}$, to the interface. That is the central problem here as well: to find the heat feedback from considerations of steady combustion and assume (the quasi-steady approximation) that the form of the result holds under unsteady conditions. The trick is to work out the relation between the feedback and the properties of steady combustion. It is in that process that the parameters (2.69)a–d appear.

The formula for the response function corresponding to (2.67) is usually written (e.g., Cozzi, DeLuca and Novozhilov 1999)

$$R_p = \frac{\nu + \delta(\lambda - 1)}{r_{ZN}(\lambda - 1) + k\left(\frac{1}{\lambda} - 1\right) + 1} \tag{2.70}$$

where

$$\delta = \nu r_{ZN} - \mu k \tag{2.71}$$

Comparison of (2.67) and (2.70) gives the formulas connecting the parameters in the two formulations:

$$A = \frac{k}{r_{ZN}}\ , \quad B = \frac{1}{k}\ , \quad n = \nu\ , \quad n_s = \frac{\delta}{r_{ZN}} \tag{2.72}$$

Much emphasis has been placed in the Russian literature on the "boundary of intrinsic stability," the locus of values of (A,B), or (k, r_{ZN}) for which the denominator of (2.70) vanishes[16]. Under those conditions, the propellant burn rate suffers a finite perturbation in the limit of a vanishingly small change of pressure. Hence, from measured values of ν and r_{ZN}, one can infer how close an actual propellant is to that stability boundary.

With these models, the opportunity exists to use experimental results to determine how accurately the QSHOD approximations capture the combustion dynamics of solid propellants:

(i) infer ν, μ, k, r_{ZN} from tests of steady combustion;
(ii) measure the real and imaginary parts of R_p;
(iii) compute R_p from (2.67) or (2.70) and compare with (ii)

There seem to be no published reports of results for this procedure, although some results exist for predictions related to the boundary of intrinsic stability.

Novozhilov and his co-workers have investigated many other detailed aspects of the combustion dynamics. However, experimental data to confirm the theoretical results either don't exist or are too sparse to allow definite conclusions. Hence despite the value of those results, we will not discuss them here.

2.2.5. Revisions and Extensions of the QSHOD Model. As we have already noted in Section 2.2.3, even with the large uncertainties accompanying the experimental results obtained with current methods, it is clear that the QSHOD model does not capture some important dynamical processes. Considerable effort has been devoted to improving the model, with a certain amount of success, but unfortunately the deficiencies in the experimental procedures still prevent definitive identification of the most significant contributions. Thus there is only weak justification for developing three-dimensional models of the processes for practical purposes. It seems that much is still to be gained by investigating extensions of the QSHOD model.

Attention has been given to all three of the regions sketched in Figure 2.12. It is important to recognize that simply changing the model for steady combustion—for example including a finite zone of decomposition in the solid phase—will *not* change the form of the QSHOD result. To affect the frequency dependence of the response function, any additional spatial zones or processes must also contain new dynamics (see, for example, Culick 1969). One cause of 'new dynamics' is spatial non-uniformity of material properties when conductive heat transfer is the dominant unsteady process. Here we attend mainly to contributions from different processes which conceivably change the dynamics.

[16]This condition is analogous to the way in which instabilities are defined for a classical control system by finding the poles of the appropriate transfer function

(a) *Additional Dynamics in the Condensed Phase.* It seems that three types of processes have been considered as modifications of the basic model of the condensed phase discussed in Section 2.2.2:

(i) temperature-dependent thermal properties;
(ii) phase transitions; and
(iii) decomposition zones.

Louwers and Gadiot (1999) have reported results for numerical calculations based on a model of HNF. Melting at some interface within the condensed phase is accounted for, as well as energy released by subsurface reactions. Combustion in the gas phase is also treated numerically. The computed response functions show that the new processes may increase the values of $R_p^{(r)}$ by as much as 10–30% and more in the frequency range above the peak. The peak value is unchanged.

Brewster and his students at the University of Illinois have produced a number of interesting works treating additional dynamics related to chemical processes in the condensed phase and at the interface (Zebrowski and Brewster, 1996; Brewster and Son, 1995). Much attention was given to this matter in the MURI Programs (Culick 2002, Krier and Hafenrichter 2002). Gusachenko, Zarko and Rychkov (1999) have investigated the effects of melting in the response function, finding quite significant consequences. Lower melting temperatures and larger energy absorption in the melt layer increase the magnitude of the response function.

Cozzi, DeLuca and Novozhilov (1999) worked out an extension of the Z-N method to account for phase transition at an infinitesimally thin interface in the condensed phase. The analysis includes new dynamics by allowing different properties of the thermal waves on the two sides of the interface. Additional heat release is allowed only at the interface of the transition and with conversion of condensed material to gaseous products. They found that the response function is increased by exothermic reaction at the internal interface and by reduced temperature of the phase transition.

(b) *Additional Dynamics in the Gas Phase.* DeLuca (1990; 1992) has given thorough reviews of the various models proposed for the gas phase. Most, however, involve no dynamics, so there are no effects on the dependence of the response function on frequency. An example of truly dynamical effects is covered in the next section, with references to previous works.

2.2.6. Some Results for a Special Extension of the QSHOD Model. The results summarized in this and the following section have been reported in a Ph.D. Thesis (Isella, 2001) and in four publications (Culick, Isella and Seywert, 1998; Isella and Culick, 2000a; 2000b; 2002). A purpose of the works was to address in a small way some of the questions raised in our discussion of prior results. Chiefly two general problems have been addressed in those works:

(1) develop a simple general analysis of the combustion dynamics of a solid propellant that will conveniently accommodate models of the relevant chemical and physical processes, especially those in the interfacial region; and

(2) investigate the influences of small changes in the combustion response function on observable features of the combustor dynamics, particularly properties of limit cycles.

Both of those problems were chosen to determine answers to the question: what properties of a solid propellant are responsible for the often observed sensitivity of the dynamics of a solid rocket to apparently small (sometimes not well-known) changes in the composition of the propellant. The main conclusions are:

(i) small changes in the composition and thermodynamic properties of a propellant have significant consequences for dynamical behavior due to pressure coupling **only** if the propellant is burning near its intrinsic instability boundary; and

(ii) on the contrary, the dynamics due to velocity coupling may be much more sensitive to small compositional changes.

We do not compare with experimental results, and some of the behavior found may be unrealistic. Our purpose is partly to demonstrate by some examples the sort of behavior one can obtain by altering the basic QSHOD model. It seems that this strategy is an effective means of exploring possibilities in a quantitative fashion. The very important task of establishing which processes are important (and under what condition) has for the most part not been accomplished.

If the conclusions are true, then future work in the area of combustion instabilities must include intensive attention to modeling and measuring the combustion dynamics—i.e. the response function—associated with velocity coupling. In any case, there are several reasons arising with observed behavior of combustion instabilities in solid rockets that velocity coupling should receive more attention than planned.

(a) *The Model Framework.* One important purpose of the work cited above was to construct a framework within which it would be possible easily to investigate the consequences of various processes participating in the combustion of a solid. Representation of the combustion dynamics must be in a form required for analyzing the global dynamics (Section 3.3). The simplest approach is an extension of the well-known one-dimensional analysis producing the QSHOD response function for pressure coupling (Culick 1968; Beckstead *et al.* 1969; T'ien 1972; among many works). Others have followed a similar tack (e.g., Louwers and Gadiot 1999). The main novel aspects of the work described here are inclusion simultaneously of surface physical dynamics (e.g., due to mobility of liquid or solid particles); dynamics, rather than quasi-steady behavior, of the gas phase; and an elementary representation of velocity coupling. The behavior we find (calculate) may not be realistic in all cases. Our main purpose is to show one way in which the QSHOD model can be used is the initial approximation in a procedure to examine possible consequences of departures from the simplest model.

On the submillimeter scale, a burning solid is heterogeneous both in the region adjacent to the interface and in the gas phase where much of the conversion to products takes place. The flow field in the chamber, in particular the unsteady acoustic field, has spatial variations normally of the order of centimeters and larger. The dynamics of the combustion processes at the surface are formally accommodated as a boundary condition, a response function of some sort, in the analytical framework for the global dynamics. Hence the vast difference in characteristic scales is accommodated, in principle, by spatially averaging the combustion dynamics. The averaging is done over a surface in some sense far from the interface so far as the propellant combustion is concerned, but practically at the interface so far as the field within the chamber is concerned. In that way, the results of solution to the "inner" problem of combustion dynamics in the surface region are used as the boundary conditions for solution to the "outer" problem of the unsteady flow field in the chamber.

We are not concerned here with the matter of spatial averaging: We assume it can be done, although it may not necessarily be an easy or obvious process. It's an important part of the general problem. Therefore we proceed from the beginning with a one-dimensional analysis. The spatial framework for the model is shown in Figure 2.19.

The strategy of the analysis is not novel and has been used in many previous works: Solve the relevant equations, or postulate a model, governing the behavior in each of the three regions: solid phase; surface layer; and gas phase, including the region called 'combustion zone' in Figure 2.19. A major purpose of the analysis has been to determine the quantitative effects of the dynamics in the surface layer and gas phase

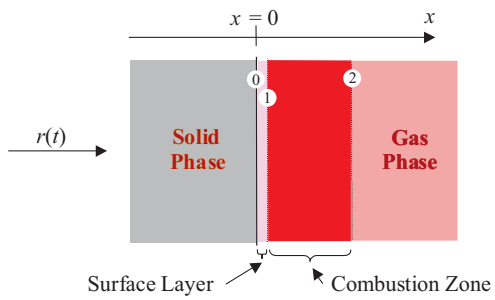

FIGURE 2.19. Spatial definition of the model.

on the response function found from the QSHOD model. Hence throughout the work we assume the same model for the solid phase: The basic dynamics is due to unsteady heat transfer in a homogeneous material having uniform and constant properties.

Separate solutions or representations are obtained for each of the three regions. Unspecified constants or functions are then eliminated by satisfying boundary conditions and applying matching conditions at the two interfaces. Initially the authors intended to find such a form for the general behavior that different models for the surface layer and gas phase could easily be substituted and their consequences assessed. That goal has not been realized and probably is unattainable in a simple form. Results require detailed numerical calculations before interesting information is obtained.

(b) *Models of the Surface Layer.* An important motivation this work was the idea that because the dynamics of the gas phase are fast (owing to the relatively low material density), then the dynamics of the surface region should have greater effect on the combustion response function in the range of lower frequencies covering the resonances of many practical rockets. Two models of the region have been examined in the analysis:

(i) first order dynamics represented by a constant time lag; and
(ii) unsteady heat transfer, with material properties different from those in the solid phase.

The idea of using a time lag is of course an old one, having been used by Grad (1949) in the first analysis of combustion instabilities in solid propellant rockets, and later by Cheng (1954)a,b as part of the Princeton group's extensive investigations (a sort of technical love affair) of time lag representations of unsteady combustion. The result (Isella 2001) for the fluctuation of mass flux is

$$\frac{m'/\overline{m}}{p'/\overline{p}} = R_p \frac{e^{-i\Omega t}}{\sqrt{1+(\Omega t)^2}} \tag{2.73}$$

where R_p is the response function found in the QSHOD theory. Thus R_p has the familiar two-parameter (A,B) representation. The dimensionless frequency is Ω, eq. (2.26) τ is the dimensionless time lag, equal to the physical time lag divided by $\kappa_p/\overline{r}^2$. Figure 2.20 shows a typical result (A = 14; B = 0.85; τ = 1.5). The graphs illustrate clearly a basic problem with a time lag theory: if the time lag is assumed constant (i.e. independent of frequency) the response (in this case the real part) possesses an oscillatory behavior with period increasing with frequency. Such behavior has never been observed in experimental results and is a consequence of an incorrect assumption, namely that the time lag is constant.

It is true that any response function for linear behavior can be written in a form showing a time lag, but in general the time lag varies with frequency (Culick, 1968). If the physical model is sufficiently detailed,

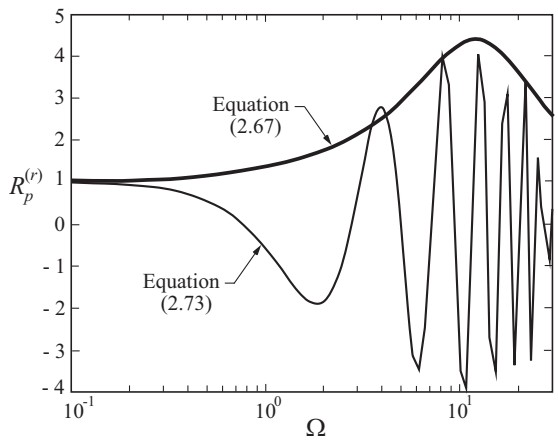

FIGURE 2.20. QSHOD response function with a time lag: thick line: QSHOD theory with $n_s = 0, A = 14,\ B = 0.85$; thin line: QSHOD model including a surface layer having first order (time lag) dynamics.

the dependence of τ on frequency is found as part of the solution. In particular, the QSHOD theory gives $\tau(\Omega)$ such that the amplitude of the response function decays smoothly for frequencies higher than that at which the single peak occurs.

The second model for the surface is the only one considered for the results discussed here. It is based on a simple representation of the dynamical behavior making use of the same solution as that for the homogeneous solid phase, with two differences:

(i) the uniform and constant properties are different from those of the condensed solid material;

(ii) the solution is forced to satisfy matching conditions of continuous temperature and heat transfer at the interfaces with the condensed phase and the gas phase.

(c) *Models of the Gas Phase.* In the following analysis, all combustion processes are assumed to occur in the gas phase; upstream, only phase changes are accounted for, assumed to take place at the interfaces. We assume distributed combustion of a simplified form, a single one-step reaction as previous treatments have used (T'ien, 1972; Huang and Micci, 1990; Lazmi and Clavin, 1992). Solutions must then be found numerically for the steady and linear unsteady temperature distributions, and subsequently matched to the solution for the surface layer. For details, consult Isella (2001) and other references cited there and at the beginning of this section.

2.2.7. Some Results for the Combustion Response Function. Many experimental results exist suggesting that the responses of actual propellants tend often to be higher than that predicted by the QSHOD model for some ranges of high frequencies; and possibly the existence of peaks in addition to that associated with unsteady heat transfer in the condensed phase. Initially the strongest motivation for much work on the response function has been the need to determine in simple and relatively crude fashion what processes might have greatest effect on the values of the pressure-coupled response at frequencies greater than that at which the peak magnitude occurs. Roughly what that means is finding one or more processes having 'resonant behavior' or characteristic times in the appropriate range. Unfortunately the analysis is sufficiently complicated that it has not been possible yet to deduce any explicit 'rules of thumb.' Therefore, we present here a few plots of computed results to illustrate the behavior. What we find may not be realistic.

A purpose here is to illustrate what one may learn with a simple procedure. The basic or reference response function computed from the simple QSHOD model is that shown in Figure 2.14. Influences of dynamics in the surface layer and gas phase will be shown relative to that reference. Because of the immediate availability of the results we extract details from the thesis prepared by Isella (2001). We will not compare the results with observed behavior. The purpose here is only to show possible indications of deviations from the basic QSHOD model, due to several well-defined processes.

(a) *Influence of Gas Phase Dynamics.* Figure 2.21 is the result when only the dynamics in the gas phase is added to the QSHOD model. The results are similar to those found by T'ien (1972) and Lazmi and Clavin (1992), not a surprising conclusion. As expected, the dynamics of the gas phase introduce a single additional peak in the real part of the response function ($\sim m'/p'$). Due to the density fluctuation $\rho'(m'/\bar{m} = \rho'/\bar{p} + v'/\bar{v})$, the real part of the admittance function ($\sim v'/\bar{v}$) shows a negative depression where the real part of the response function R_p has a rise.

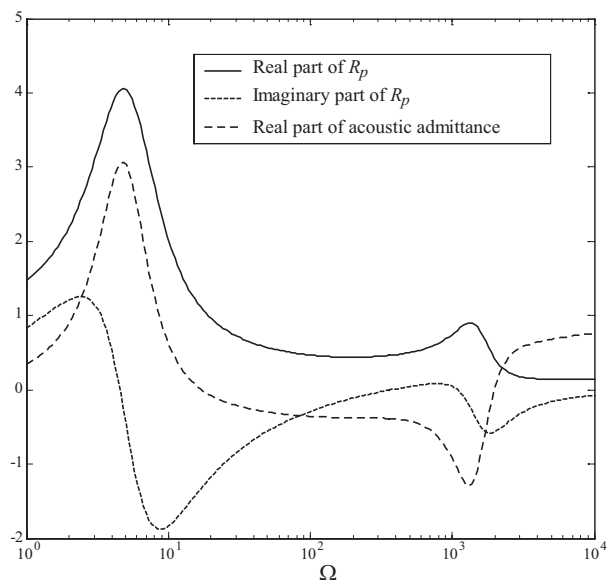

FIGURE 2.21. Combustion response, QSHOD model with gas phase dynamics (Isella 2001; Isella and Culick 2000).

(b) *Combined Influences of the Dynamics of the Surface Layer and the Gas Phase.* The dynamics of the surface layer itself are the same as those of the condensed phase, but with different values of the defining parameters. Figure 2.22 illustrates the effects of changing the surface activation energy and the material density on a function characterizing the response of heat transfer in the layer. The shape of this function differs from that (Figure 2.14) of the basic response function because it is affected by the dependence of several flow variables on frequency.

Finally, Figure 2.23 shows the result for one example of the response function with the dynamics of both the surface layer and the gas phase accounted for. Evidently for the conditions examined here the dynamics of the gas phase has a greater effect on the response, in the higher frequency range, than does the surface layer.

2.2.8. The Combustion Response and Possible Sensitivity of Global Dynamics to Velocity Coupling. A fundamental problem for practical applications concerns connections between the unsteady motions taking place in a motor and the features of the combustion processes responsible for that behavior.

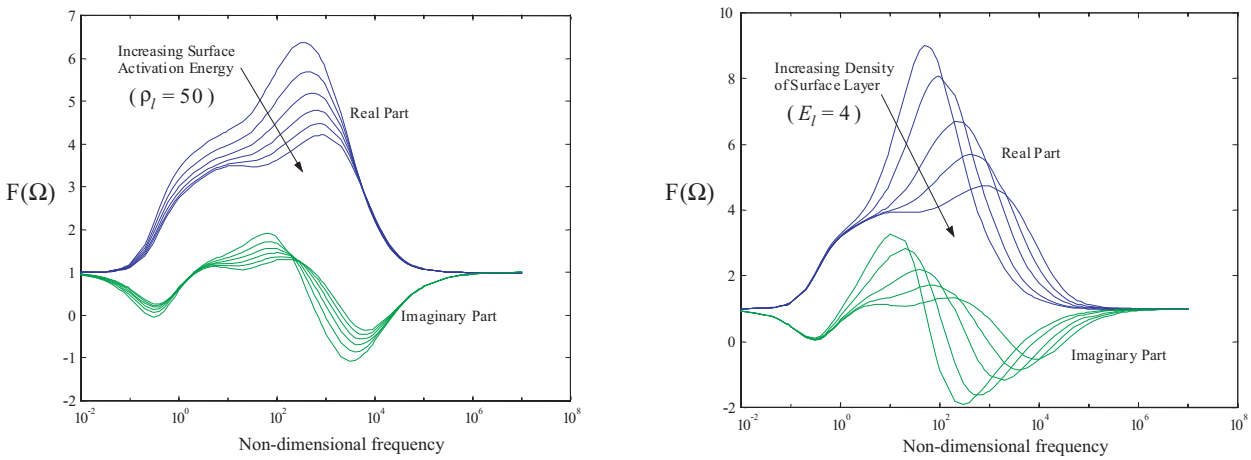

FIGURE 2.22. Effects of activation energy and density on the dynamics of the surface layer (Isella 2001; Isella and Culick 2000).

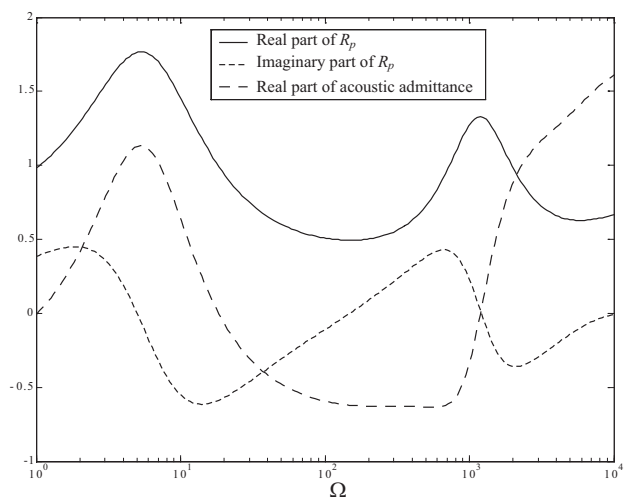

FIGURE 2.23. Combustion response function including the dynamics of the surface layer and the gas phase (Isella 2001; Isella and Culick 2000).

This is far from a solved problem, but we are able to make some tentative observations in respect to both linear and nonlinear characteristics that have already been observed or might be expected.

We will often use the term *global dynamics* to mean the dynamical behavior of the system in question, a combustion chamber, its source of energy and, in some cases, peripheral equipment. Thus we intend the term to have a general meaning, but generally we really mean global dynamics as indicated by the evolution of the unsteady pressure. Recall that the pressure is the one variable we always have available, and it is often the only variable measured. In this section we are examining only computed results interpreted as far as possible in respect to physical behavior. Hence we have at our disposal not only the amplitude of the entire motion, but the amplitude of harmonics as well.[17]

[17]The phases of the motion are also available but we will not consider them here.

In certain respects, the behavior discussed in this section is well beyond the preparation provided so far. We will be examining, without clarifying the basis, certain consequences of the dependence of nonlinear behavior on linear behavior. The main indicator is the amplitude of the limit cycle, or the amplitudes of the modal components of limit cycles. It happens, as we will see in Chapter 7, that the nonlinear gasdynamics do not introduce physical parameters other than the properties of the gas. Thus when the linear parameters—the growth rate and phase for each mode—are changed, those changes are reflected directly in the limit cycle. In other words, the amplitudes in the limit cycle serve as a diagnostic revealing the consequences of changes in the linear processes. Put another way, we evidently have a means of investigating the consequences for the global dynamics of modifying the linear behevior of the system

The idea of somehow connecting linear and nonlinear behavior is of course not new, and is widely applied in other fields. For example, without having a nonlinear theory as a basis for quantitative reasoning, early discussions by Price, McClure and others used observations as the basis for discussing the subjects treated here. We will not review experimental results. Levine and Culick (1972, 1974) appealed to both numerical calculations and an early form of the analysis developed here in Chapters 3 and 4 to investigate some properties of limit cycles with modest success. The approach was greatly extended by Levine and Baum (1984, 1985) who produced substantial results. They obtained the first quantitative theoretical results for subcritical bifurcations (pulsed instabilities) in solid propellant rockets. To obtain those results they needed a nonlinear response function, explained in Section 7.11. Burnley (1996) and Burnley and Culick (1997) confirmed a conclusion reached by Levine and Baum (1983) that a requirement for the subcritical bifurcation seemed to be that the response should contain both velocity coupling and a threshold velocity (Section 7.11). The question of what behavior of the response function is necessary remains open. Experimental results support the results qualitatively, but there seems to be little possibility at the present time of making firm quantitative connections with theory.

Currently an unsolved problem is the occasionally observed apparent sensitivity of the global behavior to relatively small changes of propellant composition (see remarks (i) and (ii) in the introductory part of Section 2.2.6). We assume that small changes of composition likely have relatively small effects on the magnitude and phase of the response function. Therefore, we are really investigating the effects of small changes in the response function on the observable global dynamics. The main (but tentative) conclusion is that the sensitivity of the dynamics to changes in the response associated with velocity coupling may be significantly greater than that for the response due to pressure coupling. The implications for directions in future research are substantial.

Isella (2001) and Isella and Culick (2000) have reported the main results. Here we will only cite a couple of examples. The idea is to use the framework described in Section 3.2 below to compute the growth and limiting amplitudes for limit cycles. Essentially a modest parameter study has been done, the response function itself (i.e. the combustion dynamics) being the parameter. Following the presentation first introduced by Culick, Isella and Seywert (1998), it is helpful to display the response function as a function of frequency, and the amplitudes of the modes forming a limit cycle, as two parts of the same figure, such as Figure 2.24 prepared as a typical case for the QSHOD response function. The vertical lines in the upper parts of the figures identify the non-dimensional frequencies. For these calculations the model chamber is cylindrical, 0.6 m long, 0.025 m in diameter, operated at a chamber mean pressure equal to 1.06×10^7 Pa. It is the same motor considered previously by Culick and Yang (1992).

Figures 2.24–2.27 show results obtained for the same motor and basic combustion response but including, respectively, surface layer dynamics; a time delay; and dynamics of both a surface layer and gas phase, all according to the analysis described above.

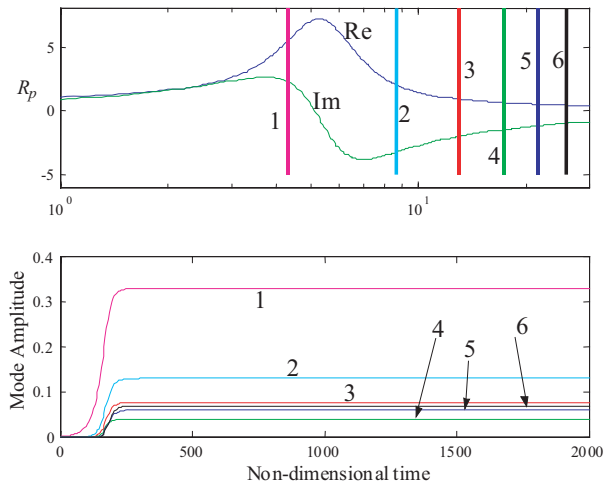

FIGURE 2.24. Results of a simulation with a QSHOD combustion response (pressure coupling: A= 8.0, B = 0.6, n = 0.8) (Isella 2001).

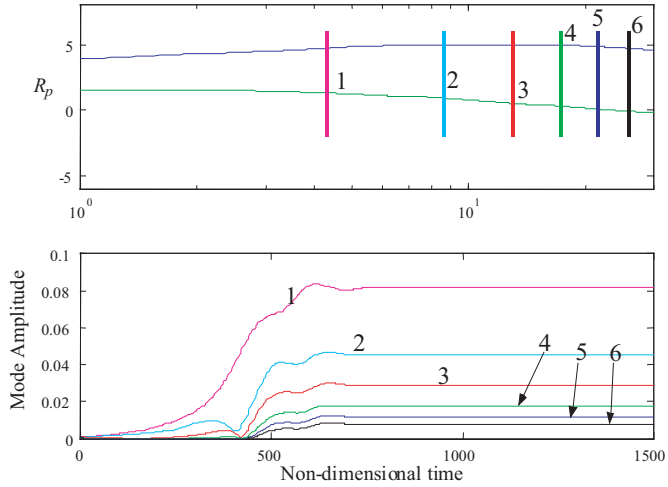

FIGURE 2.25. Results of a simulation including dynamics of a surface layer (Isella 2001).

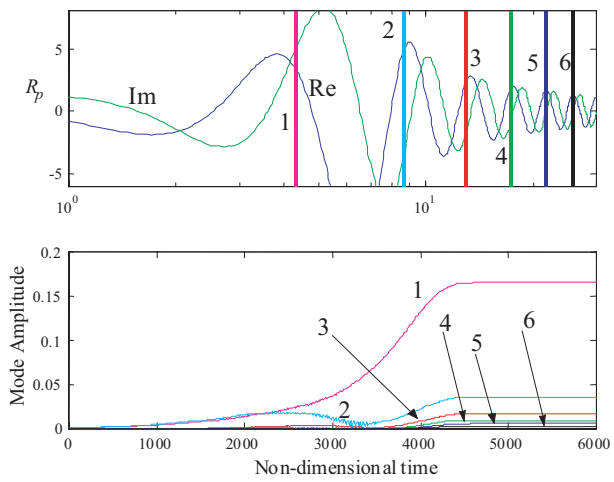

FIGURE 2.26. Results of a simulation including a time delay (τ = 1.5) (Isella 2001).

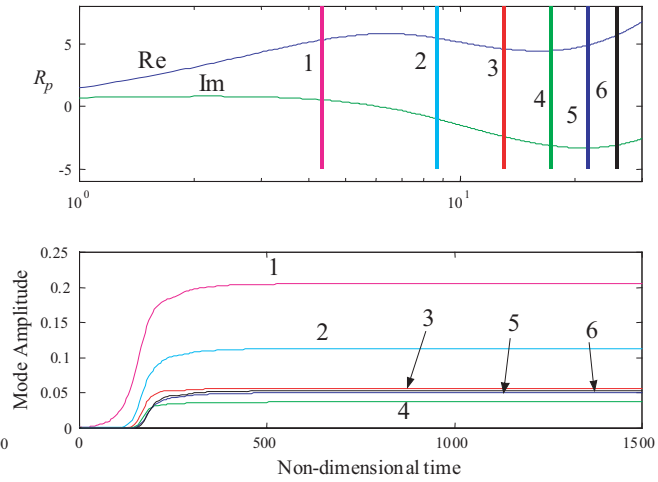

FIGURE 2.27. Results of a simulation including dynamics of a surface layer and the gas phase (Isella 2001).

Owing to the significantly different dynamics added to the basic QSHOD model, the three examples illustrated in Figures 2.26–2.27 show quite different response functions—all, it must be emphasized, representing responses due to pressure coupling. The question here concerns indirectly the sensitivity of the response function to changes of composition (not the qualitative dynamics) and consequently the sensitivity of the global chamber dynamics.

In general, models based on pressure coupling do not seem to show dramatic sensitivity of the combustor dynamics to small changes of composition. That result motivates investigation of similar problems with a simple model of the response due to velocity coupling. The idea is based on the model introduced by Levine and Baum (1988). This work is discussed at greater length in Section 7.11.1.

Some recent work done on the dependence of the global dynamics on the functional form of the equations used in the analysis by Ananthkrishnan *et al.* (2002, 2004) seems to show that the absolute value of the velocity itself, as it appears in a simple model of velocity coupling, is sufficient to produce a subcritical bifurcation (pitchfork) followed by a fold (saddle-node bifurcation). Those ideas are developed further in Chapter 7; the point is that a subcritical bifurcation, followed by a fold or turning point, provides conditions under which pulsed or triggered nonlinear instabilities may exist. Although we have not yet firmly established the point, it seems that with the QSHOD basic model, the dynamics of a chamber seems to be much more sensitive to velocity changes than pressure changes. The conclusion is apparently related to the way in which the global dynamics depends on the unsteady velocity and the phases established among the components of the motion. That is not a startling result in view of the different forms of the combustion terms provided by velocity coupling, in contrast to pressure coupling, in the modal equations.

2.2.9. Generation of Vorticity and Vortex Shedding. There are two phenomena of rotational flow that have significant influences on the stability and behavior of unsteady motions in solid propellant rockets:

(1) generation of unsteady vorticity at burning surfaces; and

(2) coupling between acoustical motions and large vortices shed at obstacles or growing out of the region adjacent to the lateral burning surface.

Both of these phenomena have motivated much interesting work that has flourished particularly in the past 10–12 years. Significant effort has been expended, mainly in the U.S. and France, on theory, analysis, numerical simulations and experiments. The reasons for the strong interests are different for the two processes. Both affect stability, but unlike the generation of distributed vorticity, shedding of large vortices has been unambiguously identified as a mechanism in several large rockets, notably the Shuttle SRM, versions of the Titan motor, and the Ariane 5 booster motors. Accordingly, several large research programs have been devoted to understanding the connections between vortex shedding and acoustic field. Blomshield and Mathes (1993) have given the most thorough discussion of the problem existing in the Shuttle motors. Much information exists in internal reports of continuing observations of Shuttle motors in flight, but little has been done to determine how the oscillations might be reduced.

In contrast, the corresponding problem in the Ariane 5 has been the subject of a great deal of work in France. See Vuillot and Casalis (2002) and several other papers in the course "Internal Aerodynamics in Solid Rocket Propulsion" given at the von Karman Institute (2002). The reason for the intensive concern has been the necessity to install vibration dampers between the solid boosters and the main vehicle. As a result, the payload has been reduced by a significant amount, apparently as much as two hundred kilograms.

(a) *Generation of Vorticity.* The generation of vorticity at a burning surface is special to solid rockets. It occurs whenever there is a variation of pressure fluctuation, and hence a fluctuating velocity, in the direction tangential to a surface from which there is average mass flow normal to surface into the chamber. The vorticity is created because the velocity inward is perpendicular to the surface—the 'no-slip' boundary condition. Imposition of a tangential velocity fluctuation, due to the non-uniform pressure along the surface, on the average inward flow constitutes an inviscid mechanism of vorticity generation. Moreover, conservation of mass in the region close to the surface causes a periodic pumping action normal to the surface. Both the vorticity generation and the pumping exist at the expense of work done by the impressed acoustic field and therefore must involve exchange of energy with the acoustic field in the chamber. Sketches of the two processes are shown in Figure 2.28.

An oversimplified and incomplete interpretation of the phenomenon due to the no-slip boundary condition is that the incoming average flow normal to the surface gains some kinetic energy because it must acquire

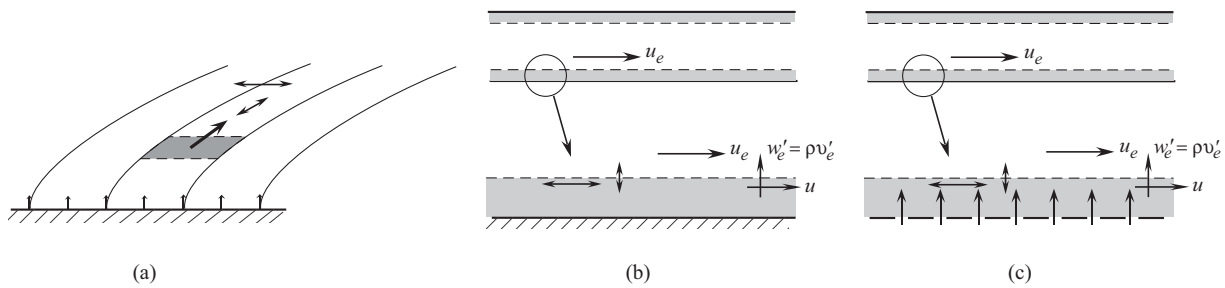

FIGURE 2.28. Sketches illustrating two primary processes involved in the generation of vorticity. (a) flow-turning; (b) 'pumping action': oscillatory motion parallel to the boundary, in the boundary layer, induces oscillatory motion normal to an impermeable wall; (c) similar to (b) with mean flow through the wall.

the oscillatory motion parallel to the surface. Thus there is effectively a "turning" of the flow in the direction of its passage out the nozzle. In a rocket chamber, for example a cylinder, both the average and unsteady velocities must become parallel to the axis of the chamber as the flow approaches the axis. The inelastic acceleration of the mass flow causes a loss that is the unsteady counterpart of the loss accompanying mass injection into a duct flow. This "flow-turning loss" was, not surprisingly, discovered in analysis of unsteady one-dimensional flow with mass injection at the lateral surface (Culick 1973). However, the connection with vorticity generation was not mentioned. It was Flandro (1995) who clarified the phenomenon in terms of the unsteady production of vorticity, emphasizing the central importance of the no-slip boundary condition. Flandro carried out the first rigorous formal analysis of the problem, work that has since prompted a stream of calculations on the basic problem at hand, as well as variations (among them are Majdalani, 1999; Kassoy, 1999; Majdalani, Flandro and Roh, 2000; Malhotra, 2004).

At least five processes must be considered to assess completely the net effect of distributed vorticity on the stability of acoustical motions in a combustion chamber:

(i) the generation process, Figure 2.28(a);
(ii) the 'pumping action', Figure 2.28(c);
(iii) interaction of the vorticity with the acoustic field in the chamber;
(iv) interaction of the vorticity with the exhaust nozzle; and
(v) interactions between the generated vorticity waves and turbulence in the chamber.

In practice, the matter of stability in the context of combustion instabilities always means stability of pressure oscillations. It is often helpful to interpret stability in terms of growth or decay of acoustic energy, but care must be exercised: Because the problem *in toto* is very complicated, even in the limit of linear behavior it is easy to obtain misleading, or incorrect, results. The presence of the mean flow and the various paths of energy transfer make intuitive construction of an equation for the time evolution of acoustic energy a delicate task. To ensure accurate theoretical results, the formalism developed here in Chapters 3–7 seems to offer the best method; see, for example, Flandro (1995) and Section 6.9.

The 'flow-turning' contribution identified in the simple one-dimensional approximation by Culick (1972, 1973) was later shown by Flandro (1995) to be, surprisingly, exactly correct. Interpretation of the process, a loss of energy for the acoustic field, in terms of generation of vorticity cannot be accomplished within the one-dimensional approximation. It was somewhat misleading that Culick vaguely related the flow-turning loss to viscous processes associated, at least partly, with flow in the acoustic boundary layer, a speculation that misses the mark. That proposition led to calculations of corrections to the classical theory of the acoustic boundary layer (Flandro 1974, Vuillot and Kuentzmann 1986) which have been superceded by the

more recent works by Flandro (1995)a,b; Majdalani and Van Moorhem (1997) and Majdalani (2000) treat essentially the same problem but contain some errors of understanding.

Unfortunately, the pumping action associated with the generation of vorticity was missed by Culick in his one-dimensional analysis.[18] Pumping in this context refers to a fluctuating velocity induced normal to the surface if the acoustic velocity tangential to the surface is not uniform, a direct consequence of continuity. This motion makes the surface appear as an effective oscillating piston tending, if the phase of the motion is suitable, to drive waves in the chamber. Flandro (1995) has shown that for a cylindrical chamber with uniform flow entering along the entire boundary, the net effect of the generation of vorticity and the pumping is zero for purely longitudinal acoustic modes. Whether or not this energy gain is accounted for is the origin of a controversy centered in the 'true' value of the flow turning, i.e. whether it is a loss, a gain, or has no net effect. At this point, the correct answer seems to be that there is no net effect for a cylindrical chamber, but the amount of loss or gain must be calculated separately for each geometry.

There is no question that the processes (i) and (ii) in the list given above are always present. Whatever may be the net effect on stability, due to these two contributions only, nevertheless waves of vorticity are generated at the surface and are carried by the average flow into the chamber. Subsequent interactions with the acoustic field in the chamber may cause energy transfer to or from the acoustic field—there seems to be presently no basis for giving a definite answer.

If the distributed vorticity survives passage to the nozzle, interactions with the non-uniform flow have no direct effect on the stability of acoustic waves. Any energy transferred between the vorticity waves and the mean flow has no consequences for the acoustic field. Thus, process (iv) will not contribute to stability. However, it is conceivable that those interactions may be accompanied by generation of pressure waves. The necessary analysis has not been carried out to determine whether the effect is stabilizing or de-stabilizing. Crocco and Sirignano (1964) have given the most thorough treatment of the influences of supercritical nozzles on stability including vorticity. No work has been done to clarify the case when the vorticity is that produced in flow turning. Culick (1961, 1963) had earlier reported a few results for the behavior of three-dimensional waves incident upon a choked exhaust nozzle, but he did not include vorticity.

On the other hand, the waves of vorticity must interact with the turbulence field necessarily present, process (v). It seems most likely that as a result the vorticity is destroyed. If the destruction occurs close to the burning surface, then the processes (iii) and (iv) become almost irrelevant to stability. We need account only for the processes of generation and pumping. At the present state of analysis and understanding, this seems to be the best resolution of the matter. Thus, for stability of longitudinal motions in a cylindrical chamber, the net effect of flow-turning is zero, as Flandro has reasoned. Contrary conclusions have been reached by others, partly supported by appeal to experimental results, which usually contain substantial uncertainties. The preceeding reasoning rests entirely on the equations of motion.

We discuss further the theoretical basis for the preceding remarks in Chapters 6 and 7. Our conclusion here is that generation of vorticity at a burning surface is a mechanism for combustion instabilities but its influence on attenuation or amplification is often small, much smaller, for example, than the damping due to a choked nozzle. Calculations must be done for the particular grain geometry in question—there is no simple generalization that can be formulated.

(b) *Shedding of Large Scale Vortices.* So far as practical consequences are concerned, the production of large vortices in motors has been far more significant than has the generation of vorticity discussed above. The latter is present in all solid rockets, and contributes always to linear stability, although the

[18] In the same paper, Culick treated the phenomenon of 'pumping' as an interpretation of the way in which an acoustic boundary layer on an impermeable surface attenuates waves. However, he overlooked the analogous process for a permeable surface. The calculations for the acoustic boundary layer are given here in Annex D. See Section 6.9 for the correct one-dimensional analysis.

true quantitative value remains controversial. On the other hand, while the prediction and influences of vortex shedding may contain uncertainties, it is fair to say that the general characteristics are well-known and settled. Moreover, vortex shedding has been identified unambiguously as the mechanism for oscillation observed in several large motors including the Space Shuttle SRM, the Titan IV SRMU and the Ariane 5 SRM. Note that the mechanism has apparently not been active in small operational motors.[19]

The main reason for that conclusion seems to be the required special near-coincidence between the frequency of shedding and the frequency of an acoustic mode. Laboratory tests demonstrated that basic feature (Magiawala and Culick 1979; Nomoto and Culick 1982; Aaron and Culick 1984). Satisfaction of the condition requires suitable combinations of geometry, mean flow speed, thickness of shear layer at the origin of the vortex shedding and acoustic frequency which depends mainly on the speed of sound and length of chamber. Nevertheless, only a simple apparatus, sketched in Figure 2.29, is required to demonstrate the phenomenon.

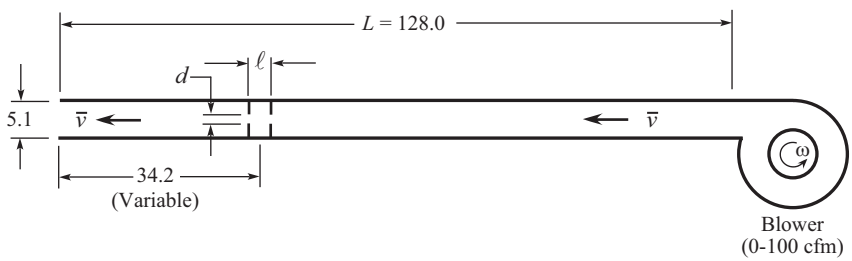

FIGURE 2.29. Sketch of an apparatus for demonstrating the excitation of acoustic modes by vortex shedding at a pair of annuli. All dimensions in centimeters (adapted from Culick and Magiawala 1979).

Three forms of vortex shedding have been unambiguously identified as mechanisms for exciting pressure (acoustic) oscillations in motors, illustrated in Figure 2.30: shedding from obstacles, usually annular rungs of restrictors or inhibiting material (Flandro, 1986; Vuillot, 1995); shedding from backward-facing steps and edges existing due to the geometry of the grain (Flandro, 1986 and Vuillot, 1995); and parietal vortex shedding in which vortices are created as a consequence of instabilities of the mean velocity profile in the vicinity of a burning surface (Casalis and Vuillot, 2002). The first two forms of vortices arise from unstable shear layers so one may state that generally the presence of vortex shedding as a mechanism is due to an instability of the average flow profile.

That conclusion suggests the obvious advice for avoiding this cause of pressure oscillations: Design the grain to exclude all possibilities for unstable velocity profiles. Thus there must be no obstacles, backward facing steps or edges, and the flow along burning surfaces must nowhere reach critical conditions for local instability. In practice those constraints may be too severe to be satisfied entirely. The design problem will then come down to producing a configuration in which the strength of the vortices, and their coupling to the acoustic field, will be minimal even though not necessarily nonexistent.

Suppose, then, that one or more instabilities of the mean flow exist in a chamber. Is it necessarily so that the vortices that may develop will excite and support unacceptable pressure oscillations? No, because we are concerned here once again with a case of coupled oscillatory systems: The system of pressure waves filling the chamber, and the array of vortices periodically shed from some relatively small region. The two

[19]The cases of vortex shedding from obstacles and from backward-facing steps have been unambiguously identified in full-scale combustors. So far as the author is aware, parietal vortex shedding, in contrast to shedding from obstacles, has not been shown definitely to exist in full-scale devices although it has been unquestionably identified in laboratory tests (Avalon *et al.* 2000; Vuillot and Casalis 2002). The Ariane 5 is the most likely candidate, but the case still remains open to question; direct observation has not been accomplished.

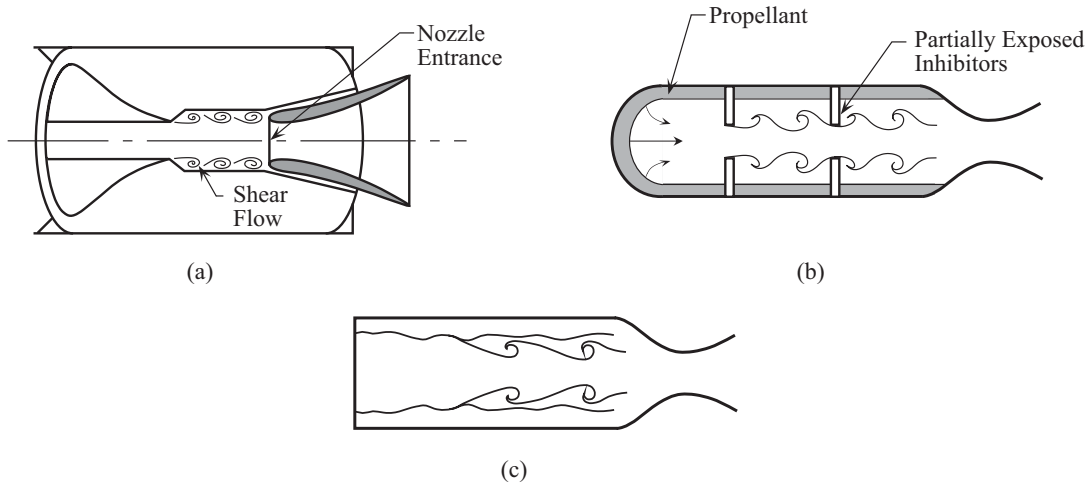

FIGURE 2.30. Vortex shedding from (a) an annular obstacle composed of residual inhibitor material; and (b) an edge of a backward facing step at a transition zone; (c) due to instability of the mean flow near a burning surface (parietal vortex shedding). Parts (a) and (b) from (Flandro 1986); Part (c) from Vuillot and Casalis (2002).

systems are coupled. The vortices, by some process such as that discussed below, may transfer a portion of their energy to the pressure waves; and the pressure waves—or their associated velocity oscillations—have strong influence on the initiation of the vortices by triggering, and, by frequency locking, on instabilities of the mean flow.

That behavior has long been known (e.g., see Rockwell and Naudascher 1979 and Naudascher and Rockwell 1980), implying that the oscillations found in rocket motors require near-coincidence between the shedding frequency and the frequency of an acoustic mode of the chamber. The truth of that conclusion for configurations appropriate to solid rockets seems first to have been demonstrated with the simple laboratory tests cited above. Satisfaction of the condition requires appropriate combinations of geometry; mean flow speed; suitable properties in the region of mean flow where the instability originates; and the acoustic frequency, which depends mainly on the speed of sound and a characteristic dimension, usually the length of the chamber. Sufficient data have been taken for the problem to construct useful scaling laws, 'rules of thumb' for design; see the references cited.

The appearance of vortex shedding in the Titan motors caused formation of a very useful program of extensive tests carried out in a subscale cold-flow model of the motor (Dunlap and Brown 1981; Brown *et al.* 1981, 1985). Those tests produced extensive data for the internal flow fields, eventually including results that formed part of the basis for the theoretical work on unsteady vorticity cited in the preceeding section.

In 1986, Flandro reported his elaboration and extension of the analysis he had carried out with Jacobs twelve years earlier. The work brought together previous ideas of instability of a shear layer as the initiation of a shear wave; growth and roll-up of the wave into a vortex; propagation of the vortex at a speed something less than that of the average flow; and impingement of the vortices on a solid surface, producing a pulse of pressure that can excite and sustain acoustic waves in the chamber. An acoustic pulse will propagate upstream to the region of the shear instability, possibly to initiate another disturbance to be amplified within the layer, later to develop into another vortex, etc., etc. The process will continue, becoming periodic when the frequency of the vortex shedding is nearly equal to the acoustic frequency. In that work, Flandro also fitted his results in the general analysis of linear instabilities covered here in Chapter 6.

When that behavior occurs in a rocket, toroidal vortices are shed from the inner edge of an annular obstruction, as in the Shuttle and Titan motors, or from edges such as those at the transition from longitudinal slots to the main cylindrical chamber (Figure 2.30(b)). The acoustic frequency is determined mainly by the length of the chamber, while the vortex shedding frequency is influenced by the local geometry and average flow. The local geometry determines the growth of the shear layer and in particular its momentum thickness, a fundamental parameter defining the conditions for instability. Flandro's analysis—an adaptation of earlier work by Michalke (1965)—and experimental results, have confirmed that the vortex shedding is characterized by the value of the Strouhal number, St, at which the growth rate of an unstable disturbance is maximum. The Strouhal number is defined as the product of shedding frequency f_s, times a characteristic length δ, divided by a characteristic speed U, so the shedding frequency is given by the formula

$$f_s = St\frac{U}{\delta} \tag{2.74}$$

where St has some value roughly constant and set by the geometry. The frequencies of the acoustic modes are only weakly dependent on the mean flow of the Mach number so small but do depend strongly on the geometry. For a chamber having length L and closed at both ends[20], the longitudinal modes have frequencies given by

$$f_a = \ell\pi\frac{a}{L} \tag{2.75}$$

where a is the speed of sound and $\ell = 1, 2, \ldots$ identifies the mode.

The results reported by Nomoto and Culick (1982) confirm the truth of the preceding ideas for a simple laboratory apparatus consisting of two annuli fitted in a tube, separated by some distance ℓ and having a mean flow in the axial direction. Figure 2.31 is a photo of the flow in the vicinity of the two baffles. Figure 2.32 shows some results with lines drawn according to (2.74) and (2.75) and data points indicating the occurences of oscillations without regard to amplitude. For the conditions of the experiment, significant oscillations were excited only in regions in which (2.74) and (2.75) are simultaneously satisfied. Note that the separate diagonal lines for shedding frequency given by (2.74) represent cases in which there are $1, 2, 3, \ldots$ vortices existing between the annuli at any given time. This interpretation of the shedding frequency was first given by Rossiter (1966).

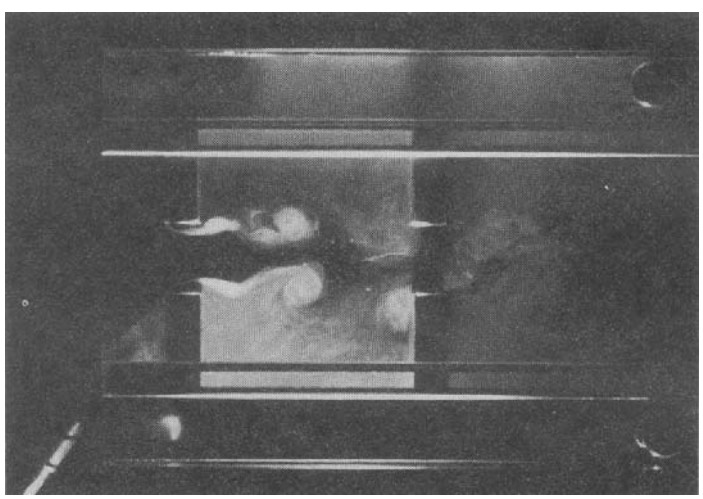

FIGURE 2.31. Typical flow between the baffles when a pure tone is generated (Nomoto and Culick 1982).

[20] A rocket physically closed at one end and exhausting through a choked nozzle appears to acoustic waves as if it is approximately closed at both ends.

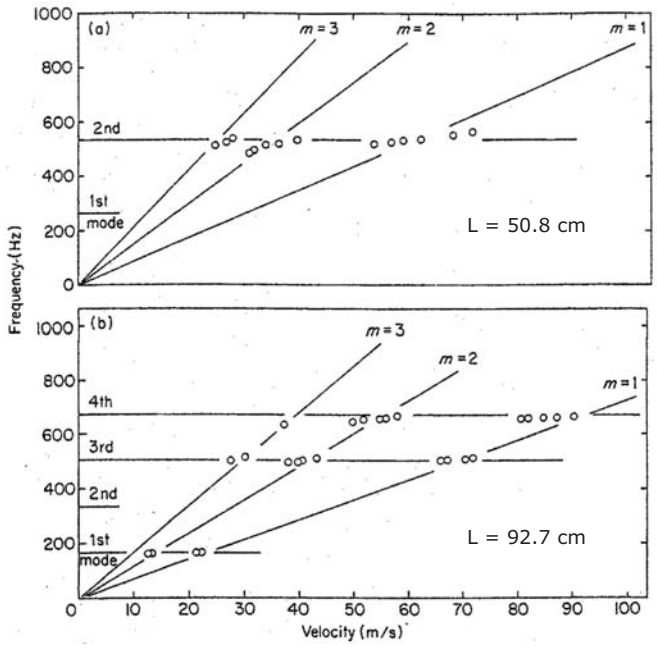

FIGURE 2.32. Experimental results for the excitation of acoustic modes by vortex shedding (Nomoto and Culick 1982). Open circles identify conditions when significant oscillations were observed. The length of the chambers from inlet to exhaust.

A potentially important implication of Figure 2.32 is that the dependence of the observed frequency of oscillation may not have an obvious—or simple—dependence on the length and mean flow speed during the firing of a solid rocket. In fact, as several researchers have noted (see, e.g., Vuillot 1995) the following reasoning shows that the shift of frequency with time is a good basis for distinguishing vortex shedding as the mechanism for oscillations. However, in practice, unambiguous distinction between this form of vortex shedding and parietal vortex shedding as the primary cause of observed oscillations may not be easy (Vuillot and Casalis, 2002).

Instabilities sustained by feedback involving combustion dynamics almost always show dependence on geometry closely given by the formulas of classical acoustics: $f_a \sim 1/L$. Thus, if there is little or no propellant cast at the head end, the longitudinal frequency is nearly constant in time. Or, if, as usually is the case for large motors, there are slots and fins at the head end, the effective length of the chamber tends to increase during a firing and hence the frequency of oscillation decreases.

However, according to the results given in Figure 2.32, because the mean velocity may increase during a burn as more propellant is exposed, the frequency of vortex shedding may increase. Coupling between the process of vortex shedding and the acoustic modes occurs over a broad range of frequency. It is possible (and has been observed) that the frequency suffers discrete changes, corresponding to transition between groups of data points shown in Figure 2.32; that is, the state of the oscillating system shifts because the number of shed vortices present between the shedding and impingement points changes.

The potentially important and very interesting second cause of vortex shedding was discovered several years ago by Vuillot and his colleagues at ONERA while investigating the mechanism for unstable oscillations observed in the Ariane 5 solid rocket boosters. Subscale firings of motors showed that large vortices were initiated, grew, and were shed from the region near the burning surface. (Vuillot *et al.* 1993; Traineau *et al.* 1997). Hence the phenomenon was called "parietal vortex shedding" by Lupoglazoff and Vuillot (1996).

In an exemplary systematic research program, the group at ONERA have established most of the characteristics of parietal vortex shedding relevant to practical applications. Some issues of scale apparently remain, but very good agreement has been found between subscale hot firings; subscale tests with flow visualization (Avalon *et al.* 2000); and numerical analyses of stability and vortex shedding. LeBreton *et al.* (1999) have given a good review of the subject, including some results for the effects of residual combustion which in this situation may not be negligible. Moreover, there is strong evidence of significant interaction between shedding from obstacles and parietal vortex shedding. The strength and significance of those interactions must clearly depend on the geometry and (changing) flow conditions in the chamber.

Possibly the most important aspect of this subject is weak understanding of nonlinear behavior. Apparently only Aaron (1985) has attempted a simple explanation, with only modest success. No simple explanation exists for the amplitudes of oscillations that can be generated by coupling with the shedding of large vortices. According to LeBreton *et al.* (1999) parietal vortex shedding produces, in their examples, larger amplitudes of oscillation than does shedding from an annulus (inhibitor ring in a segmented rocket). It would clearly be a significant aid to design and development if a rule of thumb could be constructed to place an upper limit to the amplitudes of oscillation caused by vortex shedding. Because the mechanism involves conversion of mechanical energy of the near flow to acoustic energy, it is likely that the maximum possible amplitudes must be much smaller than those that can be generated by coupling between acoustics and combustion dynamics. However, even when the amplitudes are well below values causing damage to the motor, the associated levels of oscillatory vibrations may be unacceptable to the payload.

2.2.10. Distributed Combustion. Combustion of the major components of a solid propellant—the primary oxidizer and the binder in the case of composite solids—normally takes place to completion near the burning surface. Thus the term 'distributed combustion' refers to combustion of particles as they are carried into the volume of the chamber. In particular, almost all attention has been directed to residual combustion of aluminum for which there is much photographic evidence. Steady combustion of aluminum particles has long been and continues to be a subject of research owing to its vital importance to the efficiency and performance of motors, and in the formation of slag, a general term referring to condensed material.

Relatively little notice has been taken of the possible influences of residual combustion on the stability of motors. Probably the main reason for this lack of interest is the general view that the existence of combustion instabilities in motors can be satisfactorily explained by other mechanisms, notably the dynamics of surface combustion and vortex shedding. It appears that the dynamics of aluminum combustion within the volume of the chamber must provide at most a small contribution to stability. There are at least two reasons for this conclusion: the available data contain uncertainties too large to allow identification of the influences of unsteady aluminum combustion; and any destabilizing tendencies of the particles are roughly compensated by the attenuation of unsteady motions due to the presence of particles. The second effect is known to be significant if the particles are inert and have suitable sizes for the frequencies of the instability in question.

Several works (Marble and Wooten 1970; Dupays and Vuillot 1998) have treated the effects of condensation and vaporization of non-burning particles, on attenuation of acoustic waves. Whether the attenuation is increased or decreased depends on many factors, including the sizes of particles and the rates at which the particles gain or lose mass. When, for example, a particle is vaporizing, it seems that in the presence of an acoustic wave, the phenomenon of 'flow turning' discussed in the preceding section should cause increased attenuation for a given particle size and frequency. However, while the analysis by Wooten (1966) supports that conclusion, recent work by Dupays (2000) suggests that the result is not always true. Moreover, suggestions have been made by investigators of combustion instabilities in ramjets (Sirignano *et al.* 1986) and in liquid rockets (Grenda, Vanketaswaram and Merkl 1995) that the process of vaporization of liquid drops is destabilizing. Those conclusions may be misleading, due to implied direct connections between the vaporization and burning rates. It may in fact be the case that the destabilization found in practice is due to combustion rather than vaporization *per se.*

Owing to the necessary connection between vaporization and combustion of particles, the problem of residual combustion presents certain difficulties of distinguishing what process is really responsible for attenuation or driving of waves. The most extensive experimental work on the problem in the U.S. has been done by Beckstead and his students (Beckstead, Richards and Brewster 1987; Raun and Beckstead 1993; Raun *et al.* 1993; Brooks and Beckstead 1995).

One of the most compelling reasons for investigating the matter was the discovery of anomalous (and still not completely understood) results obtained with a device called the 'velocity-coupled T-burner'. In this configuration, large areas of propellant are mounted in the lateral boundary to emphasize the interactions between surface combustion and velocity fluctuations parallel to the surface. For reasons not discussed here, Beckstead concluded that residual combustion was possibly a reason that unusually large values of the response function were found. The idea was based partly on the suspicion that the tangential velocity disturbances can strip incompletely burned aluminum from the surface. Subsequently, with both calculations and further experiments (Raun and Beckstead 1993), Beckstead has strengthened his case that the effects of unsteady residual combustion should not be dismissed out-of-hand. It is worth noting the conclusion by Brooks and Beckstead (1995) that the greatest effect of residual combustion (of aluminum) on stability is indirect, due to its effect on the mean temperature profile.

More recent work on distributed combustion has been carried out in France, motivated by the problem of oscillations in the Ariane 5 motor discussed in Section 2.2.6. The program devoted first to non-reacting two-phase flow and later to reacting flow began, apparently, with the dissertation by Dupays (1996). The most recent discussion of the work seems to be the review articles prepared by Dupays *et al.* (2002), but a broader view of the matter is presented in the excellent article by Fabignon *et al.* (2003). Aluminum combustion is discussed, not at great length, in the context of acoustic oscillations driven by vortex shedding with the Ariane 5. A main conclusion must be given close attention: Relatively small drops amplify oscillations, but large drops (diameters 125μ, burning to 60μ) attenuate the motions. It appears that little further work has been accomplished to investigate the reasons for this result which clearly has important practical implications. Simulations of unsteady two-phase flow in the Ariane 5 P230 booster motor have also been described by Lupoglazoff *et al.* (2000). See Section 6.11. It's an important topic. The subject of the effects of interactions between particles and gas seemed at one time to be quite well in hand. That view changed with recognition that at the temperature of flows in solid rockets residual combustion distributed in a chamber is likely significant under some realistic conditions. How significant, and how widespread the conditions are, has not been defined. It's an interesting subject that should be better understood.

2.3. Mechanisms of Combustion Instabilities in Liquid-Fueled Systems

Apart from differences in geometry, the primary distinctions between different propulsion systems are due to the internal physical processes. Some are independent of geometry, but others—such as flow separation—are not. In this and the following sections, we discuss the four oldest and main ideas that have been proposed for explaining combustion instabilities in liquid-fueled systems: processes associated with droplet formation and burning; interpretation with a time lag; convective waves; and vortex shedding and combustion. The ideas are not new and much of the material covered was developed during the period 1950–1990. Relatively little has been accomplished in general since that time, although in the past decade much has been done to improve the level of detail. While all have been prompted by experimental results, they differ greatly in the extent to which they have been developed.

2.3.1. Atomization, Droplet Vaporization and Burning. Some years after the time lag model had been developed, work at the NASA Research Center (Priem and Guentert 1962 and Priem 1965) showed that the stability of a liquid rocket motor could be controlled by varying the characteristics of the vaporization process. The conclusion followed from the results of numerical solutions to the equations for nonlinear

unsteady motions in a chamber. Source terms were approximated with models of the atomization, vaporization and burning. Variations of characteristic parameters showed that atomization and vaporization were the dominant rate processes determining the stability limits. That conclusion led to a series of studies particularly emphasizing vaporization.

Because of the difficulty of extracting precise conclusions from numerical analyses, Heidmann and Wieber (1966a, 1966b) devised a method for assessing the vaporization process alone. A droplet is injected axially in a steady flow. An acoustic field is superposed having the spatial distribution of the lowest first tangential mode for a cylindrical chamber, $\sin\theta J_1(\kappa_{11}r)$. The motion and vaporization rate of the droplet is calculated throughout its history. By superposing the results for an array of injected drops, assumed not to interact with one another, one may find the local fluctuation of vaporization rate throughout the chamber. That is the mass source term w_l' in the continuity equation for the gas phase (see Annex A).

Heidmann and Wieber (1966a) defined a "response factor", N, to interpret their results:

$$N = \sum \frac{w_l'/\overline{w}_l}{p'/\overline{p}} \tag{2.76}$$

where $\sum$ here denotes the sum over all droplets in the volume considered. They gave results for N as a function of various parameters. Typically, N shows a peak of about 0.6–0.9 in a frequency range 0.04–0.1 Hertz. Results obtained for n-heptane over fairly wide flow conditions were correlated with a dimensionless parameter containing droplet size, chamber pressure, gas velocity and a dimensionless amplitude of the oscillation.

In a later work, Heidmann and Wieber (1966b) used a restricted form of Rayleigh's Criterion and a simpler linear analysis to produce essentially the same conclusions. The new definition of the response factor was

$$N = \sum \frac{\int_0^{2\pi/w} \frac{\hat{w}_l^{(r)}}{\overline{w}_l} \frac{\hat{p}}{\overline{p}} dt}{\int_0^{2\pi/w} \left(\frac{\hat{p}}{\overline{p}}\right)^2 dt} \tag{2.77}$$

These analyses amount to detailed examination of a particular process contributing to the time lag discussed Section 2.3.2. Substitution of the real part of (2.94) in (2.77) gives

$$N = n(1 - \cos\omega\tau) \tag{2.78}$$

Heidmann and Wieber found that their numerical results could be approximated quite well in the range $\tau_v\omega < 1$ by the values

$$\begin{aligned} n &= 0.21 \\ \tau &= 4.5\tau_v \end{aligned} \tag{2.79}$$

where τ_v is the mean droplet lifetime. This comparison is shown in Figure 2.33 taken from Heidmann and Wieber (1966).

Note that the function (2.79) oscillates and therefore becomes a poor approximation for $\omega\tau_v > 1$, as show by the solid line in Figure 2.33. The vaporization rates seem physically reasonable for the conditions shown, so one must conclude that the time lag model fails at higher frequencies. Subsequently, Tong and Sirignano (1986a, 1986b, 1987) re-examined the problem of unsteady vaporization. With their more detailed model including the effects of unsteady heat transfer in the gas phase, they concluded that their vaporization rates are much higher than those found by Heidmann and Wieber.

More strongly, Tong and Sirignano proposed that unsteady droplet vaporization is a potential mechanism for driving combustion instabilities. Heidmann and Wieber had earlier noted that the response factor they

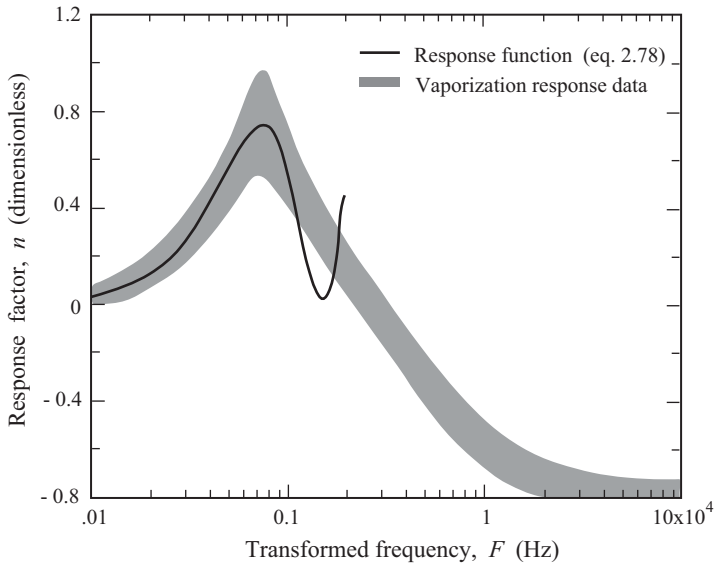

FIGURE 2.33. Vaporization response according to Heidmann and Wieber (1966).

calculated for the vaporization process was less than that calculated for the nozzle losses. Thus, although vaporization itself did add energy to the acoustic field according to their analysis, the effect was too small to be a mechanism for instabilities. Tong and Sirignano concluded that their results show sufficient energy transfer from the vaporizing droplets to the acoustic field to qualify as a mechanism in actual systems[21]. Their conclusion is based solely on the $p - v$ work done by the process of vaporization and does not include any energy release due to combustion. The proposal is evidently wrong, for the following reasons reached by reasoning from at least two points of view.

First, we must emphasize that none of the preceding conclusions involved combustion: The assertion is that coupling between pure vaporization and the acoustic field produces net flow of energy to the oscillations in the gas. The contrary conclusion was reached by Marble and Wooten(1970) and Marble (1969), that both condensing and vaporizing droplets attenuate acoustical motions. In Section 2.2.10 we noted that recent work at ONERA showed that a more complete analysis accounting for condensation and vaporization in greater detail leads to slightly different conclusions.

The reason for the opposite conclusion seems to be that not all interactions between the droplets and the acoustic field are accounted for in the calculations by Heidmann and Wieber, and by Tong and Sirignano. Their conclusions were based on using Rayleigh's Criterion, but only one term was considered. They argued that by analogy with Rayleigh's original statement concerning fluctuations of heat addition, the same criterion should apply to mass addition. Therefore, as in equation (2.77), only the integral involving w_l' was computed; a positive value indicates the possibility for driving the acoustic field. However, the derivation given later will show that the correct form of the criterion involves several contributions. Considering only those associated with the conversion of liquid to gas, the result can be found (Culick, 1988, Section 2.5)

$$\Delta\epsilon_n = \frac{\omega_n^2}{\overline{p}E_n^2}\int dV \int_t^{t+\tau_n} \left[(\overline{\gamma}-1)\left\{\delta Q_l' + (\overline{h}_l - \overline{e})w_l' + \left(h_l' - e' - \frac{p'}{\overline{\rho}_g}\right)\overline{w}_l\right\} + \overline{\gamma}\left(\delta\vec{F}_l' + \overline{w}_l\delta\vec{u}_l'\right)\cdot\vec{u}_n'\right] dt \tag{2.80}$$

[21]Later application of this work to ramjet combustors is discussed briefly in Section 2.4.5

There is indeed a term proportional to the integral of $w_l'p'$, but it is multiplied by $(\overline{h}_l - \overline{e})$ which contains the heat of vaporization. There are also significant amounts of energy transfer associated with the terms involving $\delta Q_l' + \delta F_l'$ which for non-vaporizing drops represent the attenuation of sound waves. Those effects are included in the work by Marble and Wooten: Their results show that the accompanying energy losses dominate, so that in fact if combustion is ignored, vaporizing droplets cause damping, not driving, of unsteady gas motions.

We must emphasize that the conflicting results, and the conclusion that vaporization is not a mechanism for driving combustion instabilities, rests on proper computation of the energy transfer. In the earlier work, an incorrect or, rather, incomplete form of Rayleigh's Criterion was used. It is certainly true that the process represented by $w_l'p'$ alone does cause driving if the fluctuation of mass release has a component in phase with the pressure fluctuation, but that is only part of the story.

Priem (1988) has used Heidmann and Wieber's model of vaporization, combined with the model worked out by Feiler and Heidmann (1967) for a gaseous fuel, to study combustion instabilities in the LOX/methane system. He bases his conclusions concerning stability boundaries on numerical results for the combustion responses, of which that for liquid oxygen is computed with equation (2.77) and the method described above; and on corresponding results found for the losses associated with the exhaust nozzle and baffles. His results seem to compare fairly well with some experimental work. The reason that this could be so—even though vaporization causes net energy losses if all contributions are accounted for—is that the energy released by combustion, immediately following vaporization, is the dominant factor. That is, in equation (2.79) the terms involving energy transfer are larger than those representing losses. Comparison with experimental results seems always to involve multiplicative factors which are determined to provide best fit to data, or are absent in normalized forms. Then when good agreement was found, it seems that it is largely the qualitative behavior that is being checked. The method is dated and no longer useful.

Despite the heavy emphasis, in many works, on vaporization as the rate controlling process, it is generally recognized that other processes contribute and in some situations may be dominant. The injection process itself may be affected under unsteady conditions due to the varying streams, impact of jets, and atomization all are sensitive to unsteady flow fields. Those problems are extremely complicated, difficult to describe in a fashion suitable for use in a general analysis, and are very much dependent on details of the hardware. Thus the work has largely been experimental with some effort to correlate results in a form useful for design (e.g., Levine 1965; Sotter, Woodward and Clayton 1969; Webber 1972; Webber and Hoffman 1972). The time-lag model has been used essentially as a means of correlating all of those processes without concern for details (Reardon, Crocco and Harrje 1964; Reardon, McBride and Smith 1966). Summaries of experimental results obtained prior to 1971 may be found in the reference volume edited by Harrje and Reardon (1972).

Of work in the 1980s, the most fundamental and detailed was that carried out at ONERA as a result of problems due to combustion instabilities in the Viking motor. Special effort was made to understand the unsteady behavior of the injectors used in that engine. The intentions of the research program were described by Souchier, Lemoine and Dorville (1982); and by Lourme and Schmitt (1983). Considerable effort has since been expended to characterize the steady and unsteady behavior as the basis for analyzing instabilities in the engine (Lourme, Schmitt and Brault 1984; Lecourt, Foucaud and Kuentzmann 1986; Lourme 1986; Lecourt and Foucaud 1987). The results range from detailed measurements of the spray (droplet size and velocity distributions) to the more global unsteady response of the injector, using a device adapted from a method developed for solid propellant rockets.

2.3.2. Interpretation With a Time Lag. Owing to the enormous complications associated with analysis of the time-dependent behavior of liquid-fueled systems, representation of the dynamics with a time lag was introduced early in theoretical work. The basic idea is simple, and quite general, related to the familiar experience that a forced oscillating system will gain energy if the force has a component in phase

with the velocity of the point of application. Stability of dynamical systems characterized in some sense by a phase or time lag had been studied prior to the concern with combustion instabilities (for example, see Callender *et al.* 1936 and Minorsky 1942). In 1941, Summerfield (1951) had observed low frequency "chugging" during firings of a liquid rocket. Discussion with von Karman led to the idea of a time lag as a possible explanation. Gunder and Friant (1950) independently introduced a time lag in their analysis of chugging, but it was Summerfield's paper and subsequent work at Princeton by Crocco that established the time lag theory in the firm widely used.

The essential idea in all applications of the time lag is that a finite interval—the lag—exists between the time when an element of propellent enters the chamber and the time when it burns and releases its chemical energy. Such a time lag must exist in steady operation, and, since combustion is distributed throughout the chamber, there is no unique value. Evidently a complete analysis of injection and subsequent processes could then be interpreted in terms of multiple time lags; results exist only for approximate analyses.

Now suppose that at time t the pressure in the chamber suddenly decreases, causing an increase in the flow of propellant through the injector. The increased mass burns at some later time $t+\tau$, where τ is the time lag. If the pressure is increasing when the added mass burns, the energy released will tend to encourage the pressure increase, a destabilizing tendency. This elementary process is easily interpreted with Rayleigh's Criterion. Assume that the pressure varies sinusoidally,

$$p' = \hat{p}\sin\omega t \tag{2.81}$$

and that the energy occurs later with constant time lag τ,

$$Q' = \hat{Q}\sin\omega(t-\tau) \tag{2.82}$$

Integration of the product $p'Q'$ over one period $2\pi/\omega$ gives

$$\int_t^{t+2\pi/\omega} p'Q'dt' = \hat{p}\hat{Q}\int_t^{t+2\pi/\omega} \sin\omega t'\sin(\omega t'-\omega\tau)dt' = \hat{p}\hat{Q}\frac{\pi}{\omega}\cos\omega\tau \tag{2.83}$$

Thus, according to Rayleigh's Criterion (Section 6.6), we expect that net energy is added to the oscillation if $\cos\omega\tau$ is positive, so the time lag must lie in the ranges

$$0 < \tau\frac{\pi}{2\omega}, \quad \frac{3\pi}{2\omega} < \tau < \frac{5\pi}{2\omega}, \quad \ldots\text{etc.} \tag{2.84}$$

Suppose that the system is unstable and the τ lies in the range $3\pi/2\omega < \tau < 5\pi/\omega$. Then the strategy for fixing the problem is based on modifying the system so that τ is either increased or decreased, placing its value outside the range for instability.

Because the processes subsequent to injection are surely dependent on the flow variables, pressure, temperature, velocity, ..., it is unrealistic to assume that the time-lag is constant. The most widely used form of the representation with a time lag are dominated by its dependence on pressure. Figure 2.34, taken from Dipprey (1972), is a sketch illustrating the behavior for a sinusoidal pressure oscillation imposed on the system. The total time delay to burning is supposed, in this case, to be composed of two parts due to the propellant feed system and the combustion delay (injection, atomization, vaporization, mixing, and chemical kinetics). It is the second part that is sensitive to the flow conditions in the chamber.

Let $\dot{m}$ denote the mass flow (mass/sec.) of propellant. At this point we are not concerned with details and we need not distinguish between fuel and oxidizer. The arguments based on the idea of a time lag are directed mainly to constructing a representation of the mass source term w_ℓ (mass/vol.-sec.) in the equation for conservation of mass. Thus the result is intended to express the rate of conversion of liquid to gas in a volume element of the chamber. There is no consideration of combustion processes in detail; the usual assumption is that combustion occurs instantaneously, a view that determines how the time lag model ought to be incorporated in the equations.

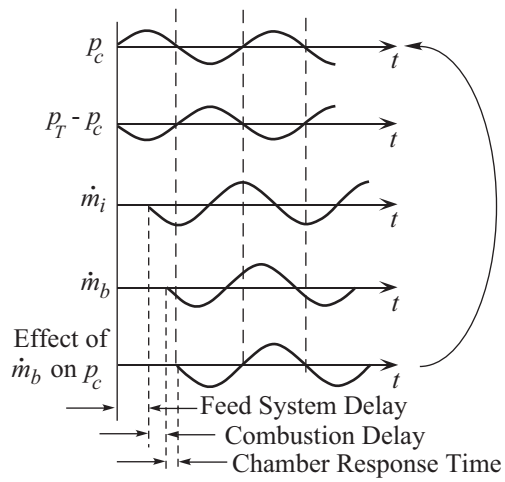

FIGURE 2.34. Graphical definition of a simple time lag (Dipprey 1972).

Let $(\vec{r},\ dV)$ denote the volume element at position $\vec{r}$ in the chamber and let $(t,\ dt)$ denote the small time interval dt at time dt. The idea is that the amount of liquid $\omega_l dV\, dt$ converted to gas in the element $(\vec{r},\ dV)$ in the interval $(t,\ dt)$ was injected as $\delta\dot{m}(t-\tau)d(t-\tau)$ at the time $t-\tau$ in the interval $d(t-\tau)$. Hence by conservation of mass,

$$w_l dV\ dt = \delta\dot{m}_i(t-\tau)d(t-\tau) \tag{2.85}$$

According to earlier remarks, the time lag is supposed to be variable, and can be written as the sum of average and fluctuating values, $\tau = \overline{\tau} + \tau'$. In steady-state operation, (2.85) is

$$\overline{w}_l dV\ dt = \delta\dot{m}_i(t-\overline{\tau}) = \delta\dot{m}_i(t-\overline{\tau})dt \tag{2.86}$$

Expanding $\delta\dot{m}(t-\tau)$ in Taylor series for use in (2.85) we have

$$\delta\dot{m}_i(t-\tau) = \delta\dot{m}_i(t-\overline{\tau}) + \tau'\left[\frac{d}{dt}\delta\dot{m}_i\right]_{t-\tau} + \cdots \tag{2.87}$$

The second term is non-zero if the injected mass flow is not constant. There are many situations (notably for low frequency instabilities) for which variations are important. But for instabilities at high frequencies, variations of the propellant flow are generally not important. Hence we ignore the second term in (2.87) and substitute (2.86) in (2.85) to find

$$w_l(\vec{r},\ t) = \overline{w}_l\left(1 - \frac{d\tau}{dt}\right) \tag{2.88}$$

The variations of the local conversion of liquid to gas depend in this simple fashion on the time-dependence of the time lag. Note that τ may in general depend on position: The reasoning here is quite widely applicable.

The difficult problem is of course to predict τ — in fact it has never been done. Crocco introduced the idea that the time lag is the period required for the processes leading to vaporization to be completed. He assumed that this integrated effect can be represented by an integral over the time lag of some function f of the variables affecting the processes

$$\int_{t-\tau}^{t} f\left\{p,\ T,\ \vec{u},\ \vec{u}_l,\ \ldots\right\} dt' = E \tag{2.89}$$

The constant E is supposed to be a measure of the level to which the integrated effects must reach in order for vaporization to occur. Almost all applications of the time lag model rest on the assumption that the time

lag is sensitive only to the pressure. The function f may then be expanded to first order about its value at the mean pressure,

$$f(p) = f(\overline{p}) + p'\frac{df}{dp} = f(\overline{p})\left[1 + p'\frac{1}{f(\overline{p})}\frac{df}{dp}\right]$$

If $f = cp^n$ then $df/dp = ncp^{n-1}$ and $(df/dp)/f(p) = n/p$. The *interaction index* n is defined as

$$n = \frac{\overline{p}}{f(\overline{p})}\frac{df}{dp} \tag{2.90}$$

and $f(p)$ is approximated as

$$f(p) = f(\overline{p})\left[1 + n\frac{p'}{\overline{p}}\right] \tag{2.91}$$

This form is now used in approximate evaluation of (2.89).

First differentiate (2.89) with $f(p) = f\{p(t)\}$ to find

$$f\{p(t)\} - \left(1 - \frac{d\tau}{dt}\right) f\{p(t-\tau)\} = 0$$

Substitution of (2.91) gives

$$1 - \frac{d\tau}{dt} = \frac{1 + n\frac{p'(t)}{\overline{p}}}{1 + n\frac{p'(t-\tau)}{\overline{p}}} \approx 1 + n\left[\frac{p'(t)}{\overline{p}} - \frac{p'(t-\tau)}{\overline{p}}\right] \tag{2.92}$$

Set $w_l = \overline{w}_l + w_l'$ in (2.88) and substitute (2.92) to find the basic result of the time lag theory:

$$w_l' = \overline{w}_l n\left[\frac{p'(t)}{\overline{p}} - \frac{p'(t-\tau)}{\overline{p}}\right] \tag{2.93}$$

For analyzing linear stability, $p' = \overline{p}e^{-i\overline{a}kt}\psi(\vec{r})$ and $w_l' = \hat{w}_l e^{-i\overline{a}kt}$, so

$$\hat{w}_l = \overline{w}_l n(1 - e^{-i\omega\tau}) \tag{2.94}$$

where the usual approximation has been made, $\alpha\tau \ll \omega\tau$ in the exponent.

Equation (2.94) is a two-parameter representation of the conversion of liquid to gas. The two parameters, the time lag τ and the interaction or pressure index n, are unknown *a priori.* All work with the time lag theory requires experimental measurements to determine their values. The general idea is simple. After substituting (2.94) in the linearized conservation equations, solution is found for the stability boundary ($\alpha = 0$) with n and τ as parameters. Experimental data for the stability boundary are used to determine n and τ. The approximate range of values for τ had been reasoned, e.g., by Crocco and Cheng (1956). Crocco, Grey and Harrje (1960) were first to obtain sufficient data to confirm the value of this approach. Figure 2.35 reproduces some of their results for the time lag and interaction index inferred from tests with two injectors. The data were taken for the stability boundary of the fundamental longitudinal mode and show the strong dependence on fuel/oxidizer ratio.

Obviously, there are many limitations within the analysis itself. The analysis leading to (2.94) is entirely phenomenological; the final result containing two parameters only is an enormous simplification of the real situation, but there is no way to assess the imperfections. The formula (2.93) can be extended to include, for example, dependence on velocity fluctuations (Reardon, Crocco, and Harrje 1964). Because the values of all parameters must be found from experimental data, the difficulties become prohibitive.

The time lag model (it is, after all, not really a theory) is based on an appealing physical argument but no processes are treated explicity. Probably the most serious deficiency is that no detailed treatment is given of combustion, which is ultimately the source of the energy driving all combustion instabilities. Nevertheless, the model has been the basis for some success in treating instabilities in liquid rockets, primarily as the basis

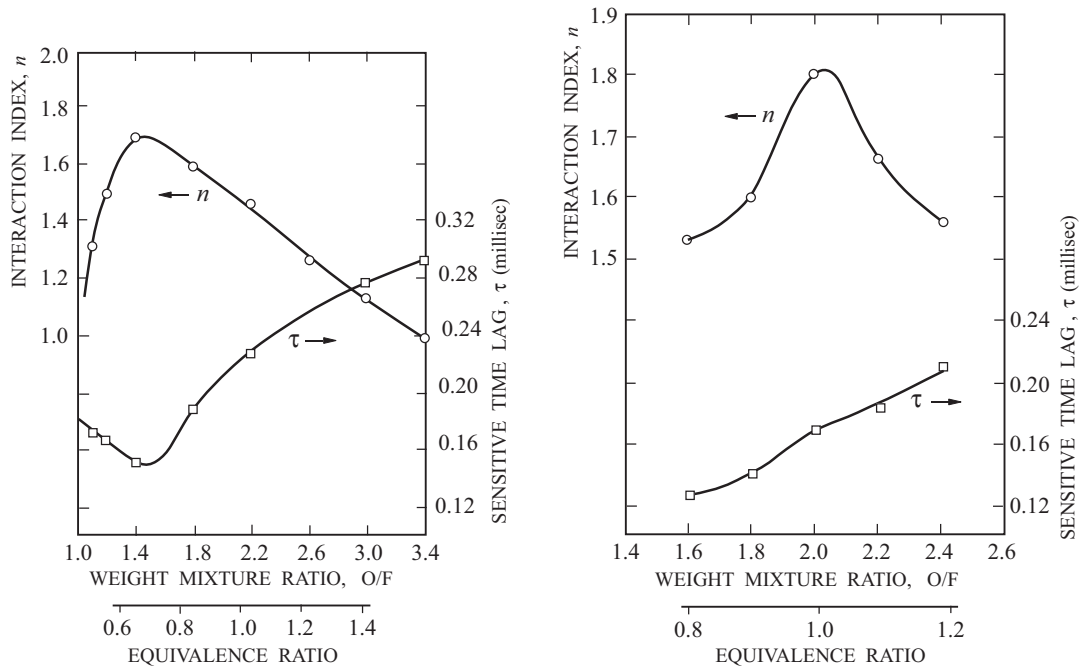

FIGURE 2.35. Early measurements of the time lag and pressure index in a gas rocket (Crocco, Grey and Harrje, 1960).

for correlating data. The two-parameter representation provides a convenient framework for detecting trends with design changes. Its illumination of basic physical processes and its predictive value are very limited indeed.

2.3.3. Convective Waves. Following work by Kovasznay (1953), Chu and Kovasznay (1957) showed one way of decomposing general small disturbances of a viscous compressible fluid into three classes: acoustic, viscous, and entropy waves. Acoustic waves carry no entropy changes, while viscous and entropy waves have no accompanying pressure fluctuations. The direct effects of viscous stresses and heat conduction on combustion instabilities are generally negligible except in the vicinity of surfaces. That entropy fluctuations evidently have second order effects on the acoustic waves is implied by the formal analysis covered in Chapter 3.

However, both viscous effects and non-uniform entropy may affect the acoustic field indirectly through processes at the boundaries. First we examine here the possible influences of entropy fluctuations. These fall within the general class of convective waves, that is, disturbances that are carried with the mean flow: their propagation speed is the average flow speed. Entropy fluctuations are associated with the portion of temperature fluctuations not related isentropically to the pressure fluctuation, such as non-uniformities of temperature due, for example, to combustion of a mixture having non-uniformities in the fuel/oxidizer ratio. In general, an entropy wave may be regarded as a non-uniformity of temperature carried with the mean flow.

As shown by Chu (1953) pressure waves incident upon a plane flame will cause generation of entropy waves carried downstream in the flow of combustion products. Thus one should expect that when combustion instabilities occur, there must be ample opportunity for the production of entropy fluctuations. That process has negligible effect directly on stability (the coupling between acoustic and entropy waves is second order within the volume) but there has long been interest in the possible consequences of entropy waves for the following reason.

When an entropy wave is incident upon the exhaust nozzle, it must pass through a region containing large gradients of mean flow properties. A fluid element must retain its value of entropy and for this condition to be satisfied, the pressure and density fluctuations cannot be related by the familiar isentropic relation, $\delta p \sim \gamma \delta \rho$. As a result, within the nozzle, pressure changes are produced that will generate an acoustic wave that will propagate upstream. Thus, an entropy wave incident upon an exhaust nozzle can produce an acoustic wave in the chamber, augmenting the acoustic field due to other sources.

An artificial elementary example will illustrate the proposition. Consider a chamber admitting uniform constant mean flow at the head end, say through a choked porous plate; the flow exhausts through a choked nozzle (Figure 2.36). Suppose that at the head end a heater is placed, arranged so that its temperature can be varied periodically, with frequency ω. This action produces a continuous temperature or entropy

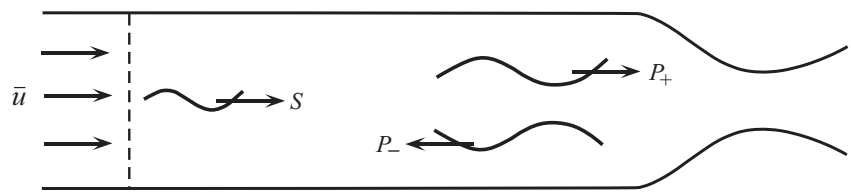

FIGURE 2.36. Sketch of a simple case with a single entropy wave (S) and acoustic pressure waves (P_+, P_-).

wave convected with the flow. An experimental realization of this situation has been described by Zukoski and Auerbach (1976). We assume no losses within the flow, so a fluid element retains its entropy; small perturbations s' of the entropy satisfy the equation

$$\frac{\delta s'}{\delta t} + \overline{u}\frac{\delta s'}{\delta z} = 0 \tag{2.95}$$

If S is the amplitude of the fluctuation at the heater ($z = 0$), the solution for s' is

$$s' = Se^{-i\omega(t-\frac{z}{a})} \tag{2.96}$$

To simplify the calculations, assume that the flow speed is vanishingly small so that we may ignore its effect on acoustic waves. Then the acoustic pressure and velocity fields can be expressed as sums of rightward and leftward traveling plane waves:

$$\begin{aligned} p' &= [P_+e^{ikz} + P_-e^{-ikz}]e^{-i\omega t} \\ u' &= [U_+e^{ikz} + U_-e^{-ikz}]e^{-i\omega t} \end{aligned} \tag{2.97)a,b}$$

As usual, the complex wavenumber is $k = (\omega - i\alpha)/\overline{a}$. The acoustic pressure and velocity must in this problem satisfy the classical acoustic momentum equation with no sources:

$$\overline{\rho}\frac{\partial u'}{\partial t} + \frac{\partial p'}{\partial z} = 0 \tag{2.98}$$

Separate substitution of the forms for the rightward and leftward traveling waves shows that $U_\pm$, $P_\pm$ are related by

$$\overline{\rho a}U_+ = P_+ \ ; \quad \overline{\rho a}U_- = -P_- \tag{2.99}$$

Assume that the head end acts as a perfect reflector for the acoustic waves, so

$$u' = 0; \quad \frac{\partial p'}{\partial z} = 0 \quad (z = 0) \tag{2.100)a,b}$$

In a real case (e.g., if the heater were actually a flame) the pressure fluctuations would cause fluctuations of entropy at the head end. To represent this effect, set s' proportional to p' at $z = 0$:

$$s' = A_0 p' \quad (z = 0) \tag{2.101}$$

Tsien (1952), Crocco (1953) and Crocco and Cheng (1956) have shown that the boundary condition at the nozzle entrance may be written in the form

$$p' + \overline{\rho a} A_1 u' + A_2 s' = 0 \quad (z = L) \tag{2.102}$$

We may now show that the problem formulated here admits solutions representing steady acoustic oscillations in the chamber, whose stability depends on the values of the coefficients A_0, A_1, A_2. We eliminate the unknown amplitudes S, P_+, P_- and obtain a characteristic equation for the complex wavenumber k, by satisfying the boundary conditions (2.99)-(2.102). Substitute equations (2.97)a,b and (2.99) into (2.100)a,b to find

$$P_+ - P_- = 0 \tag{2.103}$$

With (2.96) and (2.97)a, the condition (2.98) is satisfied if

$$S = A_0(P_+ + P_-) \tag{2.104}$$

Finally, substitution of (2.96), (2.97)a,b and (2.104) in (2.102) gives

$$[(1 + A_1)e^{ikL} + A_0 A_2 e^{i\frac{\omega}{\overline{u}}L}]P_+ + [(1 + A_1)e^{-ikL} + A_0 A_2 e^{i(\frac{\omega}{\overline{u}})L}]P_- = 0 \tag{2.105}$$

With $P_- = P_+$ from (2.103) we have the characteristic equation

$$e^{i2kL} = \frac{-1}{(1 + A_1)}[1 - A_1 + 2A_0 A_2 e^{i(k+\frac{\omega}{\overline{u}})L}] \tag{2.106}$$

Generally A_0, A_1, A_2 are complex numbers. The real and imaginary parts of (2.106) provide transcendental equations for the real and imaginary parts $(\omega/\overline{a},\ \overline{\alpha}/\overline{a})$ of k. The solutions are unstable if $\alpha > 0$, corresponding to self-excited waves. Note that in the limiting case of no entropy fluctuations ($A_0 = 0$) and a rigid wall ($A_1 \to \infty$) at $z = L$, (2.106) reduces to $e^{i2kL} = +1$ or $\cos 2kL = 1$ and $\sin 2kL = 0$. Then $k = n\pi/L$ and the allowable wavelengths are $\lambda = 2\pi/k = 2L/n$, the correct values for a tube closed at both ends.

This example suggests the possibility for producing instabilities if entropy waves are generated and *if* those waves interact with the boundary in such a way as to produce acoustic disturbances. It is in fact a genuine possibility that has been considered both in laboratory tests and as an explanation of instabilities observed in actual engines. The difficulties in applying this idea are largely associated with treating the processes responsible for causing the entropy waves.

In a combustion chamber, possible sources of entropy fluctuations may be distributed throughout the chamber. Burning of non-uniform regions of fuel/oxidizer ratio and interactions of pressure distributions with combustion zones are important causes, both producing non-isentropic temperature fluctuations. Thus in general the property that in inviscid flow free of sources an element of fluid has constant entropy, is inadequate. A proper description of entropy waves should be placed in the broader context accounting also for convective waves of vorticity was worked out first by Chu and Kovasznay (1957). We cannot provide a complete discussion here, but for later purposes it is helpful to have at hand the more general equation governing entropy fluctuations.

Combination of the first law of thermodynamics for a perfect gas and the definition $ds = dq/T$, valid if the heat transfer dq is not too abrupt, gives

$$ds = C_v \frac{dT}{T} - \frac{p}{\rho_g}\frac{d\rho_g}{\rho_g}$$

Now introduce the perfect gas law to eliminate the temperature change. Writing the result for motion following a fluid element we have

$$\frac{1}{C_v}\frac{Ds}{Dt} = \frac{1}{\rho}\frac{Dp}{Dt} - \frac{\gamma}{\rho_g}\frac{D\rho_g}{Dt} \tag{2.107}$$

where $D/Dt = \partial/\partial t + \vec{u}_g \cdot \nabla$ is the convective derivative. From the calculations in Annex A, we find the equation for entropy,

$$\frac{1}{C_v}\frac{Ds}{Dt} = \frac{1}{\rho}\frac{R}{C_v}\left[Q + \delta Q_l + \nabla\mathbf{q} + \Phi + \delta\mathbf{u}_l \cdot \boldsymbol{\mathfrak{F}}_l + \frac{p}{\rho_g}\nabla\cdot(\rho_l\delta\mathbf{u}_l) + \left\{(h_l - e) + \frac{1}{2}(\delta\mathbf{u}_l)^2\right\} w_l\right] \tag{2.108}$$

The right-hand side contains all sources of entropy changes including viscous effects, combustion and conversion of liquid to gas.

Equation (2.108) completes the set of equations required for complete analysis of combustion instabilities including entropy waves. See also Annex A and Chapter 3. The equations governing vorticity waves are obtained by splitting the velocity field into two parts: the acoustic field which is irrotational, and the rotational vorticity field which, if treated in all generality, includes turbulence as well as large vortex structures and shear waves.

2.3.4. Vortex Shedding from Rearward-Facing Steps. The presence of unplanned swirling, spinning or vortex motions in propulsion systems has long been recognized as a serious problem. They fall broadly into two classes: those with angular momentum directed along the axis, usually (if the rocket itself isn't spinning) related to standing or spinning transverse acoustic modes of the chamber; and those having angular momentum mainly perpendicular to the axis, associated with vortex shedding from bluff bodies or rearward-facing steps.

Motions identified as forms of transverse or tangential modes do not normally qualify as mechanisms: they are themselves the combustion instability. Male, Kerslake and Tischler (1954) gave an early summary of severe transverse oscillations ("screaming" at 10 kHz) and noted what has always been a serious consequence: greatly increased surface heat transfer.

Here we are concerned with vortex motions growing out of unstable shear layers. Those vortices, now commonly called "large coherent structures" (Brown and Roshko 1974) are convected downstream at approximately the average speed of the two streams forming the shear layer. Figure 2.37 shows an example of the observations made by Brown and Roshko for cold flow at relatively low Reynolds number. In propulsion systems, the shear layers in question are generally formed in flow past bluff body flameholders (in thrust augmentors) or past rearward-facing steps (in ramjet engines).

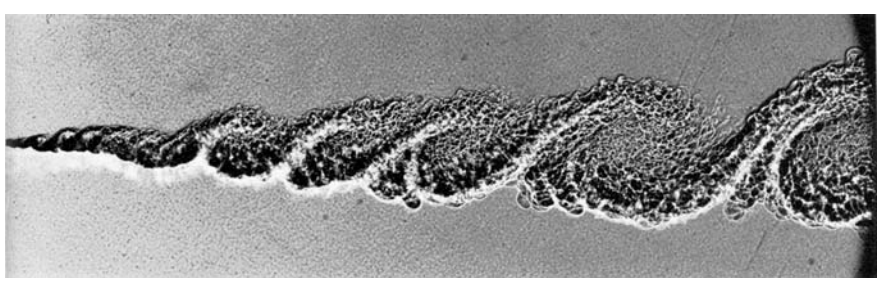

FIGURE 2.37. Large-scale coherent structures in a mixing layer at 8 atmospheres in flow past a splitter plate: upper stream ($v_1 = 10$ m/s) is He; lower stream is N_2, with $\rho_2 v_2^2 = \rho_1 v_1^2$. (Brown and Roshko 1974).

Observations of vortex shedding from flameholders, and recognition of the importance of this process as a possible mechanism for combustion instabilities were first independently reported by Kaskan and Noreen (1955), Rogers (1954) and Rogers and Marble (1956). Both experiments used premixed gaseous fuel and air

flowing past a flameholder in a rectangular channel. However, the particular mechanisms proposed were very different. Figures 2.38 and 2.39 taken respectively from Kaskan and Noreen (1955) and Rogers and Marble (1956) clearly show the vortex shedding. Particularly Figure 2.39 shows a good example of the influence of flow conditions on vortex shedding from a two-dimensional bluff body with combustion; in this case the bluff body was a two-dimensional wedge. At approximately constant speed, when the equivalence ratio in the premixed flow past the lip of the wedge was increased from about 0.75 to around 0.90 continuous vortex shedding began, and high-frequency acoustic oscillations were sustained in the channel. The oscillations were transverse to the axis of the channel.

Particularly noteworthy—and important—is the reasoning by Rogers and Marble for the presence of the oscillations. They give an appealing argument based on the idea that delayed pulses of combustion, producing pulses of pressure, occur periodically with the shed vortices. A vortex formed and shed from the lip of the flameholder entrains fuel mixture from the free stream. A short period of time passes during which the fresh (cold) gas mixes with hot combustion products entrained from the recirculation zone behind the flameholder. At the end of the ignition delay, the mixture in the vortex burns vigorously, generating a pulse of pressure which is supposed to reinforce the pressure oscillation in the chamber. For steady oscillations to be sustained, this process must evidently occur at the same frequency as that of the wave motion. For the tests typified by those shown in Figure 2.39, the ignition delay, according to results given by Zukoski and Marble (1954), was about 0.00028 seconds, suggesting a frequency around 3600 Hz. The observed oscillations (Figure 2.39) had frequencies in the range 3600–3900 Hz.

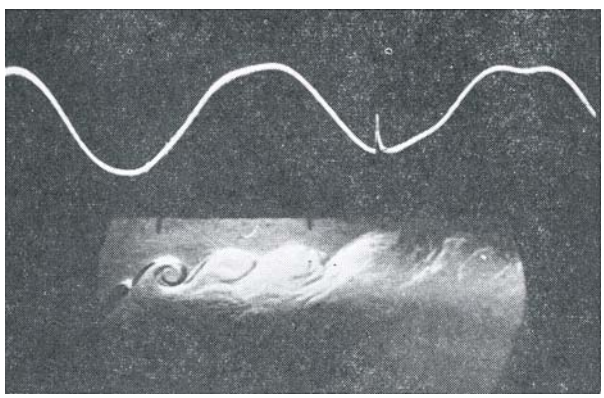

FIGURE 2.38. Photograph of vortices shed in a reacting flow (Kaskan and Noreen 1955).

Motivated partly by earlier observations of Blackshear (1953) and Putnam and Dennis (1953), Kaskan and Noreen proposed a different mechanism, speculating that stretching of the flame front accompanying roll-up in the vortex causes a pressure disturbance. Periodic disturbances generated by vortex shedding may then sustain either transverse or longitudinal acoustic fields. (They observed both in their tests, but transverse waves were most common.) As a quantitative basis for interpreting their results they modified a theoretical relation derived by Chu (1953) for plane flames. Although they had modest success comparing their reasoning with their data, Kaskan and Noreen did not provide a complete explanation of the closed-loop process required to generate self-excited oscillations. This mechanism has subsequently received much notice as a possible cause for combustion instabilities after the idea was revived in the 1980s in connection with work on ramjet combustion. More recently, several groups have used the idea of changing flame to represent a possible mechanism in problems of active control; for example see Section 2.5.

During the past twenty years, the idea that vortex shedding is a dominant factor in mechanisms for many combustion instabilities in liquid-fueled systems has gained growing support. Practically all of the work has been motivated by problems of longitudinal oscillations in ramjet engines. Even though the frequencies are

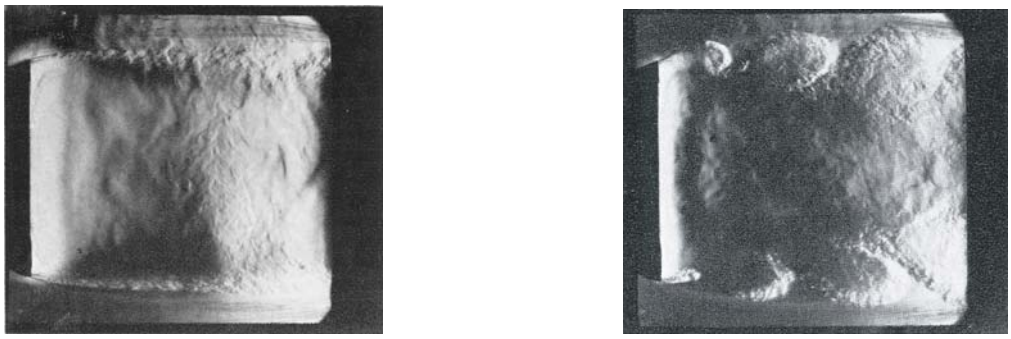

(a) (b)

FIGURE 2.39. Flow past a bluff body flameholder under two conditions of flow at approximately the same speed. (a) low equivalence ratio, $\phi\tilde{<}0.75$, no oscillations; (b) high equivalence ratio $\phi\tilde{>}0.90$, acoustic oscillations in the channel (Rogers and Marble 1956).

substantially lower than those of the oscillations treated by Rogers and Marble, the essentials of the idea seem to hold true.

The problem of longitudinal oscillations in ramjet engines was found quite early in their development although the direct connection with instabilities in combustors was not immediately clear (Conners 1950). Longitudinal oscillations in small ramjet engines was apparently first recognized by Hall (1978). Rogers (1980a, 1980b) gave thorough summaries of the available experimental work. Those reports marked the beginning of widespread attention and work which continued until the early 1990s. In particular, Rogers' investigation served as the basis for an early analysis of the problem by Culick and Rogers (1983); that work did not include a satisfactory mechanism. Vortex shedding as a possible mechanism for causing the longitudinal modes in a ramjet engine seems to have been discussed first at a JANNAF workshop in 1979 (Culick 1980). Byrne (1981, 1983) gave the first detailed discussion of the mechanism. His 1983 paper is a very nice description of the problem and touches on several problems understood only later, in particular with work at the Naval Weapons Center. Apparently unaware of the earlier work by Rogers and Marble on transverse oscillations, Byrne based his argument on established results for cold jet flows. He used known results for the stability of shear layers and jets, vortex shedding and vortex merging to argue that the frequencies of those processes taking place under the conditions occurring in ramjet engines are in the range of frequencies of the oscillation actually observed. He supported his conclusions by good comparisons of his estimated frequencies with data taken by others for both coaxial and side-dump configurations. Waugh *et al.* 1983 showed modest success in their Appendix B correlating amplitudes of instabilities with Strouhal number.

Since the early 1980s a great deal of attention has been given to the role of vortex shedding in dump combustors, both in cold flow and in laboratory combustion tests (e.g., Keller *et al.* 1982; Smith and Zukoski 1985; Biron *et al.* 1986; Schadow 2001; Sterling and Zukoski 1987; Poinsot *et al.* 1987a,b; Yu *et al.* 1987a,b). There is little doubt now that indeed the coupling between shed vortices and the acoustic field is the dominant mechanism in dump combustors. That coupling may or may not be accompanied by energy release due to combustion. The extent to which the same mechanism is active in contemporary thrust augmentors is less well-established but there is good reason to believe that it is often the main cause.

Extensive experimental work on vortex shedding in shear layers and jets at room temperature has provided a fairly complete picture of the formation of vortices; vortex pairing; and the general features of the flow without heat addition (see Schadow *et al.* 1987b for a brief review of the literature relevant to problems in ramjet engines). Tests in various configurations, including those appropriate to ramjets (e.g., Flandro *et al.* 1972; Culick and Magiawala 1979; Dunlap and Brown 1981; Brown *et al.* 1981, 1983; Schadow *et al.* 1987,

1989; Schadow and Gutmark 1992; Schadow 2001) established the ability of shed vortices to drive acoustic resonances over a broad range of flow conditions. See Section 8.6 for further discussion of experimental work on vortex shedding with no combustion. The works cited above have extended that conclusion to flows with large heat addition accompanying combustion under circumstances simulating those found in actual ramjet engines. We will discuss those results further in Section 8.6.

The obvious qualitative importance of combustion in large vortices has prompted several analytical investigations of the process. Broadly the idea is that the shear layer is formed at the edge of a bluff body, the high speed stream consisting of an unburnt mixture of reactants; the low speed stream is composed largely of hot combustion products forming the recirculation zone behind the body. As Smith and Zukoski (1985) and Sterling and Zukoski (1987) have shown, the shear layer exhibits widely varying degrees of stability depending on the operating conditions. We are concerned here with cases when the layer is highly unstable, a situation encouraged by the action of the acoustic velocity forcing oscillations of the layer at the lip. Large vortices may then rapidly form, entraining unburnt mixture on one side of an interface, with the combustion products on the other side. A flame is initiated at the interface and the question to be answered is: how does the rate of combustion, and therefore heat release, vary as the vortex rolls up and propagates downstream?

Marble (1984) treated an idealized case of a diffusion flame initiated along a horizontal plane when simultaneously the velocity field of a line vortex is imposed along an axis in the interface. Elements of flame initially in the interface are caused to execute circular motions and are stretched by the vortex field, causing an increase in the rate at which reactants are consumed. The expanding core contains combustion products but as the vortex roll-up continues, the rate of consumption always remains greater than that for flame in the flat interface having the same length as that in the rolled-up vortex. Karagozian and Marble (1986) carried out a similar analysis accounting for the influence of stretching along the axis of the vortex. They found that, following a transient period during which the core grows to its asymptotic form, the augmented consumption rate is unaffected by axial stretching. In those cases the rate of heat release reached a constant value monotonically: there is no distinguished period of pulsed combustion as required for the mechanism for instability described above.

Subsequently, Laverdant and Candel (1987a,b; 1988) analyzed both diffusion and premixed flames in the presence of vortex motion with finite chemical kinetics. Their analysis is entirely numerical giving good agreement with the results obtained by Karagozian and Marble (1986) and Karagozian and Manda (1990) for a vortex pair.

Norton (1983) also analyzed the influence of finite chemical kinetics in the problem posed and solved by Marble (1984) who had assumed infinite reaction rates. Under some conditions, the heat release rate shows a modest peak in time. However, neither his results, nor those of Laverdant and Candel, suggest the sort of time delay to pulsed combustion one might like to see to complete the picture.

No work has been accomplished to determine whether or not the augmented reaction rates found in the analyses are sufficient to explain the mechanism of instabilities driven by vortex combustion. On the other hand, the experimental results reported by Smith and Zukoski (1985), Sterling and Zukoski (1987), and Yu *et al.* (1987)a,b show vividly and beyond doubt that unsteady combustion associated with vortex motions is a vigorous source indeed. Figure 2.40 is a sequence of photographs taken by Smith and Zukoski during one cycle of a high amplitude oscillation. They propose the following mechanism. A vortex is initiated at the edge of the step at a time determined partly by the local acoustic velocity. The vortex propagates downstream, releasing energy of a rate that seems to reach maximum when the vortex impinges on the wall. In order for impingement to occur at a favorable time during the acoustic oscillation, the propagation rate and hence strength of the vortex must increase with frequency. Because the vortex strength depends on the magnitude of velocity fluctuation initiating the motion at the lip, it is necessary that the steady amplitude of the acoustic field increase with frequency. That behavior is observed. Moreover, numerical calculations

by Hendricks (1986) have shown quite similar behavior for the unsteady flow induced by an abrupt change of velocity past a rearward-facing step. Figure 2.41 is a sketch taken from Hendricks' work showing the development of a vortex calculated for those conditions.

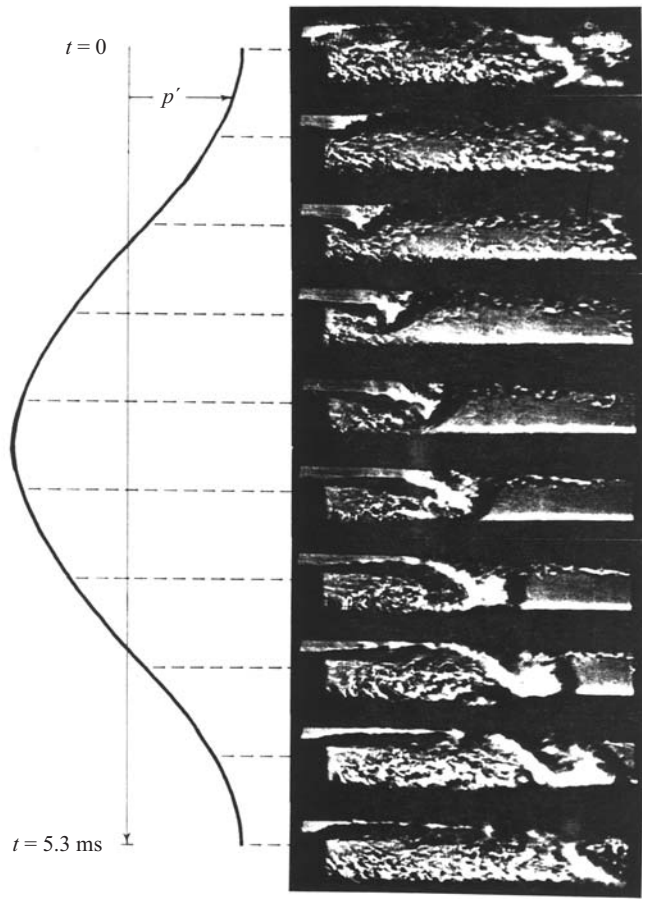

FIGURE 2.40. Development of a vortex during one cycle of a pressure oscillation (Smith and Zukoski 1985).

The essential ideas of vortex combustion as a mechanism for driving instabilities can be incorporated in the approximate analysis developed here. There is ample experimental evidence that large vortices in cold flow can sustain resonances in a duct; Flandro (1986) has shown one means of handling the process analytically, based on direct fluid mechanical coupling between vortical and acoustic motions. See also Aaron (1984) and Aaron and Culick (1985) for an elementary model of coupling associated with impingement of a vortex on an obstacle. Tests with combustors have shown, however, that the amplitudes of oscillation are substantially greater when burning occurs. That result is most likely due to the unsteady energy release. We therefore assume that this is the main source of the driving.

Hence in the forcing function F_n^L, equation (1.21), we retain only the term containing Q', giving equation (1.23) written now for the time-dependent amplitude of the nth mode:

$$\frac{d^2\eta_n}{dt^2} + \omega_n^2\eta_n = \frac{\gamma - 1}{\overline{p}E_n^2}\int \psi_n \frac{\partial Q'}{\partial t} dV \tag{2.109}$$

A formula for Q' must be constructed to account for the trajectory of the vortex and its associated rate of energy release along the trajectory. To illustrate with a simple example, we consider excitation of longitudinal

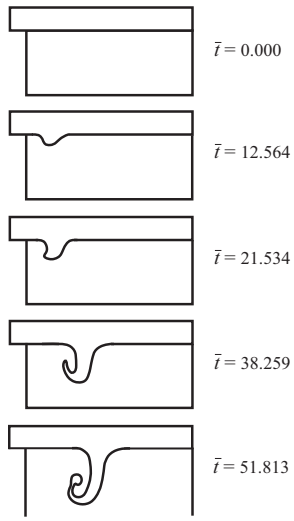

FIGURE 2.41. Development of a vortex at the interface of two unlike fluids (Hendricks 1986).

modes and assume that the vortex travels parallel to the axis. Within the one-dimensional approximation, that implies averaging the presence of the vortex over planes transverse to the axis. The situation is sketched in Figure 2.42. The origin $z = 0$ is at the step, which is not the location of a pressure anti-node. In fact, we must allow the acoustic velocity to be non-zero at the beginning of the shear layer at $z = 0$, so the mode shape is

$$\psi_n(z) = \cos(k_n z + \phi) \tag{2.110}$$

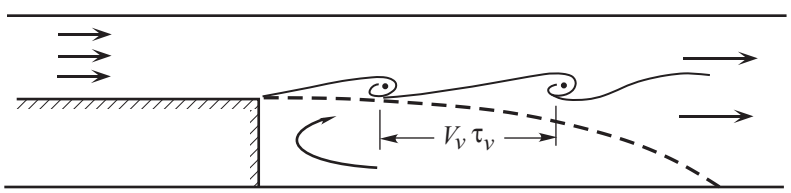

FIGURE 2.42. An elementary model of combustion in vortices as a mechanism for driving acoustic waves.

The values of k_n and ϕ can be set by imposing a boundary condition at $z = l$ and choosing some location $z < 0$ for a pressure anti-node. For example, if pressure anti-nodes occur at $z = -\delta L_0$ and $z = L + \delta L_1$, the two conditions must be satisfied

$$\begin{aligned} \sin(-k_n \delta L_0 + \phi) &= 0 \\ \sin[k_n(L + \delta L_1) + \phi] &= 0 \end{aligned} \tag{2.111}$$

from which k_n and ϕ can be determined. For the purposes here, the particular values of k_n and ϕ are immaterial. With (2.110), the acoustic pressure and velocity are

$$\begin{aligned} p' &= \overline{p}\eta_n(t)\cos(k_n z + \phi) \\ u' &= \frac{\dot{\eta}_n}{\overline{\gamma} k_n}\sin(k_n z + \phi) \end{aligned} \tag{2.112)a,b}$$

For simplicity, assume that the vortices propagate with constant speed v_v and are launched periodically with period τ_v at the times $t = 0$, τ_v, $2\tau_v$, $\cdots$. Assume further that these are point vortices releasing energy

at the rate $q(t)$ each. Hence the energy release associated with a train of shed vortices can be represented by δ-functions moving with speed v_v, multiplying the energy release:

$$\begin{aligned} Q'(z_1 t) &= q_1(t)\delta[z - v_v t] + q_2(t)q[z - v_v(t - \tau_v)] + q_3(t)\delta[z - v_v(t - 2\tau_v)] + \cdots \\ &= \sum_{j=0}^{\infty} q_j(t)\delta[z - v_v(t - j\tau_v)] \end{aligned} \tag{2.113}$$

In accordance with the behavior reported by Smith and Zukoski we should relate the strength of each vortex and, therefore by assumption its energy release, to the velocity fluctuation causing its birth. For simplicity we ignore the influence of the mean flow speed and set q_j proportional to the acoustic velocity at the step and at the time when the vortex is launched. Hence, we assume

$$q_j(t) = \overline{q}_j(t)u'(0, j\tau_v) = -\overline{q}_j(t)\frac{\dot{\eta}_n(j\tau_v)}{\overline{\gamma}k_n}\sin\phi \tag{2.114}$$

where $q(t)$ is supposed to be common to all vortices. With (2.114) for $q_j(t)$, differentiate (2.113):

$$\frac{\partial Q'}{\partial t} = -\sum_{j=0}^{\infty}\frac{\dot{\eta}_n(j\tau_v)}{\overline{\gamma}k_n}\sin\phi\left\{\dot{\overline{q}}_j\delta[z - v_v(t - j\tau_v)] - \overline{q}_j v_v\delta[z - v_v(t - j\tau_v)]\right\} \tag{2.115}$$

Now substitute (2.110) and (2.115) in the integral on the right-hand side of (2.107), with $dV = S_c dz$ where S_c is the cross-section area of the chamber:

$$\int \psi_n\frac{\partial Q'}{\partial t}dV = S_c\int_0^L \cos(k_n z + \phi)\sum_{j=0}^{\infty}\frac{\dot{\eta}_n(j\tau_v)}{\overline{\gamma}k_n}\sin\phi\left\{\dot{\overline{q}}_j\delta[z - v_v(t - j\tau_v)] - \overline{q}_j v_v\delta[z - v_v(t - j\tau_v)]\right\}dz$$

Use the properties

$$\int \delta(x - a)f(x)dx = f(a); \quad \int \delta'(x - a)f(x)dx = -f'(a)$$

to find:

$$\begin{aligned} \int \psi_n\frac{\partial Q'}{\partial t}dV = &- S_c\sum_{j=0}^{\infty}\xi_{nj}\left\{\dot{\overline{q}}_j(t)\cos[k_n v_v(t - j\tau_v)]\right. \\ &\left. + \overline{q}_j(t)k_n v_v\sin[k_n v_v(t - j\tau_v)]\right\} \end{aligned} \tag{2.116}$$

with

$$\xi_{nj} = \frac{\dot{\eta}_n(j\tau_v)}{\overline{\gamma}k_n}\sin\phi \tag{2.117}$$

Thus we have an expression for the right-hand side of (2.107) representing the forcing due to a train of burning vortices, launched at $t = 0$, τ_v, $2\tau_v$, ... from the lip of the step at $z = 0$. This model has been the starting point for two analyses by Matveev and Culick, 2002b and 2003a; the following section is a summary of the work.

By far most attention has been directed to vortex shedding as the most likely mechanism for combustion instabilities in ramjet engines, although recently more attention has been paid to the phenomenon in gas turbines. In addition to extensive experimental work related to those ideas, much has been done, both with laboratory tests and analysis, to clarify the acoustical characteristics of the modes of oscillation. Much more is known, and understood, about vortex shedding and its role as a mechanism for causing combustion instabilities chiefly because that phenomenon is easily identified in experiments and is commonly encountered. Although vortex shedding is arguably the dominant feature causing instabilities in dump combustors—and might therefore be termed the most important mechanism—it cannot be separated completely from convective waves. Furthermore, neither mechanism can be understood apart from the acoustics of the chamber

in which they occur; the type of mode that is unstable always provides some clues about the mechanism. For convenience here we nevertheless treat the phenomena separately. One distinction between the two mechanisms that seems to be true, is that if direct coupling between large vortices and the acoustics field dominates, the frequencies of oscillations tend to be close to those of classical resonances. If convective waves are involved, the frequencies may be quite different, as shown with the elementary example in Section 2.3.3.

As we discussed above, the earliest ideas based on vortex shedding were developed in the 1950s to explain the occurrence of high frequency transverse or tangential waves in afterburners. Periodic combustion of reactants entrained in large vortex structures served as sources of acoustic energy. If properly phased, the sources may supply energy to an acoustic mode of the chamber. The fluctuations of velocity associated with the mode initiate vortex shedding, completing the cycle.

Roughly two decades later vortex shedding was again proposed as a possible mechanism for instabilities in solid rockets, but periodic combustion was not part of the argument (Flandro and Jacobs 1975; Culick and Magiawala 1979). Laboratory tests in cold flow established the result that if vortices shed from a step or corner impinge on an obstacle downstream, there is sufficient coupling with unsteady motions to excite the sustain standing acoustic modes in a duct (Culick and Magiawala 1979; Dunlap and Brown 1981; Dunlap *et al.* 1981; Nomoto and Culick 1982; Aaron and Culick 1985). In all those cases, longitudinal modes were driven. Large "vortex-like" structures were observed in some flow visualization work on dump combustors at AFWAL sometime in the late 1970s [Private communication, F.D. Stull].

Since 1980, a large number of experimental works have established both by visualization and quantitative measurements that vortex shedding is a distinctive feature of dump combustors. (Schadow *et al.* 1985, 1987b; Smith and Zukoski 1985; Brown *et al.* 1985; Biron *et al.* 1986; Sterling and Zukoski 1987; Poinsot *et al.* 1987; Yu *et al.* 1987; Davis and Strahle 1987). All of those tests were performed either in cold flow or with premixed gaseous reactants. The most extensive summary of the subject has been given by Schadow *et al.* (1987b) who included also references to related work not discussed here.

The work by Schadow and co-workers at the Naval Weapons Center (e.g., see the summary by Schadow and Gutmark 1992) is particularly noteworthy for its systematic progression from tests in cold flow to experiments in dump combustors with burning, as well as for studies of vortex combustion in diffusion flames. Their program used at least four different experimental facilities and involved both forced and self-excited oscillations. They also performed limited tests in a water tunnel to show the formation of large vortices in their configuration. Overall, the work at NWC established the existence of vortex shedding at the frequencies of instabilities in realistic coaxial configurations. Moreover, they showed that combustion processes drive oscillations to much higher amplitudes than found in the cold flow tests. We should emphasize that for the cases cited earlier, of oscillations driven by vortex shedding in solid rocket motors, the vortices were formed in essentially non-reacting combustion products. The amplitudes of such instabilities have always been relatively small (<5% of mean pressure). Thus it seems true, as found also in the work by others cited above, that truly large amplitude oscillations require the presence of combustion processes and the conversion of heat released to mechanical energy.

Hegde *et al.* (1986, 1987) and Reuter *et al.* (1988) studied oscillations in a duct driven by a flame sheet, in a situation similar to that devised by Kaskan and Noreen (1955) and by Dowling and co-workers at Cambridge for afterburners (Figure 2.57). In the Georgia Tech tests by Hegde *et al.*, the flame (or flames) is stabilized on one or two wires spanning a duct. Under broad conditions, the flame is unstable and vortices grow in the sheet. Interactions with the flow field are sufficiently strong to excite acoustic waves in the duct. The authors proposed that fluctuations of the flame surface area—and hence of the reaction rate are responsible. They gave data based on emitted radiation, showing that the oscillations of surface area are in phase with the pressure variations. By Rayleigh's Criterion (Section 6.6) for heat addition, it follows that

the heat addition encourages growth of acoustic waves, a result established also by Sterling and Zukoski (1987) for a dump combustor.

Although most experimental work related to vortex shedding in ramjets has been done with coaxial configurations, the phenomenon has also been found in side-dump combustors. Stull *et al.* (1983) reported early work with that geometry and Nosseir and Behar (1986) have examined similar cases in a small scale. More extensive results with full-scale hardware were discussed by Zetterström and Sjöblom (1986) who investigated a configuration having two or four inlets. Visualization in a water tunnel revealed the presence of vortex shedding. Instabilities in the operating engines were avoided by modifying the fuel injection systems in such a fashion as to minimize combustion within the vortices. That's an important practical result clearly supporting the general picture of vortex shedding as a dominant mechanism.

2.3.5. A Model for Vortex Shedding and Excitation of Acoustic Waves. Despite the widespread recognition of vortex shedding as an important mechanism for the excitation of oscillations in dump combustors, there is no analysis that captures the main features of the process. Since the early observation and interpretations by Kaskan and Noreen (1955) and by Rogers and Marble (1956) there have been a number of experimental works, especially motivated by problems with ramjets in the 1980s and 1990s. There are few theoretical works and they have produced only modest success. The basic ideas are probably understood correctly, but until they have been successfully developed into a predictive theory, one cannot be sure. In this section we summarize one recent attempt to construct a quantitative description of the basic process, based on the model sketched in Figure 2.42.

Expressed in simplest terms, the central idea in most, if not all, treatments of the excitation of acoustic waves by vortex shedding and combustion is simply stated. Vortices are periodically generated, at a backward-facing step in the present case, propagate downstream with little or no burning, and at some later time undergo vigorous combustion, releasing "pulses" of energy. The energy added in a small volume is accompanied by a rapid rise of pressure locally, which is available to augment the pressure in the flow. Whether a sequence of such pulses will in fact cause a wave, or a mode of oscillation, to be sustained is a matter to be worked out by available methods for solving problems of acoustics with sources in a finite volume, a combustor. The simplest governing equation for the process is (2.109), with a damping term included to agree with Matveev and Culick (2003):

$$\frac{d^2\eta_n}{dt^2} + 2\zeta_n\omega_n\frac{d\eta_n}{dt} + \omega_n^2\eta_n = \frac{\gamma-1}{\overline{p}E_n^2}\int \psi_n\frac{\partial\dot{Q}}{\partial t}dt \tag{2.118}$$

The unsteady motions are treated as one-dimensional, but small deviations can be accommodated in $\psi_n(x)$. That is a relatively minor deviation here. We are primarily concerned with the action of periodic burning in vortices which are small compared with characteristic dimensions of the enclosing volume or chamber. A basic assumption is that the burning occurs instantaneously and releases an amount of energy that is proportional to the circulation Γ_j of the jth vortex. Passing to the limit of point vortices, we use the expression for $\dot{Q}$,

$$\dot{Q} = \beta\sum\Gamma_j\delta(x-x_j)\delta(t-t_j) \tag{2.119}$$

where β is a constant to be given a value later. To be definite, we suppose that instantaneous burning occurs when a vortex strikes a wall or obstacle, Figure 2.43, or after an induction time as described by Rogers and Marble (1956).

A shed vortex moves with the total flow velocity at the instantaneous position of the vortex. For the case shown in Figure 2.42 a vortex located close to the boundary between the recirculation zone and the primary flow moves with a speed $\dot{x}_j$ which may be approximated as

$$\dot{x}_j(t) = \alpha\overline{u}(x_j) + u'(x_j,t) \tag{2.120}$$

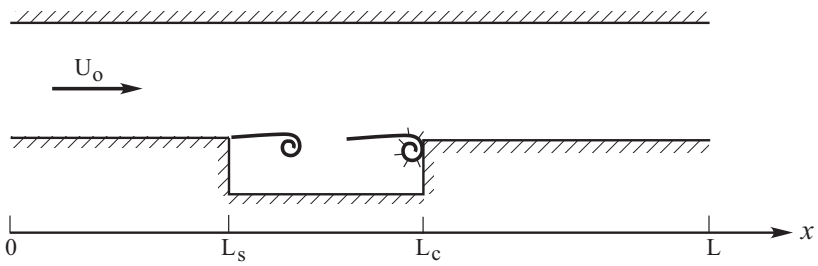

FIGURE 2.43. Vortex shedding from a backward-facing step, followed by impingement on an obstacle.

where α usually lies in the range 0.5 – 0.6 (Dotson *et al.* 1997) for segmented rocket motors. With (2.120) substituted in (2.119), the equation governing η_n in the time interval (t_{j-1}, t_{j+1}) is

$$\ddot{\eta}_n + 2\zeta_n\omega_n\dot{\eta}_n + \omega_n^2\eta_n = c\psi_n(x_j)\Gamma_j\dot{\delta}(t - t_j) \tag{2.121}$$

Following Andronov *et al.* (1987), (2.121) gives the usual result for the motion of an oscillator in the interval (t_{j-1}, t_{j+1}) except at the instant t_j when the jump conditions are satisfied:[22]

$$\begin{aligned} \eta_n(t_j+) - \eta_n(t_j-) &= c\psi_n(x_j)\Lambda_j \\ \dot{\eta}_n(t_j+) - \dot{\eta}_n(t_j-) &= 0 \end{aligned} \tag{2.122)a,b}$$

The relation (2.122)b means that the velocity is instantaneously unchanged while the amplitude η_n changes discontinuously by the amount $c\psi_n(x_j)\Gamma_j$ at the instant t_j. Such behavior is characterized as that of a "kicked" oscillator.

The time at which a vortex separates from the step, and its strength are modeled following the idea introduced by Clements (1973). A vortex is formed from the vorticity contained within the thickness of the boundary layer shed from the step. With a relatively simple argument the result for the circulation of a shed vortex is

$$\Gamma = \frac{\overline{u}D}{2St} \tag{2.123}$$

where D is a characteristic dimension roughly equal to the momentum thickness of the boundary layer and St is the Strouhal number for vortex shedding at frequency $f_s : St = \frac{\overline{u}}{f_s D}$. The formula (2.123) has the interpretation that a vortex detaches from a step when its circulation reaches the "critical" value given by the right-hand side of (2.123). Matveev and Culick propose that a vortex is shed in unsteady flow when its circulation reaches the value given by (2.123) with $\overline{u}$ replaced by the instantaneous velocity $\overline{u} + u$:

$$\Gamma(t) = \frac{u(t)D}{2St} \tag{2.124}$$

The Strouhal number is assumed to have the same value in steady and unsteady flow. This formula shows fairly good argument with experimental results for vortex shedding from a rising in oscillatory flow (Castro 1997). However, the result has been only weakly tested; perhaps most seriously, data is available only for isothermal flows.[23]

The model was used by Matveev to calculate a two-dimensional case, Figure 2.43, representative of the experimental results reported by Smith (1985), Sterling (1987), Smith and Zukoski (1985), and Sterling and Zukoski (1991). The damping coefficient was set according to information provided by Sterling and Zukoski,

$$\zeta_n = \frac{1}{2\pi}\left(0.135\frac{\omega_n}{\omega_1} + 0.015\sqrt{\frac{\omega_1}{\omega_n}}\right) \tag{2.125}$$

[22]Damping is neglected ($\zeta_n = 0$) for derivation of these conditions.
[23]Schadow and Gutmark (1992) have discussed vortex shedding for various geometries in isothermal and reacting flows.

in which end losses are represented by the first term and the second term accounts for the attenuation due to acoustic boundary layers. As identified by Smith, five acoustic modes were accounted for, having frequencies (in Hertz) 180, 229, 385, 470, and 590. Values for the various parameters in the model, and reasons for the choices, are given by Matveev and Culick (2002)b, (2003)a and by Matveev (2004). With (2.121), (2.122)a,b and (2.124), the unsteady pressure field may be estimated. Figure 2.44 shows some results.

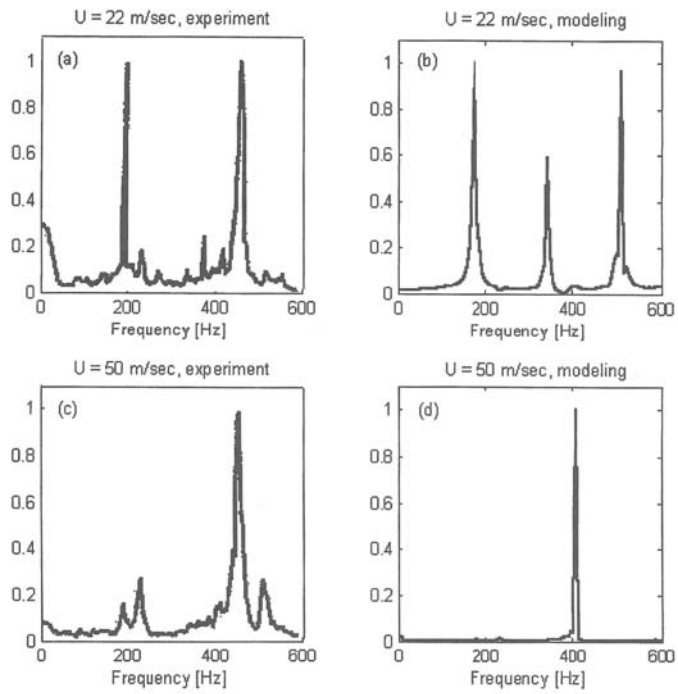

FIGURE 2.44. Normalized spectra of pressure fluctuations at the step of Figure 2.43 for two mean flow velocities at the dump plane. (a), (c) experimental results (Smith 1985); (b), (d) results from the kicked oscillator model.

In its present state, the 'kicked oscillator' model has no practical value except as a view or interpretation of a mechanism for oscillations in a combustor. The analysis we have briefly and incompletely described is suggestive and has wider possibilities than discussed here. This example illustrates the relative ease with which results can be obtained without tedious integration of the partial differential equations governing 'exact' solutions.

2.4. Further Remarks on Particular Forms of Liquid-Fueled Systems

Most of the discussion in Section 2.3 was concerned with matters common to all types of liquid-fueled systems. Much of the work was in fact carried out in the U.S. originally for liquid fueled rockets, the strongest motivation being applications to engines intended for the Apollo vehicle. Some of the ideas and methods developed for liquid rockets have subsequently been modified or extended for analysis of combustion instabilities in augmentors and ramjets. Moreover, there are special problems peculiar to the different systems themselves. We therefore examine now those particular matters.

2.4.1. Combustion Instabilities in Liquid Rockets. Little work was done outside the USSR on the problem of instabilities in liquid rockets during the 1970s. With the flight failure of an Ariane vehicle due to combustion instability in a first stage Viking motor, a comprehensive research program was initiated in France in 1981. Most of the available reports of that work have already been referred to and little more needs to be added here.

Within the present context, the most important parts of the French work are the experimental and analytical efforts to characterize the liquid spray; and the extensive numerical simulations of unsteady motions, incorporating the results obtained for the propellant sprays. The problem causing the failure involved coupling between the pressure oscillations in the chamber and structural vibrations of the injector which is placed in the lateral boundary as sketched in Figure 2.45 taken from Souchier, Lemoine and Dorville (1982). Figure 2.45(b) shows the computed distortion of the injector plane. As a result, the fuel and oxidizer jets were shaken, causing (apparently) perturbations of the distribution and phase of the energy release, thereby closing the loop and making possible self-excited motions.

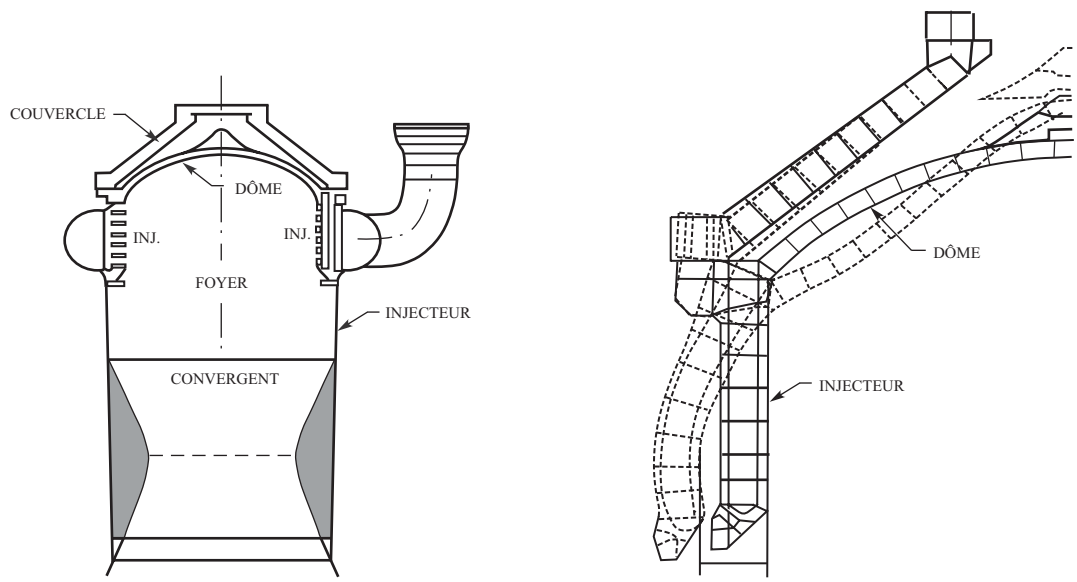

FIGURE 2.45. Coupling between pressure oscillations, structural vibrations and the injection system (based on drawings appearing in Souchier, Lemoine and Dorville 1982).

Such effects on the injection processes have long been known to be a possible cause of instabilities (Levine 1965; Harrje and Reardon 1972) but they have yet to be well-characterized.[24] They are likely to be particularly important in cases when the amplitudes of motion are large. It is quite possible that the forms of the representation of the unsteady sources of mass and energy are strongly dependent on the amplitudes of motion as well as on the hardware design. Such behavior is far outside any successes of the time lag model and is likely to remain so. Careful experimental work is essential to clarify the situation.

During the mid-1980s, serious interest in developing new liquid-fueled rockets grew in the U.S., primarily for use in proposed heavy lift launch vehicles. Because of their high densities and good performance, liquid oxygen and hydrocarbon fuels were considered as propellants. In particular, methane was selected by the NASA Lewis Research Center is the favored fuel. As a result, studies of combustion instabilities were carried out at the Aerojet TechSystems Company and at the Rocketdyne Division of Rockwell International.

[24]The more recent work by Bazarov, cited briefly in Section 8.5, has done much to correct this situation.

Rocketdyne designed and fabricated two engines, for the Lewis Research Center (LeRC) and for the Marshall Space Flight Center(MSFC). Both used LOX/methane and had identical thrust chambers but different injectors. The MSFC engine had an acoustic resonator; the LeRC engine had no damping device. A small number of firings directed to determining stability characteristics were completed (Jensen, Dodson and Trueblood 1988; Philippart and Moser 1988).

A computer program for analysis of instabilities was developed from an earlier program, IFAR. (Fang 1984, 1987; Fang and Jones 1987; Mitchell, Howell and Fang 1987; Nguyen 1988). The program IFAR (Injector Face Acoustic Resonator) had been in existence for some years; the time lag model was used to represent the combustion process. That program was revised and modified for application to both rectangular and axisymmetric chambers to become HIFI (High Frequency Intrinsic Stability) (Nguyen 1988).

With all other variables and parameters specified, the values of n and τ are calculated on the stability boundary. Then to predict whether the engine is stable or not, the values of n and τ must be determined. Traditionally this has been done with correlations for injectors using hydrocarbon fuels, so as part of their work the group at Aerojet performed sub-scale tests and carried out analysis of the injector response (Muss and Pieper 1987; Nguyen and Muss 1987). The analysis and tests were intended to provide correlations of n and τ for the injector with those on the stability boundary calculated with the analyses cited above.

Aerojet carried out a program combining analysis, sub-scale tests using both rectangular and axisymmetric chambers prior to full-scale firings. The chief purpose was to provide as certain as possible basis for confidently predicting the stability of the large engines, thereby reducing development costs. This program was described by Muss and Pieper (1988).

Philippart (1987) and Philippart and Moser (1988) reported comparisons of predictions of the sort mentioned above, with firings of the two Rocketdyne engines. One operating condition was examined for which the LeRC engine was stable and the MSFC engine was unstable. Three calculations of the stability boundary in the $n - \tau$ plane were done, using the program IFAR, HIFI and a modified from (NDORC) of Mitchell and Eckert's (1979) MODULE. Figure 2.46, taken from Philippart and Moser, shows the results obtained with HIFI for the two engines. Results obtained with the other two programs differ in details that are unimportant here. Also shown as filled regions are estimates of the 'combustor response' (i.e. the values of n and τ) based on correlations for LOX/hydrogen injectors. Apparently the predictions of the three codes agreed fairly well. However, there are uncertainties owing to differences between the codes; a significant distinction is that IFAR and HIFI assume that combustion is concentrated in a transverse plane, while MODULE is written for distributed combustion. Comparison with the test data is ambiguous and must be viewed as estimates because the true characteristics of the injectors are unknown.

Jensen, Dodson and Trueblood (1988) gave an early progress report in their tests with the LeRC engine. They measured growth rates and, using the MODULE program, inferred the necessary values of n and τ. Two examples are shown in Figure 2.47. The striking result is that the values of the interaction index are found to be considerably greater than those computed by Philippart and Moser and those provided by previous correlations of data. It is impossible at this point to determine the cause for these differences. The existence of such significant differences probably betrays the absence of a fundamental basis and understanding of any *ad hoc* approach based on a time lag 'model'.

Also at Rocketdyne some interesting work to analyze the characteristics of sprays vaporizing and burning under steady conditions was reported by Liang *et al.* (1986, 1987a,b,c). The calculations were done for various injector types placed in chambers, with provision for computing the internal flow field. When extended to cover transient motions, this work seemed to be potentially an important contribution to analysis of combustion instabilities but it seems that the potential was not realized. Indeed, it appears that among the

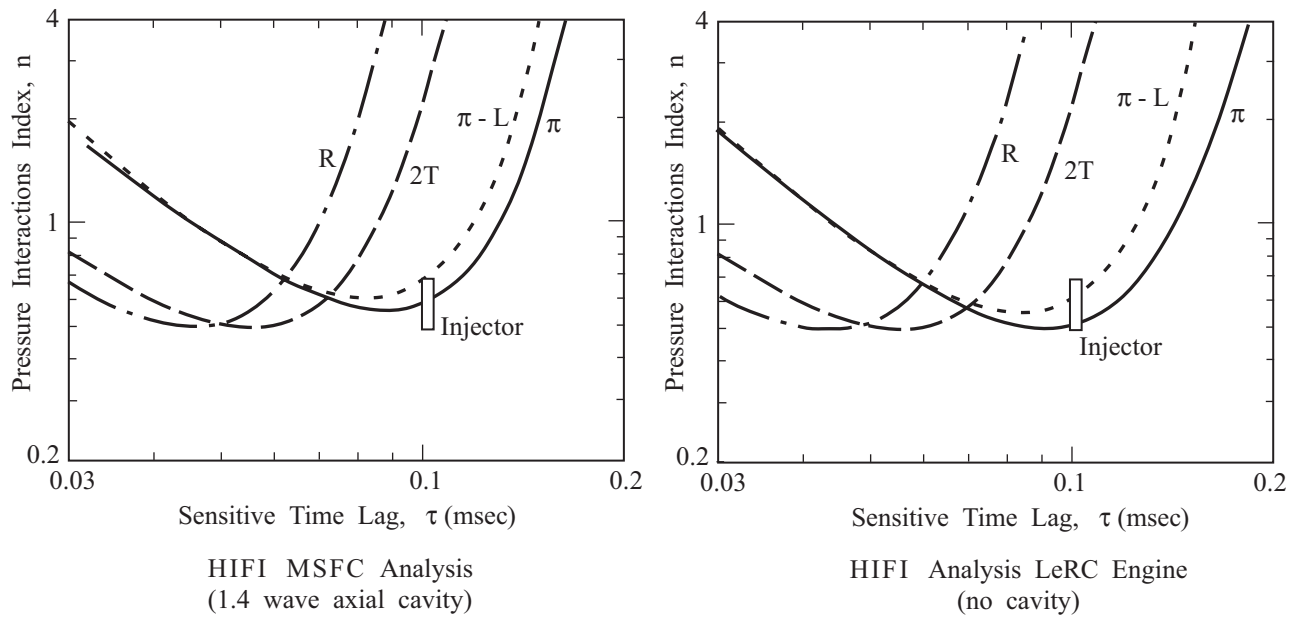

FIGURE 2.46. Some results of calculations based on the n-τ model (Philippart and Moser 1988).

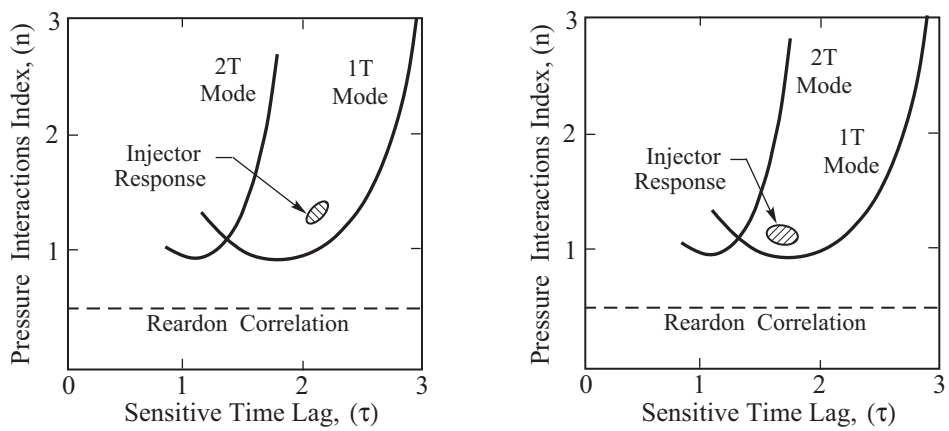

FIGURE 2.47. Comparison of calculations and some experimental results interpreted with the n-τ model (Jensen, Dodson and Trueblood 1988).

most important outstanding problems in the subject are the production of the liquid drops; unsteady spray combustion; and incorporation of the results in a complete formation allowing realistic numerical simulations.

2.4.2. Application of the Time Lag Model to Gas and Liquid Rockets. By 'time lag model' we mean here the most common form, expressed by equation (2.94) for the unsteady conversion of liquid to gas. Crocco and Cheng (1956) examined various elaborations, including spatial variations of the sensitive time lag, but here we shall assume τ to be uniform everywhere and the same for all elements of injected propellant. Also we will not distinguish between oxidizer and fuel. Both assumptions have been adopted in almost all applications, a notable exception being an analysis of chugging in which two time lags were introduced (Szuch and Wenzel 1968).

Although some analysis has been done of nonlinear behavior with the time lag model (see Chapter 7 for work by Sirignano and Crocco 1964; Mitchell, Crocco and Sirignano 1969; and Mitchell and Crocco 1969) by far most results, and all applications, have been worked out for linear behavior. To illustrate here, we appeal to the approximate analysis described later. Although differences in detail will arise, the results will contain all the essential ideas discussed in previous works.

Broadly, the central idea is to use the formula for the growth constant, α, *evaluated on the stability boundary,* so $\alpha = 0$. Those terms containing ω will of course depend on the interaction index, n, and the time lag, τ. If we assume that all other contributions to the formula are known, then the condition $\alpha = 0$ provides a relation between n and τ that must, within the approximations used, hold on the stability boundary.

There is no need to work out details here; see Chapter 6. The equation defining α will take the form

$$\alpha = C_1 \int \psi_n \hat{w}_l^{(r)} dV - C_2$$

where C_1, C_2 are constants. The constant C_2 contains the various effects of liquid/gas interactions, the nozzle, mean flow/acoustics interactions and damping devices. Now with $\hat{w}_l$ given by (2.94), its real part is $n(1 - \cos\omega\tau)$, and for $\alpha = 0$, the last equation gives

$$n(1 - \cos\omega\tau) = \frac{C_1}{C_2 \int \overline{w}_l \psi_n^2 dV} = G_R \tag{2.126}$$

The function G_R is supposed to be known, with value depending on the various parameters (geometrical, etc.. . .) defining the system. Then equation (2.126) is the relation between n and τ referred to above.

Figure 2.48 shows the unstable regions defined by equation (2.126). This is a reproduction of Figure 4.2.2a, p. 180, in an article prepared by Crocco (Harrje and Reardon 1972). The calculations carried out by Crocco were quite different from those summarized here, but the result has the same form, another illustration of the fact that there is, in a deep sense, only one 'linear stability problem'. Differences in detail among analyses arise only because representations of processes, and therefore characteristic parameters, may differ.

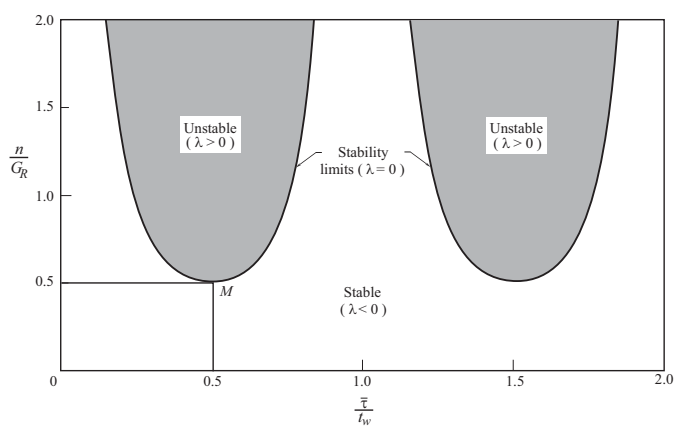

FIGURE 2.48. A general representation of stability based on the $n-\tau$ model (Crocco, Figure 4.2.2a in Harrje and Reardon 1972).

In this normalized form, Figure 2.48 is a kind of universal chart for the $n-\tau$ model. The multiple regions appear because of the factor $1-\cos\omega\tau$ in (2.126) and correspond to the multiple peaks in the response, noted

in respect to Figure 2.33. They are usually not physically realistic and are another reflection of limitations of the elementary time lag model. A formulation of the $n-\tau$ model showing only a single peak was reported by Crocco (1966) but will not be discussed here.

For applications, equation (2.126) and Figure 2.48 have always been unfolded to give plots of n and τ versus some characteristic parameter, such as the fuel/oxidizer ratio as in Figure 2.48 above; or in some cases the stability boundaries have been presented in terms of system variables, with n and τ parameters along the curves.

An example of the latter is reproduced in Figure 2.49 taken from Crocco, Grey and Harrje (1960). The preparation of this figure, and other quantitative results for n and τ, rests on extensive experimental work. In all cases the strategy is the same: the stability boundary, marking the transition between stable and unstable small amplitude waves, is located experimentally, as a function of the variables defining the instabilities. Then the theoretical relation (2.126) is used to compute the required values of n and τ along the boundary.

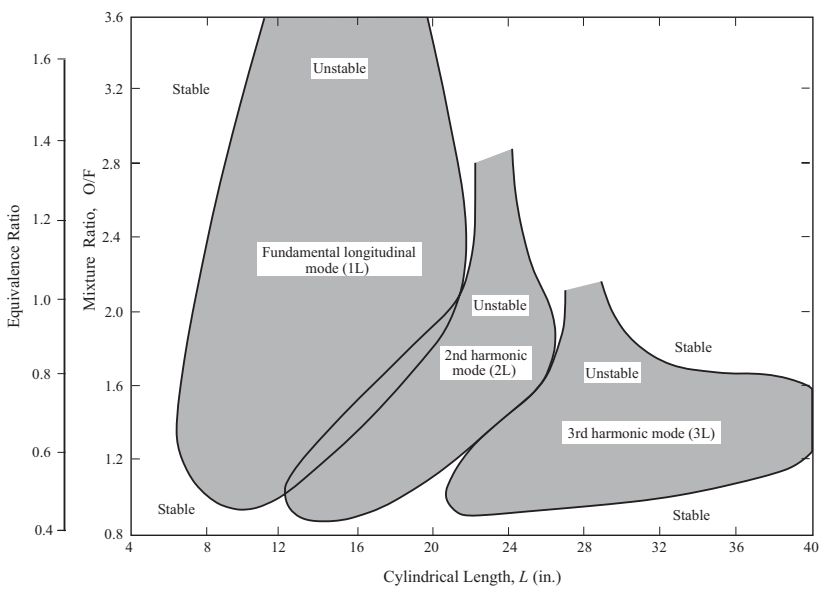

FIGURE 2.49. Stability boundaries inferred with the $n-\tau$ model applied to a gas-fueled rocket (Crocco, Grey and Harrje 1960).

That procedure has been used successfully to interpret longitudinal modes (Crocco, Grey and Harrje 1960) and transverse modes (Crocco, Harrje and Reardon 1962 and Reardon, Crocco and Harrje 1964). By applying the method to large numbers of tests, extensive correlations have been worked out for the interaction index and time lag as functions of geometric variables, injector design, propellant types and operating conditions. A brief summary has been given by Reardon in Harrje and Reardon (1972), pp. 277–286. Figure 2.50 is an example of results for n and τ determined from tests for storable hypergolic propellants, with various types of injectors.

Having values of n and τ, one is now presumably in a position to return to the theoretical result for the growth constant and apply the results to designing new systems. An obvious shortcoming is that the data correlations can be assumed valid only for the systems actually tested. How far the results can be extrapolated cannot be known with any confidence. Nevertheless, this semi-empirical approach has been apparently used successfully both as a framework for correlating data and as an aid to design. It is essential

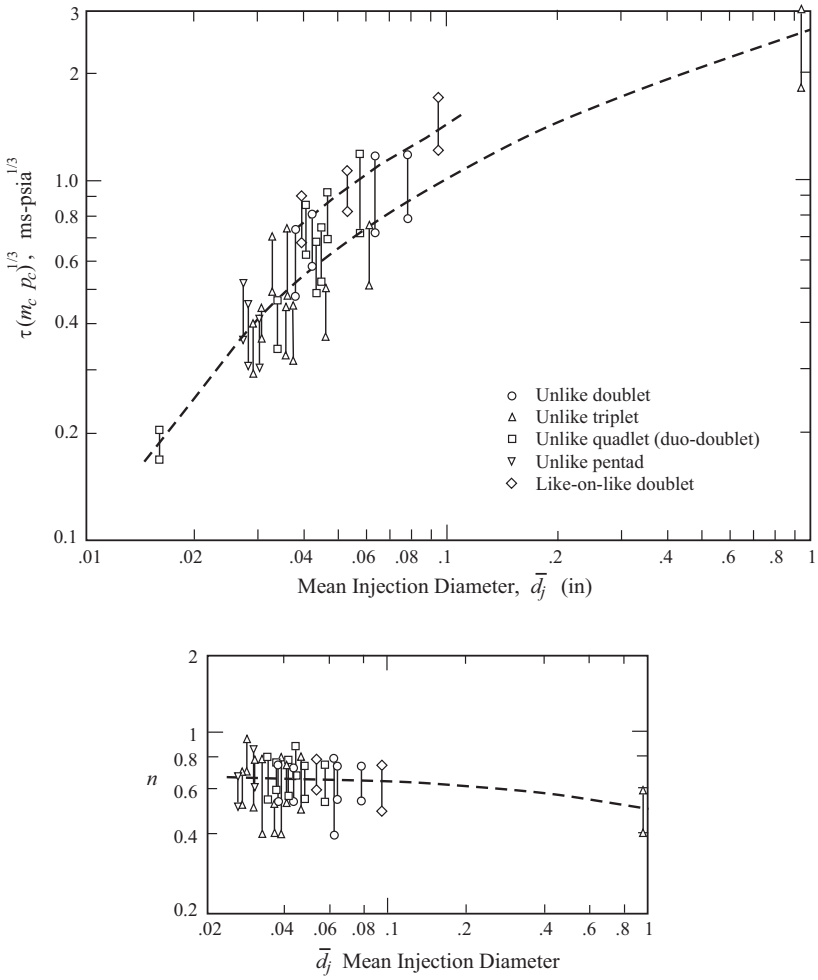

FIGURE 2.50. Experimental results for n and τ, using stable hypergolic propellants and various injectors (Reardon, Figures 6.33 e and f in Harrje and Reardon 1972).

in this procedure that the same theoretical result for the growth constant be used for correlating the data and for subsequent predictions. Otherwise, inconsistent and meaningless results will be obtained.

Although the ideas leading to the definitions of n and τ are appealing, the time lag model should be regarded truly as a framework for correlating data and not as a theory explaining fundamental mechanisms of combustion instabilities. With a different two-parameter representation of the unsteady process, the left-hand side of (2.126) might have a different functional form, but the formula could be used in the same fashion to interpret stability boundaries. Only the forms of the correlations would be changed.

We must also note that because only the single formula for the growth constant (2.126) has been used, the method described above uses one equation to determine two unknowns (n, τ). Thus in practice, some difficulties may arise in obtaining consistent results. That trouble is avoided if, more correctly, both the real and imaginary parts of the complex wavenumber are used. In that event, measured values of the frequency are used and since (2.90) contains the imaginary part of the unsteady mass source (2.94), the two equations

for the frequency and growth constant have the form

$$\omega = \omega_n + C_3 \int \psi_n \hat{w}_l^{(i)} dV - C_4$$

$$\alpha = C_1 \int \psi_n \hat{w}_l^{(r)} dV - C_2$$

Hence with (2.94)

$$\begin{aligned} n \sin \omega\tau &= \frac{\omega - \omega_n + C_4}{C_3 \int \psi_n^2 \overline{w}_l dV} \\ n(1 - \cos \omega\tau) &= \frac{C_2}{C_3 \int \psi_n^2 \overline{w}_l dV} \end{aligned} \qquad (2.127)\text{a,b}$$

The left-hand sides could equally be regarded, within a multiplier, as the real and imaginary parts of the mass source,

$$\begin{aligned} \hat{w}_l^{(r)} &= \overline{w}_l n(1 - \cos \omega\tau) \\ \hat{w}_l^{(i)} &= \overline{w}_l n \sin \omega\tau \end{aligned} \qquad (2.128)\text{a,b}$$

and correlations could be done with $\frac{\hat{w}_l^{(r)}}{\hat{w}_l} = \hat{w}_r = n(1 - \cos \omega\tau)$ and $\frac{\hat{w}_l^{(i)}}{\hat{w}_l} = \hat{w}_r = n \sin \omega\tau$ instead of (n, τ). Thus, even though the heuristic argument leading to $\hat{w}_l$ in the form (2.128)a,b is based on a time lag associated with motions of the propellant (a Lagrangian view), the end result is equivalent to a purely Eulerian representation of local combustion process. The time lag associated with motions in space can be reinterpreted as a phase lag in time at a fixed location in space.

The formulas (2.128)a,b have been deduced from the approximate analysis discussed in Section 2.3.2 and therefore have a particularly simple form. Although it is true that a linear analysis will always produce two formulas, for the real and imaginary parts of complex wavenumber, the forms may be wildly different in detail, depending in the method of solution. Crocco, Grey and Harrje (1960) solved their differential equations directly, a method used later by Crocco, Harrje and Reardon (1962) and Reardon, Crocco and Harrje (1964) to study transverse modes.

The time lag models of the combustion process have been used also in analysis of nonlinear behavior, both for longitudinal oscillations (Sirignano and Crocco 1964; Mitchell, Crocco and Sirignano 1969; Crocco and Mitchell 1969) and for transverse oscillations (Zinn 1966; Zinn and Savell 1968). In those and other works discussed in Chapter 7, either n and τ are assigned values; or the unsteady behavior is studied as a function of n and τ quite analogous to the handling of linear problems. Thus, sufficient experimental data had been gained to support the time lag model that it could be used in a general fashion for theoretical work. However, remarks above emphasize that this practice really amounts to using any combustion response having real and imaginary parts related to n and τ by equations (2.128)a,b. Expressing results and interpreting behavior in terms of n and τ carries no uniqueness.

2.4.3. Pogo Instabilities. The problem of low frequency POGO instabilities is well-documented and understood. Due to the POGO instability in the Apollo vehicle, it is also probably the best known among people otherwise not familiar with combustion instabilities.

Low frequency instabilities ('chugging') arise due to coupling between the fluid dynamics in the combustion chamber, and the propellant supply system. They are perhaps the first sort of combustion instability definitely identified and analyzed for liquid rockets (see the remarks at the beginning of Section 2.3.2). POGO instabilities involve the further complication of coupling between the propulsion system and the structure of the vehicle. The low frequency structural vibrations are the origin of the name, by analogy with the motions of a POGO stick.

During the 1960s, the POGO instability received much attention as a serious problem in several vehicles including the Thor, Atlas, and Titan vehicles. Rubin (1966) has given a clear brief summary, including particular emphasis on pump cavitation and wave propagation in the propellant feed lines. Those are matters often overlooked by those concerned with motions in the combustion chamber. Yet they provide significant contributions to time lags in the system and are crucial items in treating POGO instabilities.

More recent work in France was reported by Dordain, Lourme and Estoueig (1974) for the Europa II and Diamant B vehicles; and by Ordonneau (1986) for the Ariane.

2.4.4. Combustion Instabilities in Thrust Augmentors. Augmentors or, as earlier forms are called, 'afterburners,'[25] have a long history and offer the most varied examples of passive control applied to propulsion systems. The main reasons for this special ranking are basic and simply expressed. First, the geometry is typically ideal for the excitation and sustenance of acoustic oscillations. Figure 2.51 shows two examples of widely used engines; both are turbofans with augmentors. In all designs the injection of fuel takes place at the upstream end of the device. Although the boundary condition does not cause a velocity fluctuation to vanish there, the value is relatively low and the pressure fluctuation can be relatively large. Thus, the product $u'p'$ is likely to have a significantly non-zero positive real part, representing acoustic energy flowing into the region.

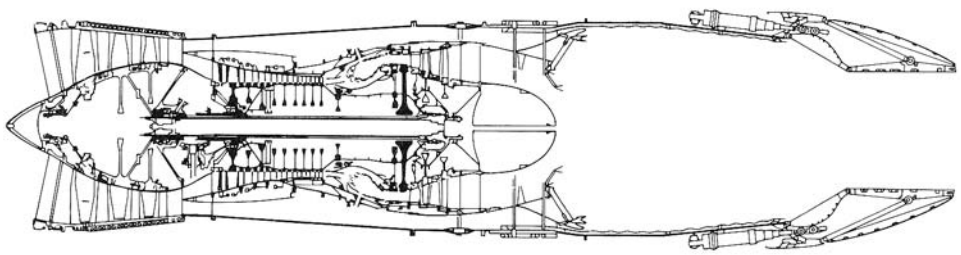

(a)

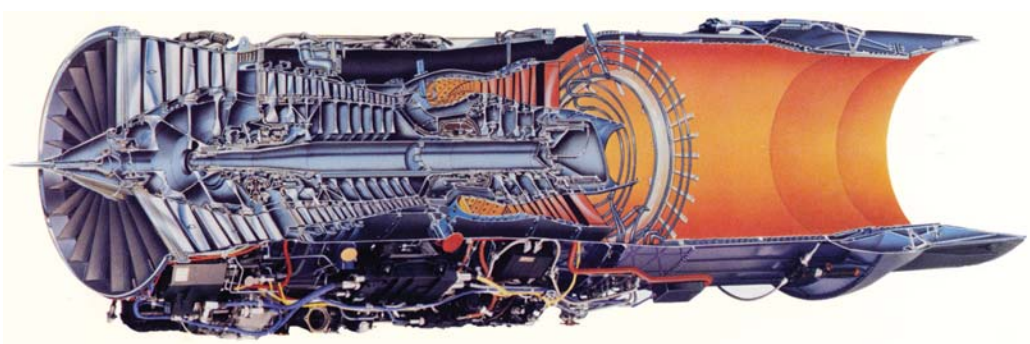

(b)

FIGURE 2.51. Two examples of aircraft gas turbine engines with thrust augmentation (a) General Electric F110 engine (taken from *Jane's All The World's Aircraft*, 1988–1989); (b) Pratt and Whitney F100 engine (taken from Pratt and Whitney advertising material).

[25]The main difference between augmentors and afterburners is that the entire flow in the latter passes through the turbine and therefore the afterburners. To simplify writing, we will use the term 'augmentor' to mean afterburner as well.

Second, fuel is usually introduced through radial vanes, perhaps with circumferential supply tubes as well. Those parts, whatever the configuration, are obstructions to the flow, and are sources of vortex shedding, a potential cause of acoustic oscillations. Third, the conditions for instabilities in flow may be enhanced by a bypass design in which the cold outer flow and the hot core from an unstable cylindrical shear layer between them.

Finally, it is apparent from Figure 2.51 that the system has low losses. Thus it has long been standard practice to incorporate acoustic liners as integral parts of thrust augmentors. That is, they are part of a design and not added later when a problem arises. It is virtually guaranteed that as the operational envelope of any augmentor is expanded, problems with oscillations will be found.

Since high frequency or 'screech' instabilities were first encountered as a serious problem in the late 1940s and early 1950s, liners have been developed largely by trial and error to act as passive control devices designed to suppress the oscillations. The staff of the Lewis Laboratory[26] (1954) compiled most of the existing data and performed some tests to provide a basis for general guidelines for design; Harp *et al.* (1954) reported the results of extensive tests, also at Lewis Laboratory. Of the methods investigated to solve the problem, including baffles and vanes as well as adjusting the distribution of injectors, perforated liners worked best. Groups at Pratt and Whitney Aircraft and the United Aircraft Research Laboratory had already tried Helmholtz resonators and in 1953 demonstrated the first successful use of perforated liners is a full-scale afterburner on a J57. The physical basis for the success of liners is explained in Chapter 8.

Despite several attempts to develop analytical methods and a more quantitative basis for design, treatment of combustion instabilities in thrust augmentors has remained almost entirely an empirical matter. Kenworthy, Woltmann and Corley (1974) reported the results of an experimental program devoted to studying screech instabilities in three different designs of augmentors. The report also contains analysis used to correlate data and to provide some guidance for design of acoustic liners. This seems to be the last reported work on high frequency instabilities in full-scale augmentors; the mechanisms remain obscure. Chamberlain (1983) gave the most recent status report: it seems that little has changed over several decades in respect to augmentors shown in Figure 2.51.

Perforated liners effectively attenuate the high frequency oscillations related to radial and tangential acoustic nodes. Low frequency instabilities, often called 'rumble', tend to be more troublesome. Liners are ineffective at low frequencies and the problem of rumble is solved or reduced in practice by careful control and coordination of the distribution of injected fuel and the nozzle opening. It's a costly process to develop the system, inevitably requiring several designs of the injection system and flameholders, and expensive full-scale tests in altitude simulation test facilities.

The problem of combustion instabilities in thrust augmentors is arguably more difficult then that in liquid rockets for at least two reasons: the processes involved in flame stabilizations are sensitive to pressure and velocity fluctuations; and the device is usually required to perform over a wider range of operating conditions. The first explains the importance of injector and flameholder design. As a result of the second, the high and low frequency instabilities are typically found in different regions of the flight envelope. Figure 2.52, reproduced from the excellent summary of early work by Bonnell, Marshall and Rieche (1971) illustrates the point.

Instabilities in the lower frequency range became increasingly troublesome with the development of turbofan engines, a consequence of the geometry (see Figure 2.53 taken from Bonnell, Marshall and Rieche (1971) and Figure 2.54 taken from Zukoski (1985)). In the pure turbojet, the fluctuations may propagate upstream past the turbine disk but the turbine generally seems to act as a good reflector. In fan engines, it is common that the entire length of the fan duct participates in the oscillations, reducing the frequencies

[26] Now the NASA Glenn Research Center.

sometimes as low as 50 Hz. See Nicholson and Radcliffe (1953) for an early report of very low frequency oscillations; observations in turbofans have been discussed by Bonnell, Marshall and Rieche (1971); Mach (1971); Ernst (1976); Underwood *et al.* (1977); and Cullom and Johnsen (1979). Figure 2.55 reproduces power spectral densities taken from turbofan augmentors [Bonnell, Marshall and Rieche (1971)]. Because of the rotating parts, spectra of the acoustic field in gas turbine engines tend to exhibit a greater variety of discrete oscillations than do those for liquid rockets. The peaks at the higher frequencies in Figure 2.55(b) are 'screech' modes.

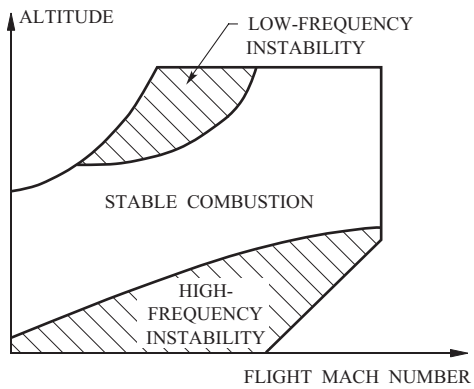

FIGURE 2.52. Schematic flight envelope showing typical regions of high- and low-frequency instabilities in thrust augmentors (Bonnell, Marshall and Rieche 1971).

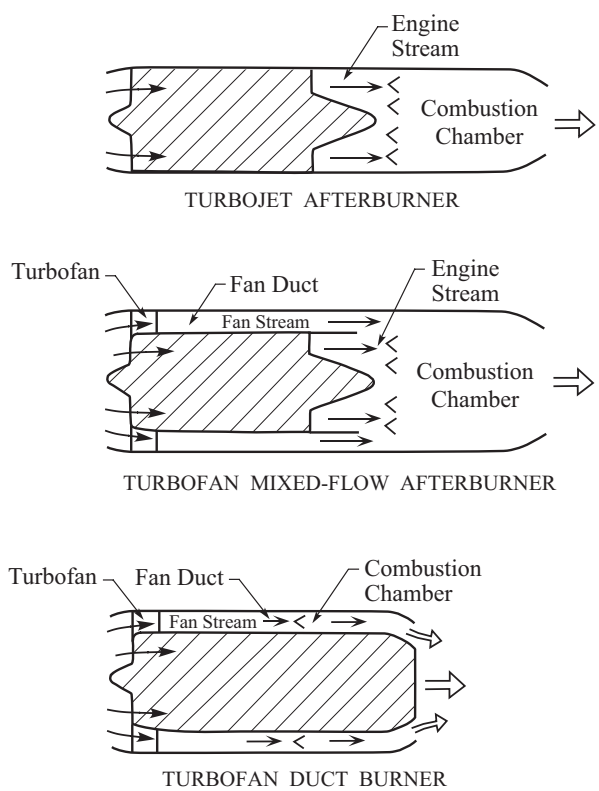

FIGURE 2.53. Sketches of the evolution of the geometry of gas turbine engines (Bonnell, Marshall and Rieche 1971).

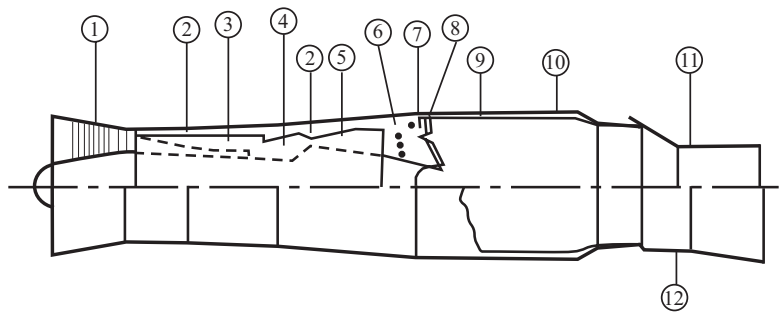

FIGURE 2.54. Pratt and Whitney F100-PW-100 Augmented Turbofan Engine. (1) three stage fan; (2) bypass air duct; core engine compressor(3), burner(4), and turbine(5); (6) fuel injectors for core engine gas stream; (7) fuel injectors for bypass air stream; (8) flame stabilizer for afterburner; (9) perforated afterburner liner; (10) afterburner case; nozzle closed to minimum area (11) and opened to maximum area(12). (Zukoski 1985, Figure 21.0.2).

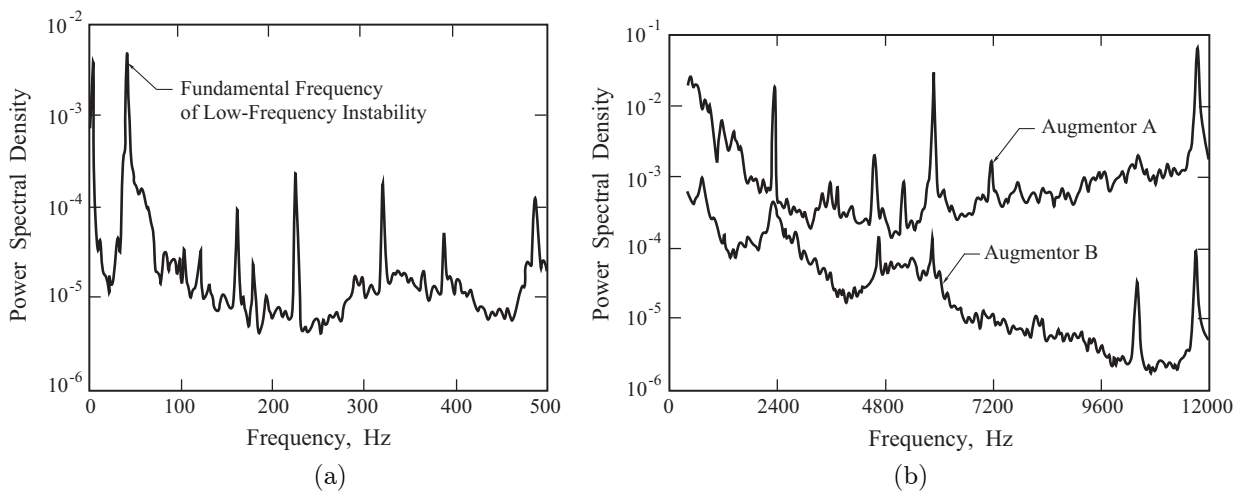

FIGURE 2.55. Spectra of pressure oscillations observed in thrust augmentors. (a) low-frequency range ('rumble'); (b) high-frequency range ('screech'). (Bonnell, Marshall and Rieche 1971).

The combustion processes in an augmentor differ in several fundamental respects from those in a liquid rocket. Only fuel is injected as liquid; the oxidizer is unburnt oxygen in the fuel-lean flows from the bypass and the core engine. There are no impinging fuel and oxidizer liquid stream, but the formation of drops and vaporization of the fuel must obviously occur. Normally, it is intended that the fuel drops should be entirely vaporized prior to ignition in the core flow so burning occurs in the fuel/air gaseous mixture. Because the flame propagation speed is less than the flow speed, a continuous source of ignition is required, normally supplied by the wake of a bluff body, the flameholder. Clearly, the performance of such a system depends not only on the flow conditions and physical properties of the fuel but also very strongly on the geometry of the injectors and flameholders. In the cooler bypass flow, vaporization is not completed upstream and liquid impinges on the flameholders; then liquid may be torn off the flameholder by the high speed of gas stream, or the liquid layer vaporizes. Zukoski (1985) has provided a thorough and readable discussion of the combustion processes in afterburners. Figure 2.56 taken from his article, illustrates the general features of the flow in the vicinity of various flameholders.

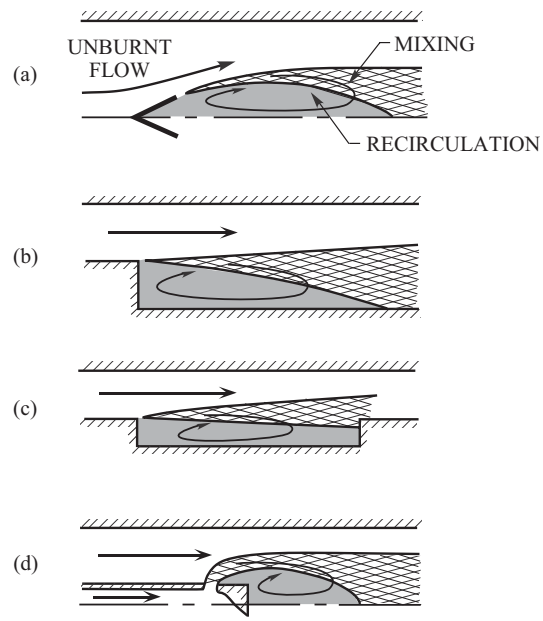

FIGURE 2.56. Flow in the vicinity of typical flameholders emphasizing the recirculation zones (Zukoski 1985).

According to the preceding remarks, it appears unlikely that vaporization of the fuel droplets is a dominant mechanism for combustion instabilities in augmentors. Nevertheless it is certainly quite possible that interaction of the acoustic field with the injection system could produce fluctuations of the fuel flow and hence subsequent fluctuations of fuel/oxidizer ratio and heat release in combustion. The process might be modeled most simply in terms of a time lag but there seems to be no treatment of this sort in the published literature.

One would suspect that processes associated with the flameholder may dominate. That view is generally supported by practical experience with the strong effects of flameholder design on instabilities. We have discussed in Section 2.3.4 the mechanism based on vortex shedding and combustion suggested by Rogers and Marble (1956). Their argument is persuasive and there has never been evidence disproving that process as a possible mechanism of screech. Similar ideas also can be applied to describe a possible 'rumble,' a low frequency instability (see Section 8.6). Theoretical developments and the necessary laboratory tests have not been carried far enough to incorporate the proposal in an analysis suitable for general design work with arbitrary geometries.

Russell, Brant, Ernst, and Underwood (1978), worked out a one-dimensional analysis of instabilities in augmentors; the work is also discussed by Underwood *et al.* (1977). Broadly the analysis represents the acoustic field as a synthesis of up and downstream traveling acoustic waves, and entropy waves, as in the example discussed earlier here in Section 2.2.3. The unsteady heat sources are derived as models of mixing and combustion in the wakes of the flameholders. Bypass and core flows are treated separately and superposed in parallel. It's a linear analysis; the equations for the time-dependent variables are solved by applying the Laplace transform. Conditions for stability are determined by applying the Nyquist criterion. It is difficult to understand all details of the analysis from the available (abbreviated) description. Although some success was evidently achieved with this work, it seems not to have been widely applied. Moreover, the results are mainly in a computer program which has not furthered general understanding of the problem although it may have been useful in treating particular cases.

Over a period of several years Dix and Smith and co-workers developed an analysis based on the formulation published by Culick (1963) for liquid rockets. See Dix and Smith (1971) and references cited there for a description of the work. Although that sort of approach should be useful in treating augmentors, that analysis has also not be widely applied. It is important to note that while their linear analysis is correct, Dix and Smith committed some basic errors in trying to extend their calculations to nonlinear behavior. The results they have reported for the influences of the amplitudes of oscillations are wrong.

A different course of recent work in instabilities in augmentors was reported by Dowling and Bloxsidge (1984); Langhorne (1988) and Bloxsidge, Dowling, Hooper and Langhorne (1988) at Cambridge University. Laboratory experiments were done in a configuration intended, roughly, to represent a longitudinal segment of an augmentor (Figure 2.57). A flame stabilized on a single vee gutter in a duct supplied with premixed gaseous reactants entering through a choked nozzle. With modifications that may have significant influences on the unsteady behavior, this has long been a common configuration (Kaskan and Noreen 1954; Hegde *et al.* 1986, 1987, 1988; Reuter *et al.* 1988). The work by Kaskan and Noreen has already been described briefly (see Figure 2.38). They worked with a flame stabilized on a vee gutter whereas Hegde and co-workers at Georgia Tech used one or two wires to stabilize the burning, although their work has presumably been directed to applications in ramjet engines.

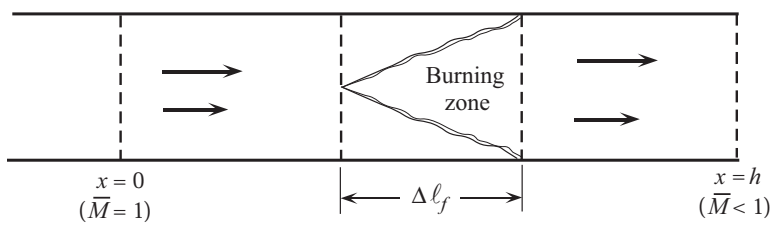

FIGURE 2.57. A flame stabilized on a gutter in a tube (Langhorne 1988).

All of these works are concerned in some broad sense with flames and flame instabilities. The instabilities are often ultimately manifested as vortices, so the mechanism for the instabilities discussed here could be classified as vortex shedding and combustion, as discussed in Section 2.3.5. Another similarity among these works is the use of electromagnetic radiation to identify the heat released by combustion products.

Langhorne (1988) concludes that for the device shown in Figure 2.57, two types of coupling exist between the burning processes and pressure oscillations. The transition between the two occurred in a narrow range of stoichiometric ratio around 0.65. For $\phi < 0.65$ a convective wave of entropy or spots of high temperature appeared to propagate well downstream of the flameholder. With increasing ϕ, that convective aspect seemed to have been confined to a short length and in the remainder of the duct the heat release (as measured by radiation from C_2 and C) seemed to be in phase with the pressure oscillation. No results of flow visualization are available to confirm the behavior directly, but vortex shedding apparently may be involved.

At least partly as a result of the two kinds of coupling, two frequencies of instability were observed with larger amplitudes produced at higher stoichiometric ratios. Bloxsidge, Dowling, Hooper and Langhorne (1988) have worked out an interesting and useful one-dimensional analysis to interpret their observations.

Certain aspects of the Cambridge results are similar to those reported by Heitor, Taylor, and Whitelaw (1984), Sivasegaram and Whitelaw (1987) and by the Georgia Tech group (Hegde *et al.* 1990). The reasons for the similarities and yet only partial reconciliation of differences are not known; a sufficiently general analysis has not been constructed to accommodate all the results on a common basis. There is little doubt that more than one mechanism may act, one or another dominant under different conditions. Because this

is a relatively well-defined situation, (a premixed flame in a duct) the problem merits further attention both experimentally and theoretically to bring clearer understanding of the behavior.

The work at Cambridge seems to have been partly motivated by the idea of using feedback control of combustion instabilities. In fact the results just described were soon followed by laboratory work at Ecole Centrale (Poinsot *et al.* 1988) concerned also with active control. Those are the beginnings of modern work on active control of combustion instabilities, the subject of Chapter 9.

2.4.5. Combustion Instabilities in Ramjet Engines. Particularly from the late 1970s to the early 1990s, substantially more attention has been paid to combustion instabilities in ramjet engines then can be discussed here. Much progress has been made but several essential problems remain unsolved, mainly associated with the conversion of liquid fuel to gaseous reactants; coupling between combustion processes and the unsteady motions; and the inlet/diffuser.

Sketches of two typical configurations are shown in Figure 2.58. Most contemporary liquid-fueled ramjets are "integral ramjet engines." The combustion chamber is initially filled with solid propellant that is burnt to boost the vehicle to supersonic speed. Liquid propellant is injected upstream of the region where the flow area abruptly increases at the "dump plane." Flame stabilization is achieved through continuous ignition by the hot combustion products in the recirculation zone. In some designs additional bluff body flameholders may also be used; and occasionally continuous burning of a pilot light may be required.

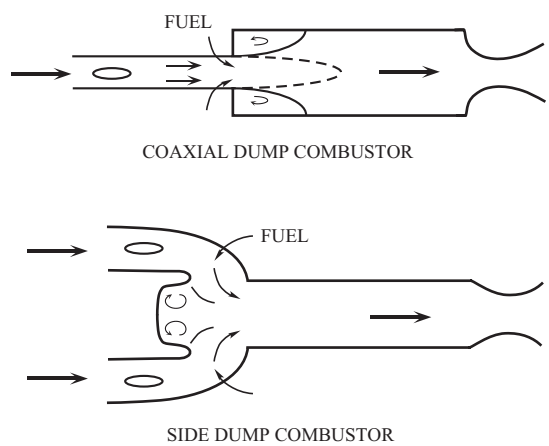

FIGURE 2.58. Two simple ramjet configurations using stabilization at abrupt changes of area.

Zukoski (1985) has given a thorough discussion of steady flame stabilization in thrust augmentors. Much of that material applies with virtually no change to the corresponding problems in ramjet engines. The presence of the rearward-facing step and the sensitivity of shear layers and recirculation zones to fluctuations in the flow are major factors in the problem of combustion instabilities in ramjet engines.

Much of the material we have covered for liquid-fueled rockets and thrust augmentors is relevant as well to ramjet engines. There are, however, several distinguishing features. First, unlike the case for liquid rockets but similar to that for afterburners, spray combustion seems a lesser issue. Although the published evidence is perhaps not wholly conclusive, (see, e.g, Edelman 1981, Edelman *et al.* 1981 and Harsha and Edelman 1982), it appears that in operating engines, the liquid droplets are largely vaporized before the flow reaches the zones of flame stabilization and combustion. Hence the processes in those regions involve mostly gaseous reactants, a great simplification for carrying out research on combustion instabilities; very

little experimental work has been done recently in the coupling between spray combustion and unsteady motions. Laboratory tests have for the most part used gaseous fuels.

That is not to say that transient processes of droplet heating and vaporization are unimportant, for they are surely influential in arranging the distribution of fuel over the plane at the entrance to the combustor. But there is no operational or experimental evidence to support the proposal by Tong and Sirignano (1986a, 1986b, 1987) that the unsteady conversion of liquid to vapor is a potential mechanism for instabilities. This matter has already been discussed in Section 2.3.1 with the conclusion that if all processes *except combustion* are accounted for, the presence of evaporating liquid drops is a stabilizing influence on unsteady motions.[27] We will not consider further problems associated with injection, atomization and vaporization. However, it is true that insufficient attention has been paid to the distribution of fuel/oxidizer ratio in the flow. Little is known of the details, either theoretically or experimentally; yet laboratory tests (e.g., Schadow *et al.* 1987b) have shown that the distribution of fuel can have a substantial effect on instabilities, a fact that has long been known qualitatively from experience gained in engine development (Rogers 1980a, 1980b; Grenleski *et al.* 1977). There seems to be no evidence of coupling between oscillations in the flow and the fuel supply system. Thus no oscillations have been observed in ramjets corresponding to 'chugging' or POGO instabilities in liquid rockets.

2.4.6. Unsteady Behavior of the Inlet/Diffuser. So far as combustion instabilities are concerned, the principal feature distinguishing ramjet engines from liquid-fuel rockets and afterburners is the inlet/diffuser. Within the inlet a system of shock waves exists to provide the mass flow and stagnation conditions demanded by the conditions set in the combustion chamber and exhaust nozzle. Under normal operating conditions the shocks are located downstream of the geometric throat in the expanding supersonic flow. The position of the shocks depends chiefly in the stagnation pressure in the combustion chamber; increasing the stagnation pressure causes the shocks to move upstream where the Mach number and therefore loss of stagnation pressure are less. It is this sensitivity of the flow in the inlet to pressure changes downstream that has caused longitudinal oscillations to be such a serious concern in ramjet engines. In the late 1970s (Hall 1978, 1980; Rogers 1980a, 1980b) first qualitative and later limited quantitative relations were established between the amplitudes of pressure oscillations and the loss of dynamic pressure margin.

Since those early works, extensive tests by Sajben and co-workers (Chen, Sajben and Krontil 1979; Sajben, Bogar and Krontil 1984; Bogar, Sajben and Krontil 1983a, 1983b) have shown that the unsteady behavior is greatly more complicated due to flow separation and instability of shear layers. High speed schlieren pictures (see also Schadow *et al.* 1981) have shown large shock oscillations as well as the formation of vortex structures. Although computations based in the one-dimensional approximation to flow in the diffuser (Culick and Rogers 1983; Yang 1984; Yang and Culick 1984, 1985, 1986) are useful and seem to capture some of the dominant features of the behavior, it is quite clear that the true motions can be simulated well only by numerical analysis based on the Navier Stokes equations for two- or three-dimensional flows (Hsieh, Wardlaw and Coakley 1984; Hsieh and Coakley 1987; and references cited there).

There is evidence that under some conditions inlets exhibit self- excited or 'natural' oscillations. Energy is transferred from the mean flow to the fluctuations associated at least partly with separated flow. Although a one-dimensional calculation (Culick and Rogers 1983 and an approximation to some of Sajben's data by Waugh *et al.* 1983, Appendix D) suggests the possibility that the inlet may drive combustion instabilities, there is no firm evidence from tests with combustors that those conclusions hold. Most experimental results strongly suggest that the major source of driving unstable motions is likely associated with processes in the combustion chamber. Nevertheless, because the flow from the inlet is the initial state for flow in the chamber, it is fundamentally important that processes in the inlet be well-understood. In that respect, as we remarked above, perhaps the greatest deficiency is knowledge of the history of the injected fuel and the distribution of liquid droplets and gaseous fuel at the inlet phase.

[27] This conclusion is not generally true. See the discussion in Section 6.13.

In practice, the first indications of combustion instabilities are almost always fluctuations in recordings of the pressure. If there is only one pressure transducer, one can infer only the amplitude and frequency—best displayed as a power spectral density. While the frequency alone may suggest what modes are involved, the configurations used for ramjet combustors are sufficiently complicated that the modes are not always easily identified. Moreover, in laboratory tests there may be an upstream plenum chamber and other parts of the apparatus that participate in the oscillations. As a general rule, it is essential that measurements of the pressure be taken at several locations in order to provide unambiguous identification of the modes. Sufficient care should be taken that distributions of both the amplitude and relative phase can be determined. This information has also proven extremely useful for confirming the results of analyses.

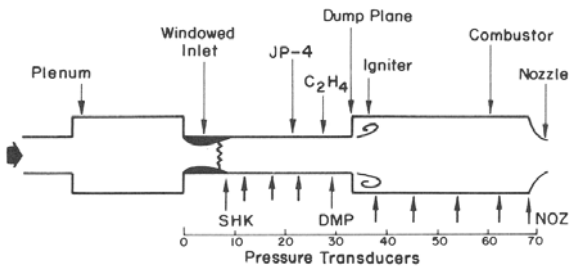

FIGURE 2.59. Model used for measurements in the inlet to a dump combustor (Crump *et al.* 1986).

The most extensive measurements of mode shapes in dump combustors were made at the Naval Weapons Center by Schadow and co-workers. A summary of the results, with references to the previous work, was published by Crump *et al.* (1986). Figure 2.59 shows the geometry of the sub-scale laboratory device; some results of measurements and analysis are reproduced in Figure 2.60. A case in which a bulk mode is excited in the combustion chamber (175 Hz) is shown in Figure 2.60(a); the fundamental wave mode was excited in the chamber excited for the case shown in Figure 2.60(b) (540 Hz). The calculated results were based on a one-dimensional analysis (Yang 1984) in which combustion was ignored and the mean flow was accounted for only in the inlet. The good agreement is further evidence of the point emphasized already that the mode shapes and frequencies for combustion instabilities are often well-approximated by results based on classical acoustics. Here we also find that the one-dimensional approximation works well. For those calculations, the inlet shock was represented with the admittance function computed by Culick and Rogers (1983). It is apparently a good approximation that for these cases, the shock system is highly absorbing: the reflected wave has much smaller amplitude than the upstream-traveling incident wave. That fact, and the presence of the high speed average flow, explains why the relative phase varies linearly in the inlet.

Clark and Humphrey (1986) have also reported fairly good results obtained with a one-dimensional analysis applied to a side-dump configuration. The engine was supplied from a large plenum through inlets that were not always choked. Although the frequencies of oscillation, phase distributions throughout the device, and amplitude distributions within the combustor were predicted well, the amplitude distributions within the inlets diffuser considerably from the measured results. The reasons for the differences are not known. Yang and Culick (1985) later carried out a numerical analysis including vaporization of the liquid fuel and were able to predict quite well both the distribution and level of the pressure field.

A series of tests in a coaxial combustor have been reported by Sivasegaram and Whitelaw (1987), intended to examine the consequences of changing geometric parameters and fuel/air ratio. Data are given for frequencies and sound intensity at one location. Mode shapes were evidently not measured and no results of analysis are cited. It would appear that these data offer an opportunity for a straightforward application of a simple one-dimensional analysis.

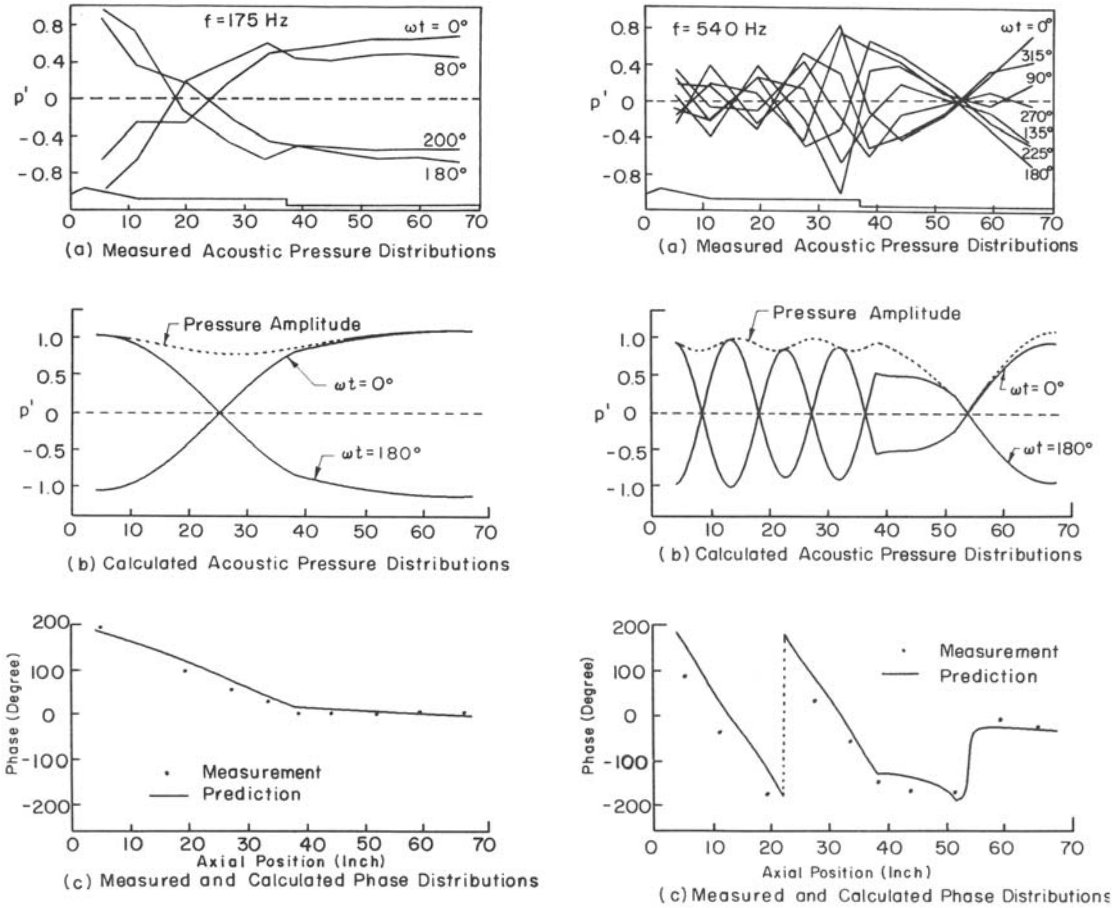

FIGURE 2.60. Comparison of measured and calculated mode shapes in the inlet of a laboratory dump combustor (Crump *et al.* 1986).

The one-dimensional approximation with the average flow accounted for works surprisingly well for rapid estimates of mode shapes and frequencies. It is worthwhile remarking on its application. Few exact solutions exist for arbitrary variations of cross-section area $S_c(z)$, but in the case of ramjet configurations it is generally required to obtain results for piecewise variations. The problem comes down to solving the wave equation

$$\frac{d^2\hat{p}}{dz^2} + k_\ell^2 \hat{p} = -\frac{d\hat{p}}{dz}\frac{1}{S_c}\frac{dS_c}{dz}$$

where dS_c/dz vanishes everywhere except at discontinuities of area where it is infinite.

Hence the general procedure is straightforward to find normal modes of the chamber. In uniform sections, the pressure field is represented by the usual forms, $A_i \cos(k_\ell z + \phi_i)$ or its equivalents, where A_i, ϕ_i are associated with segment i, and k_ℓ is the wavenumber for mode ℓ. These solutions are matched at the discontinuities by requiring continuity of the acoustic pressure and mass flow. Eventually the amplitudes A_i can be found to within a multiplicative constant, and the values of h_ℓ are determined as roots of the characteristic equation.

This sort of analysis has long been known to give satisfactory results if the changes of area are not too large (see Section 5.7.2 and more complete analyses by Culick, Derr, Price 1972; Derr and Mathes 1974).

Simple resonance tests at room temperature have confirmed the calculations, a method that is still useful for investigating the acoustic modes of combustion chambers. For application to actual systems, significant differences between these approximate results and observed values may arise due to uncertainties in the boundary conditions at the inlet and exit planes.

2.4.7. The Time Lag Model Applied to Combustion Instabilities in Ramjet Engines. During the past seven years, Reardon (1981, 1983, 1984, 1985, 1988) has used the time lag model to-correlate and interpret the extensive data taken by Davis (1981). The time lag model is unwieldy (at best) to use if combustion is allowed to be distributed and the time lag is variable. Hence as in many previous applications to liquid rockets, Reardon assumes that the energy release is concentrated in a transverse plane; that the parameters (n, τ) are constant; and that the flow field is one-dimensional. Then the combustion response is given by the part of equation (2.94) depending on frequency; to represent concentrated combustion, the average distribution $\overline{w}_l$ is replaced by δ-function. A modest change in the argument allows one to use this form for the unsteady conversion of liquid to vapor, or for unsteady energy release.

Reardon assumes that the oscillations observed by Davis are bulk modes in the combustor: the pressure is essentially uniform in space and pulsates in time. Hence the mode shape $\psi(\vec{r})$ is approximately constant and one may assume that the total unsteady energy release due to combustion processes in the chamber, E_c, is given by

$$\dot{E}_c = \dot{E}_0 n(1 - e^{-i\omega\tau})\frac{p'}{\overline{p}}$$

The rate of change of energy in the chamber is the net result of energy released by combustion and the rates at which energy is convected in and out of combustor:

$$\frac{dE}{dt} = \dot{E}_c + \dot{E}_{in} - \dot{E}_{out}$$

This relation is the basis for Reardon's treatment of the experimental results.

As we discussed earlier, in applications of the time lag model to instabilities in liquid rockets, both parameters (n, τ) were determined by matching a theoretical result to experimental results for the stability boundary. The idea then is that those values of (n, τ) can be used to predict the stability characteristics for new (but in some sense similar) designs. In this case, Reardon has chosen to use values of n calculated by Crocco and Cheng (1956) and to compute the time lag independently, using previous results obtained by others. In short, Reardon essentially assumes that the combustion model is known (defined by the two parameters (n, τ) with concentrated combustion) and then uses the relation for the balance of energy in the chamber to correlate data.

Stability of oscillations may be determined by application of the Nyquist criterion after the unsteady energy balance is rewritten by using the Laplace transform. This possibility arises because, as we have briefly described earlier, the problem of self-excited combustion instabilities can be interpreted as a linear system with a negative feedback loop. The stability criterion, expressed with the growth constant α, depends on other processes included in the energy balance. The formal result may therefore be used to test the importance of those processes by comparison with data.

Reardon has used this procedure to study the effects of several processes and geometrical parameters, with mixed results. It seems that this sort of approach suffers from the intrinsic limitation noted earlier: It is really only a method for correlating data and therefore in the first instance has little predictive value without assurance that the models used are accurate. Confidence in the results comes only from good correlations with data over broad ranges of parameters. The results to date do not seem to provide that confidence.

2.5. Dynamics of Flames and Flame Sheets as a Mechanism

Interpreted in the broadest sense, the dynamics of flames includes mechanisms which may be active in any system based on the conversion of energy by combustion processes. Conventionally the term has come to refer only to situations in which the flame or flames are rather well-defined and not spread out in space. What is probably the first example of a "combustion instability" remains virtually a canonical example. In 1777, (that's only 50 years after Newton's death!) Byron Higgens (1777) recorded his observations of a "singing flame", published twenty-five years later in Nicholson's Journal. The phenomenon has attracted much attention as a curiosity, as a simple informative example of fundamental behavior, and as an elementary guide to understanding the complexities presented by actual combustion systems.

Figure 2.61 is a sketch of Putnam's apparatus which is easily assembled for observation of a basic singing flame. Two variations are shown, to demonstrate the influence of changing the upstream boundary condition. Figure 2.62 shows some results (Putnam 1945) obtained for the two cases sketched in Figure 2.61. Putnam (1971, pp. 9–16) has given a good brief discussion of Jones' observations.

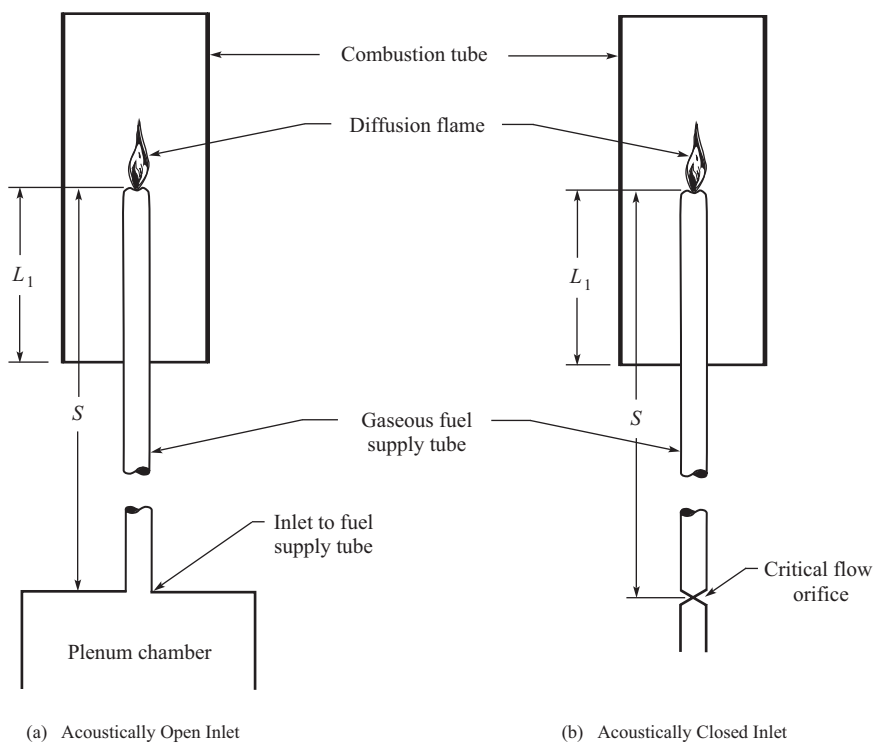

FIGURE 2.61. Simple apparatus for demonstrating a singing flame (Putnam 1971).

The connections between the behavior of the singing flame and results obtained for the Rijke tube (Section 2.7) are fairly evident; they will not be pursued here. These elementary situations are instructive examples of phenomena causing the excitation of acoustic waves by energy released in combustion processes.

Prior to the late 1940s and early 1950s, there was virtually no effort to work out true theories of flames. There were no detailed quantitative representations having predictive value. The idea that at atmospheric pressure most of the chemical reactions in a combustion process take place quickly and in thin regions had long been known, but there were few quantitative consequences. That view, that flames are thin, is at least implicit in practically all of the literature alluded to in the paragraph above. Then, a few years after World

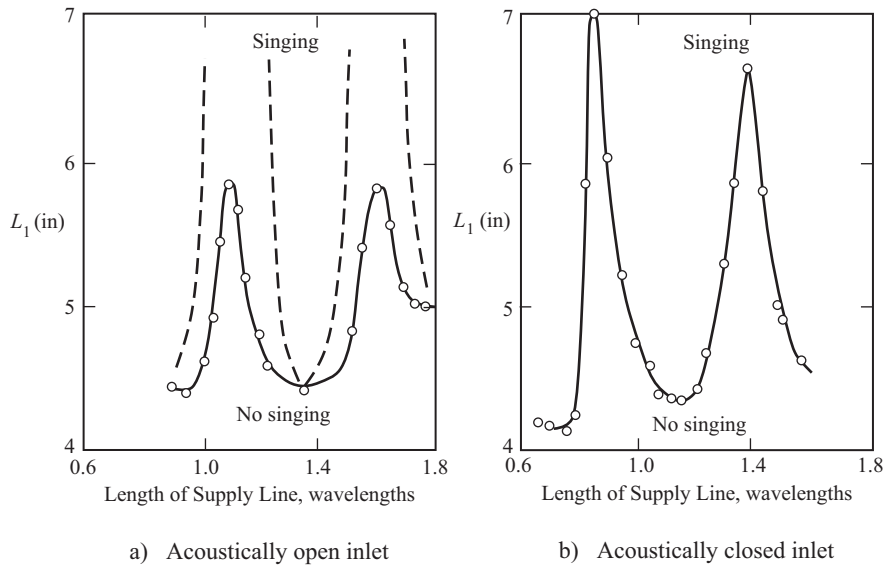

FIGURE 2.62. Location of the flame shown in Figure 2.61 to maintain a continuous tone, i.e. 'singing' (Putnam 1971).

War II, the field of combustion began to develop in the form now understood, most clearly the subject broadly covered by the proceedings of the Combustion Institute. Within that extensive field, the representation of reacting flows with thin flames, or 'flame sheets' became and has remained a useful model developed for many research and practical applications.

Consequently, it was a natural development that unsteady problems of combustion in gaseous systems should be modeled and analyzed with reaction zones treated as flame sheets. A significant increase of activity occured in the late 1980s with accomplishments at Ecole Centrale, Paris (Poinsot *et al.* 1987) and at Cambridge University (Bloxsidge *et al.* 1988). Those were the first of many works based on variations of similar apparatus at approximately atmospheric pressure. In both programs, the primary goal was successful application of active control to problems of combustion instability. A similar strategy was followed in work at M.I.T. (Annaswamy *et al.* 2000 and Fleifel *et al.* 2000).

All of those works involve models of combustion zones as flame sheets. The analyses are closely tied to investigations of active control and are therefore more appropriately discussed in Chapter 9.

2.6. Fluctuations of Mixture Ratio as a Mechanism

The influence of mixture ratio, or more precisely its fluctuations, in combustion instabilities received little attention until oscillations caused serious problems in the development of combustors for gas turbines. Reduced emissions, perhaps most importantly NO_x, oxides of nitrogen, has been a practical goal for more than fifteen years. Pressure to adopt stronger regulations has increased with time, one consequence being significantly greater investments of people, money and time devoted to research. Many related special topics of research have been, and are investigated; fluctuations of fuel/oxidizer ratio (F/O) hold a special position due to their direct connection with local reaction rates, energy release and therefore potential effects on the presence of combustion instabilities.

An interesting question is: Why do changes in the design, or operation of gas turbines to achieve lower emission of NO_x lead to combustion instabilities? The reason can be explained quite simply. First we should note that there are three main mechanisms for the formation of NO (nitrogen oxide) in combustion of conventional fuels: (1) oxidation of nitrogen contained in the fuel, the principal source of NO in the combustion of coal; (2) production of NO early in flame zones, at a rate faster than that predicted by quasi-equilibrium calculations (called 'prompt' NO); and (3) oxidation of atmospheric nitrogen. It is the last that is the main cause of NO production by gas turbines.

Production of NO is commonly estimated by the 'Zel'dovich mechanism', an approximation to the more accurate mechanism. The approximation by an overall reaction (Zel'dovich *et al.* 1985) is

$$\frac{d[\mathrm{NO}]}{dt} = 1.45 \times 10^{17} \frac{1}{\sqrt{T}} [\mathrm{O_2}]_{eq} [\mathrm{N_2}]_{eq} e^{-\frac{69,460}{T(^\circ\mathrm{K})}}$$

The rate of production of nitric oxide is strongly dependent on temperature, the origin of the descriptive label 'thermal NO'. For example, if the temperature is increased by 90°K at 2200°K, the rate doubles. Conversely, the practical implication is that less NO is produced at lower temperatures.

In the interest of reducing pollution by NO (more generally NO_x), combustion should be encouraged at low temperatures. However, at lower temperatures, the rate of production of another pollutant, carbon monoxide, is increased. At high temperatures, the equilibrium of CO_2 and CO is shifted as CO_2 dissociates to form more CO. Thus in practice, the production, or rather the equilibrium concentration of carbon monoxide, is minimum in a range of temperature not too high, not too low. Figure 2.63 shows some results of calculations carried out at the United Technologies Research Center (UTRC). It follows from these results that combustion is most favorably accomplished in a range of moderate temperature.

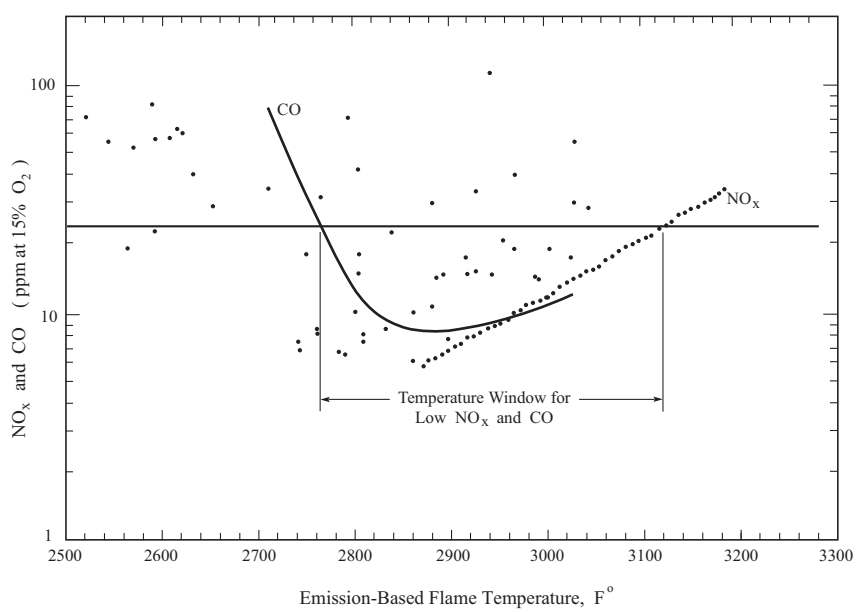

FIGURE 2.63. Concentrations at equilibrium of carbon monoxide and oxides of nitrogen (T. Rosfjord, UTRC; published in AGARD Report 820, Schadow *et al.* 1997).

The combustion temperature is reduced from its normal—i.e., traditionally accepted—value by operating the combustor at lower values of the equivalence or fuel/oxidizer ratio. But as F/O is reduced to give desirably lower levels of NO_x, the combustor operates near the lean blowout limit. Then the combustion zone becomes sensitive to fluctuations and approaches a condition under which it is both statically and dynamically unstable. Flame 'anchoring' and stabilization become insecure and can be lost due to small

disturbances. Local motions of the combustion zone may then couple to the chamber dynamics (acoustic) and grow into a combustion instability. The global consequences of that sequence of events is displayed in Figure 2.64. It is this general behavior that has motivated substantial and widespread research on combustion instabilities during the past decade and more.

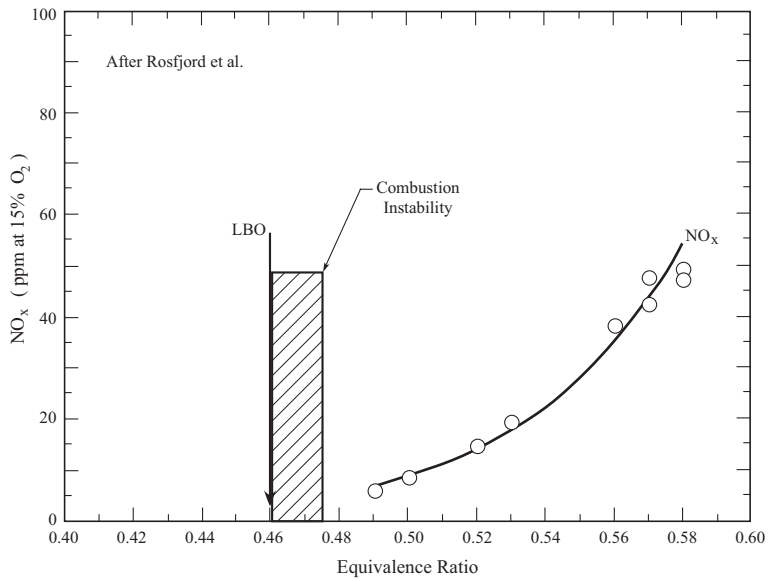

FIGURE 2.64. General behavior as the equivalence ratio is reduced near the lean blowout limit (T. Rosfjord, UTRC; published in AGARD Report 820, Schadow *et al.* 1997).

Eventually the mixture ratio holds a special position as a state variable identifying the change of the operating point of a combustor, as in Figure 2.63. It does not directly follow that F/O is in any sense a 'mechanism'. On the other hand, because the fuel/oxidizer ratio affects directly such basic properties as energy release (or heat of reaction) and flame speed, it is quite easy to make a convincing case that variations of F/O can certainly produce oscillations. For example, imposing changes in F/O is a convenient means of initiating combustion instabilities in numerical simulations.

Probably the experiments reported by Langhorne (1988) and Langhorne, Dowling and Hooper (1990) were the first works to make explicit use of fuel/oxidizer fluctuations in studies of combustion instabilities. Since then, research on the role and consequences of unsteady variations of mixture ratio has been carried out by several groups; see, for example, reports by Lieuwen and Zinn (1998); Richards, James and Robey (1999); and by Cho and Lieuwen (2003). Those and other works have been motivated mainly by intentions to develop practical methods of active control, for application to problems of combustion instabilities in lean premixed systems as explained above. That is a principal subject of Chapter 9.

2.7. The Rijke Tube: Simplest Example of Thermoacoustic Instabilities

One of the fundamental guiding principles in the field of feedback control is that time delays can cause serious problems with stability and control. We have already mentioned on several occasions the presence of a time delay as a factor in instabilities. It is preferable to view a time delay as a characteristic of the mechanism of an instability rather than a mechanism *per se*. In this section we will treat two physical mechanisms—energy addition from an electrical heater and from a flame sheet—each of which present time delays. In both cases, delays exist between the action of a flow variable (pressure or velocity) and the energy added to the flow. That is, the delays arise in the internal feedback path shown in Figure 1.1.

The role of a time delay is clearly displayed in these special situations. Because heat addition is the root mechanism, the oscillations observed experimentally are often called 'thermoacoustic instabilities.' Understanding their behavior is a significant aid to comprehending more complicated instabilities generated by mechanisms quite different in their details.

A second purpose of this section is to introduce the analytical framework developed in the following chapters. The general formalism is quite generally applicable to combustors of any shape operating with any form of reactants, solid, liquid or gaseous. Simple examples share many of the features of the behavior found even in the most complicated applications to operational systems. Consequently, much of general value can be learned from investigating the details of an elementary example.

2.7.1. The Electrically Driven Rijke Tube. Rijke (1859) invented and first studied his device nearly 150 years ago. The experimental results were described and explained by Rayleigh (1878, 1945) as the chief basis for his formulation of the principle that came to be known as Rayleigh's Criterion (Chu 1956; Zinn 1986; Culick, 1987a, 1992). In recent years the Rijke tube has received much attention because of its potential relations to combustion instabilities generally and for other reasons as well. Raun *et al.* (1993) have published the most complete summary of work with the Rijke tube to 1993. The article contains a virtually complete set of references and useful comments on much of the observed physical behavior, including experimental confirmation of Rayleigh's Criterion. Still a basic 'rule of thumb' in the field of combustion instabilities, Rayleigh's Criterion is derived here in Chapter 6.

Figure 2.65 is a sketch of the device to be analyzed here, the form of the device originally used. A tube open at both ends is supported vertically and contains an electrically heated grid mounted some distance ℓ_g above the lower end. In the original form of the tube used by Rijke, in place of the grid, a screen is heated by a flame which is subsequently removed. Soon after the flame is removed, a tone of growing intensity is produced. After maintaining a seemingly constant level for some time, the tone decays and ceases as the screen cools. Rijke attributed the sound to periodic heating and expansion of the air rising through the tube, alternating with compression due to cooling by the walls. Twenty years later, partially motivated by his belief that cooling by the walls was too slow to be a controlling process, Rayleigh gave his explanation for the excitation of the tone. He related the cause to the location of the heated screen relative to the form of the acoustic field. It is in that work that we find the succinct statement of conditions under which heat addition will cause oscillations, the famous 'Rayleigh's Criterion' explained in Section 6.6.

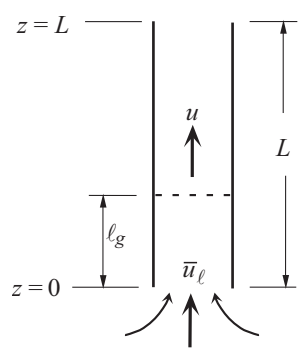

FIGURE 2.65. Sketch of an electrically heated Rijke tube.

Rayleigh's reasoning was not intended to include explicitly quantitative details of the phenomenon. Another twenty years passed before Pflaum (1909) incorrectly attributed the origin of the sound to friction between the rising current of air and the heater. The idea was essentially an analogy between the tones produced in a Rijke tube and the oscillations excited by wind blowing past electric wires or telephone lines (or a flexible bridge!). Thus the heater served only as the prime mover of the rising air.

In 1937, more than a quarter century after Pflaum's work, Lehmann (1937) carried out experiments with the notable addition of a fine screen above or below the heater. Some of his observations misled him to formulate a 'theory' predicting that the amplitude of oscillation should continually increase with the draft velocity, not having the maximum value shown by experiments. Lehmann's conclusions had no influence, for not until fifteen years later did Neuringer and Hudson (1952) carry out what might be regarded as the first 'modern' discussion of the problem. They assumed that the time-dependent heat transfer depended mainly on the gradient of the local instantaneous velocity. Lehmann's experimental conditions served to define variables of the flow required in the calculations. The results found by Neuringer and Hudson were not extensive, but satisfied the authors that the local velocity gradient contributes crucially, suggesting further that turbulence is likely an important factor. There is little concrete connection between the analysis and observations cited in their discussion.

Carrier (1954) carried out the most detailed analysis of the Rijke tube driven by heat transferred from a heater made of wires or strips of metal. The work was apparently prompted by some experiments carried out by Bailey, who later gave an extended account of tests he performed with a Rijke tube operated with a gas burner (Bailey 1957). The greater part of Carrier's paper is devoted to a careful analysis of the mechanism, unsteady heat transfer from the heater to the gas stream; and to construction of the wave field in the tube. Carrier gave only brief comments regarding comparison with experimental results. The analysis has much instructional value.

Three papers by Merk (1956b, 1957a,b) began with a calculation of one-dimensional motions in flow of premixed combusting gases, and ended with a detailed examination of some possible unstable motions in a Rijke tube. Merk's calculations are linear, for one-dimensional flow and involve use of admittance functions. He eventually uses Carrier's result for the complex transfer function for a metal heater made of thin ribbons. The unsteady heat transfer to the air flow is then proportional to the velocity parallel to the ribbon, with a small phase difference. The physical content of Merk's model of the Rijke tube is essentially the same as Carrier's but his discussion of the observable behavior is much more extensive. He obtained a result for the neutral stability curve given below.

In a short note, Maling (1963) gave what is probably the simplest quantitative analysis of the linear behavior of the Rijke tube. The unsteady pressure is taken to obey the wave equation with a heat source (energy/mass-time) and no explicit effects of mean flow:

$$\frac{\partial^2 p'}{\partial x^2} - \frac{1}{\bar{a}^2}\frac{\partial^2 p'}{\partial t^2} = -\frac{(\gamma-1)}{\bar{a}^2}\bar{\rho}\frac{\partial \dot{q}}{\partial t} \tag{2.129}$$

The heater is supposed to be an infinitesimally thin screen providing energy at a rate proportional to the velocity. In the notation used here, $p'(x,t) = \hat{p}(x)e^{-i\bar{a}kt}$ and $\dot{q} = F(\bar{u})u'$, so

$$\frac{d^2\hat{p}}{dx^2} + k^2\hat{p} = \frac{(\gamma-1)}{\bar{a}}\bar{\rho}kF(\bar{u})\hat{u}(x_h-\epsilon)\delta(x-x_h) \tag{2.130}$$

where the heater is located at x_h and ϵ is a small quantity required when the momentum equation is satisfied just upstream of the heater. As in Merk's analysis, Maling used Carrier's results to set $F(\bar{u})$. Limited test results with a three-foot tube and a blower in plenum chamber upstream of the tube established the lower limit speeds for oscillations, 0.84, 0.87, 0.91 m/s with total heater powers equal to 930, 1100, and 1290 Watts. Those can be viewed only as qualitative results because precise behavior is very sensitive to construction imperfections.

The first experiments with a horizontal Rijke tube were done by Friedlander in his thesis work reported by Friedlander, Smith and Powell (1964). Limited tests served only to establish correlations among some variables, mainly the sound pressure level, heater location, tube length and flow velocity which was provided by external means not described. The length of the tube could be adjusted by moving pistons which, while admitting flow, closed the ends. Apparently the observed behavior was consistent with the calculations by Maling. Insufficient details are given in the note to make further use of the report.

Saito (1965) seems to have misunderstood some of the previous work (e.g., he did not fully appreciate the basic nature and generality of Rayleigh's Criterion), and he incorrectly criticized application of Merk's calculations to an electrical heater. The apparatus he used is not described well, and several of his photographs are not clear. His Figures 7 and 8 clearly show that oscillations in his Rijke tube grow out of a linear instability. Unfortunately the work seems not to have fulfilled the author's hope for a new theory, or even for providing the experimental basis for a new theory.

The most extensive experimental results to that time were provided by Marone and Tarakanovskii (1967) using conventional square tubes having various lengths, an electrical heater and a controlled flow of air provided by a fan. Their basic results are reproduced in Figure 2.66. Unfortunately, the velocity V, which appears in the Strouhal number, $St = \omega d/V$, where d is the diameter of the heater, was not given in the paper. The results are therefore qualitative and have limited value. From Figure 2.66(a) it is clear, however, that a longer tube (lower frequency and lower losses/length) has a larger region of oscillation for a given heater power. Figure 2.66(b) shows that for a given tube, the region of oscillations increases with heater power. Marone and Tarakanovskii also give some results obtained when an unheated auxiliary grid was installed. Oscillations at the fundamental frequency could then, under some conditions, be excited by a heater placed in the upper half of the tube. That apparent violation of Rayleigh's Criterion has never been explained. Owing to the incompleteness of the information, a satisfactory explanation probably cannot be worked out with the given data alone.

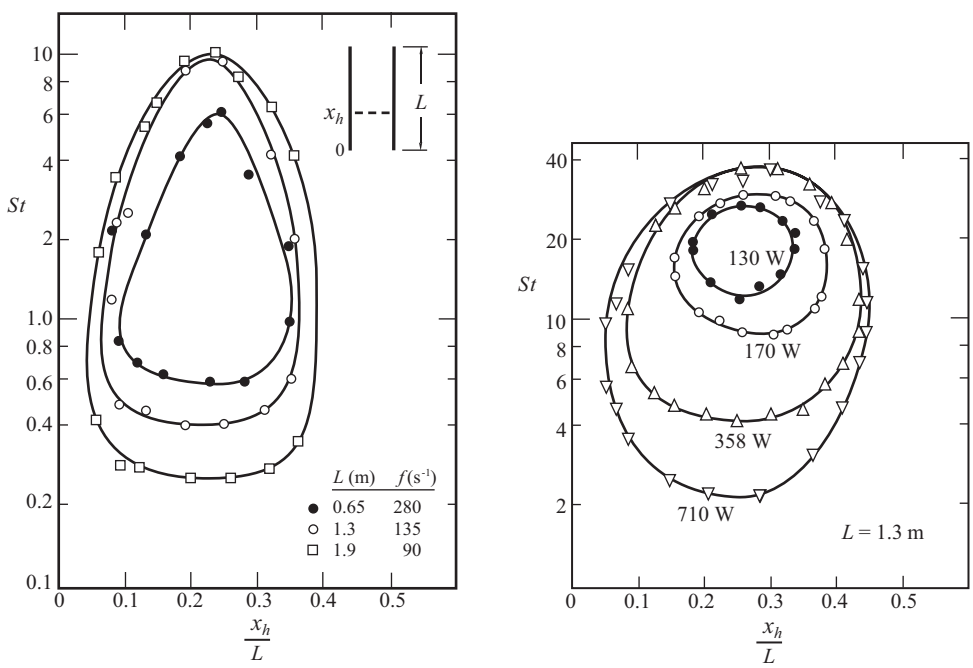

FIGURE 2.66. The effect of tube length and heater location on the generation of oscillations in a Rijke tube, $St = \omega d/V$; (a) heater power input 500W, (b) $L = 1.3$m (Marone and Tarakanovskii 1967).

In a short note, Marchenko and Timoshenko (1970) later gave incomplete results for some aspects of nonlinear behavior. For example, they found that the ratio of the amplitudes of the second harmonic to that of the fundamental decreased linearly as the heater was moved from 20% to 30% of the tube length. Their data is suggestive but too little to advance understanding.

Collyer and Ayres (1972) briefly explored the generation of harmonics in a Rijke tube by one or two screen heaters appropriately placed in the tube. They reported exciting as many as nine harmonics in a

cold 79 cm tube and eight harmonics when it was 'hot'; the average temperatures were 28°C and 68°C respectively. Apart from a brief comment regarding an explanation for the presence of the second harmonic noted by Marchenko and Timoshenko, the authors merely report their observations without interpretation or explanation. Thus the work adds little to explaining the behavior of the Rijke tube.

Apparently inspired partly by Saito's work a dozen years earlier, and motivated by some fundamental weakness of both the available experimental results and analyses, Kalto and Sajiki (1977) reported quite extensive results for the onset of oscillations, but gave no analysis. Their apparatus was a vertical tube with supporting equipment essentially the same as Saito's. Figure 2.67 shows an example of their results which were always plotted as heater power versus flow rate measured in liters per minute. They show the usual

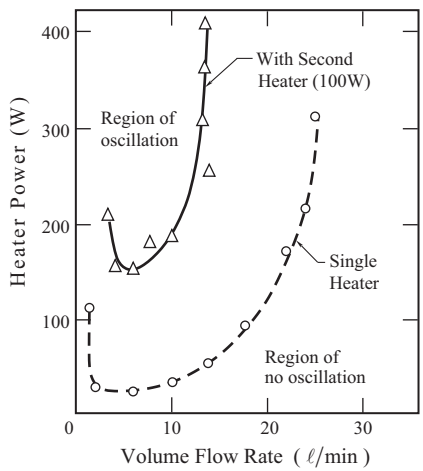

FIGURE 2.67. The effect of a second heater on the stability of oscillations; adapted from Figure 7 of Kalto and Sajiki (1977).

broad region of oscillations with a single heater placed at one-quarter of the tube length from the lower end. A series of tests were carried out with a second heater at one-quarter of the length from the top. The power to the second heater was constant, equal to 100W. When placed at the middle of the tube, the second heater had no effect, a result to be expected on the basis of Rayleigh's Criterion. Kalto and Sajiki examined the consequences of changing other variables, including tube length and form of the heater, which we will not discuss here.

The last of the papers from the University of Tokyo covers results obtained by Madarame (1981) who paid particular attention to the rates at which energy flows to the oscillations. It is unfortunate that the author ignores two hundred years of previous work on the problem: the only citations are the papers by Saito, and Kalto and Sajiki; and the book on boundary layer theory by Schlicting (1968). Madarame reports data for the growth of oscillations and for the limiting amplitude. Some effects, for example, of flow rate and heater power input are given for several lengths of tube. The author found fairly good agreement between observations and a simple analysis for small oscillations and for flow rates which are not high. Madarame speculates that transition to turbulent flow may be responsible for some of the anomalies found.

Probably the first thorough analysis of the stability of small motions in a Rijke tube was worked out by Kwon and Lee (1985). Their best result was the curve of stability limits reproduced here as Figure 2.68. Despite the obviously good agreement, which shows that the calculations contain some truth, the analysis does not constitute a theory of the Rijke tube, nor do Kwon and Lee make such a claim. Only the example shown in Figure 2.68 was given in the paper; the authors note that in other cases they examined, the experimental values of heat input were larger than predicted for large flow rates and smaller for low flow

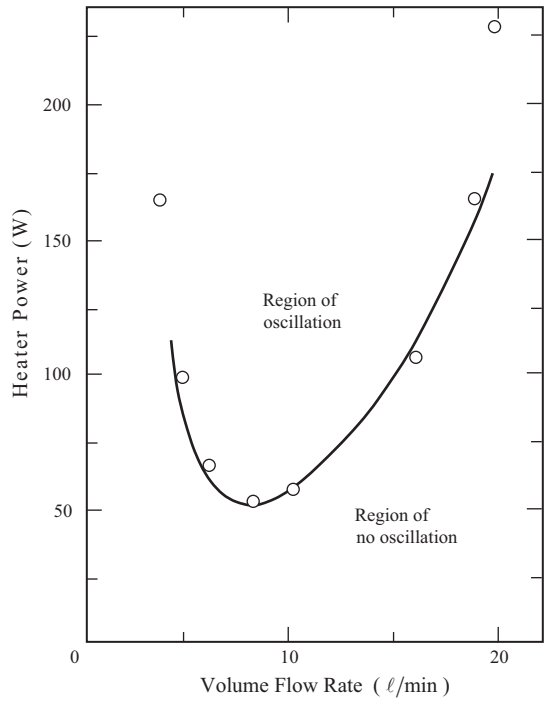

FIGURE 2.68. A prediction of a stability limit (Kwon and Lee 1983) with data reported by Kalto and Sajiki (1977).

rates. Kwon and Lee attribute those differences to a faulty representation of the heat provided by the heater for low flow rates, and to an unaccounted for increase of mean temperature T_m in the tube. In fact, even crude measurements demonstrated that their assumption that T_m is equal to the temperature of the air at the inlet to the tube is simply not valid.

Kwon and Lee define their "stability limit" for oscillations as the condition when the generation of power by the heater and absorbed by the gases exactly equals the acoustic energy dissipated in the tube. Convection of energy at the ends, and radiative losses were estimated to be negligible so the condition for oscillations is equality of the absorption of power and the rate at which acoustic energy is lost due to viscous effects, including heat conduction at the lateral boundary (Appendix C). The rates of generation and dissipation are

$$W_g = \frac{(\gamma-1)\bar{\rho}_m\bar{a}_m}{4\gamma\bar{p}(\omega\kappa)^{1/2}} E Q_0 |\hat{u}_p|^2 \sin\left(\pi\frac{\ell_g}{L}\right) \tag{2.131}$$

$$W_a = \frac{\pi^2 R\bar{\rho}_m\bar{a}_m}{2\sqrt{2}}\left(\frac{\bar{\nu}_m}{\omega}\right)^{1/2}\left(1+\frac{\gamma-1}{\sqrt{Pr}}\right)|\hat{u}_p|^2 \tag{2.132}$$

where $(\quad)_m$ denotes values at the 'mean temperature' of the gas flow; $|\hat{u}_p|$ is the magnitude of the peak velocity oscillation; $\bar{\nu}_m$ is the mean kinematic viscosity; Q_0 is the "overall steady heat input to the air from the heater"; and E is an efficiency factor measuring the part of heat release in phase with the pressure. Equating (2.131) and (2.132) leads to the formula for Q_0:

$$Q_0 = \frac{\sqrt{2}\pi R(\kappa\bar{\nu}_m)^{1/2}\gamma\bar{p}}{E\sin\left(2\pi\frac{\ell_g}{L}\right)}\left(1+\frac{\gamma-1}{\sqrt{Pr}}\right) \tag{2.133}$$

The heat input is least when $\sin\left(2\pi\frac{\ell_g}{L}\right) = 1$, or $\ell_g = \frac{L}{4}$, a well-known result. Some additional ancillary calculations are required (see the paper by Kwon and Lee) but the preceding conveys the gist of the matter.

In the greater part of practical cases, the presence of oscillations in combustors is simply not wanted. Hence the main problem is avoiding them in the first place, or supressing them when they do appear. It seems to be generally true that if an existing combustion system is developed further in the interest of improving its performance in some sense, then unwanted oscillations of pressure will inevitably appear. That is one reason why the Rijke tube has continued to attract attention; it is the simplest system displaying many aspects of general behavior. Given the problem, the practical question arises–how can the oscillations be avoided or suppressed? With an interesting paper, Sreenivasan, Raghu and Chu (1985) used an electrically-driven Rijke tube to introduce the idea and first example of actively controlling acoustic oscillations. Their basic idea was to convert "acoustic to thermal energy so that the acoustic oscillations are quenched and the system is stabilized."

The apparatus Sreenivasan *et al.* used was a vertical tube with a primary heater mounted in the bottom half and a control heater in the upper half. As part of their study the authors measured the temperature of the air system to be 26°C before the primary heater, 92°C before the control heater and 97° in the exhaust. Thus the temperature rise was about 30% of the initial ambient value, not the small change assumed by Kwon and Lee. As a point we will return to in Chapter Nine, the oscillations in the tube were suppressed by using control heater power roughly 3% of the primary heater power, whereas the acoustic power was approximately 1/100 as much. Active control may be very costly.

Subsequent to the work just described, the Rijke tube has been used either in slightly different forms using various fuels to provide the driving power from combustion (e.g. Putnam and Dennis, 1954, who apparently made the first flame-driven Rijke tube; and Raun and Beckstead, 1993, among many); or as the object to investigate the application of active control. The recent investigation by Matveev (2003) seems to be the latest based on the historically 'conventional' form of the electrically powered tube. Matveev and Culick 2002a–d; 2003b,c have discussed the work. Matveev took special care to obtain data having precision as high as possible, a demand that required lengthy tests to reach thermal equilibrium or, better, steady-state. The apparatus was a perfected form of that described by Pun (2001) and sketched in Figure 2.69. Figure 2.70 shows two examples of experimental results and calculations for the stability boundary with two

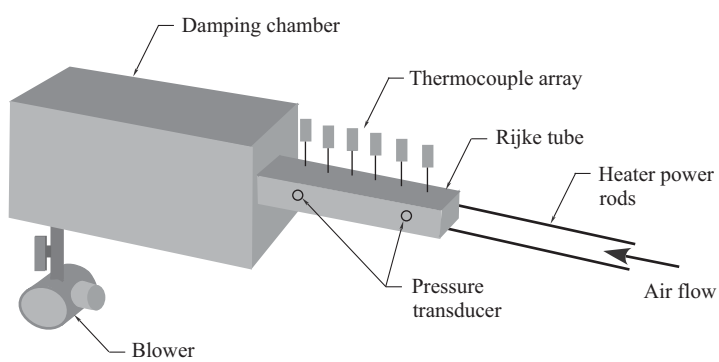

FIGURE 2.69. A sketch of the horizontal Rijke tube used by Matveev (2003).

positions of the heater. The crossed short lines represent experimental error bars; the heavier short vertical lines illustrate the shifts of the computed stability boundary when the impedance of the chamber is assigned an uncertainty of ± 20%.

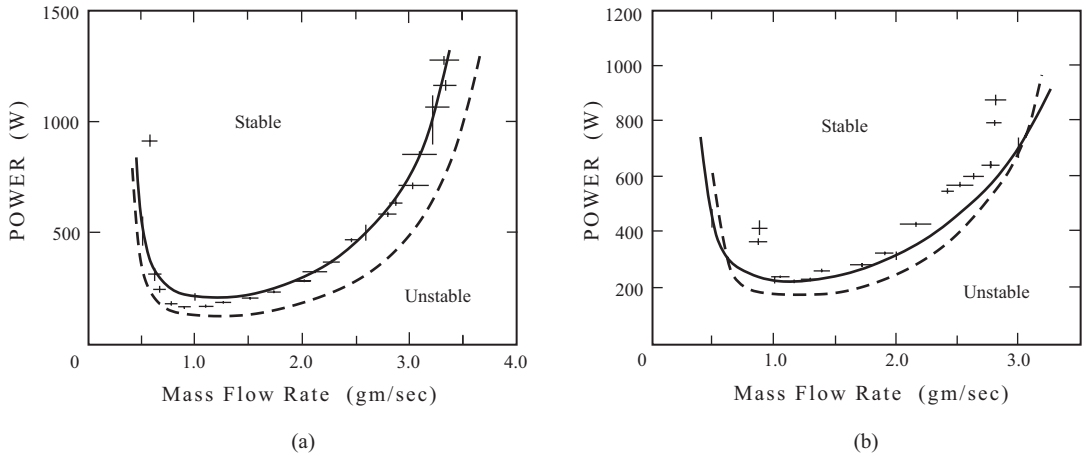

FIGURE 2.70. Comparison of experimental data and calculations for stability boundaries of the Rijke tube in Figure 2.69. Heater position: (a) 1/4 tube length; (b) 1/8 tube length.

These results support the conclusion that we can compute the stability of the electrically driven Rijke tube quite well, but considerable care is required. See Matveev and Culick (2003) for a more detailed discussion. Even in the crudest execution of the experiment, three elementary results are found, implicit in the references cited, if not discussed explicitly:

(a) If the heater is in the lower half of the tube steady acoustic oscillations can be sustained;
(b) The frequency of the sound is close to the fundamental frequency $\overline{a}/2L$ of the tube;
(c) If the tube is tilted, the intensity of sound decreases and is zero when the tube is horizontal.

Correspondingly, three basic questions are raised:

(i) What determines the frequencies of the observed oscillations?
(ii) Why does the location of the grid matter?
(iii) Why does the vertical orientation of the tube affect the oscillations?

All three questions can be answered with linear analysis of the field in the tube and consideration of modest nonlinear behavior of the heat transfer from the heater. The steps in the procedure followed in Section 2.7.2 are in direct correspondence with those followed in the general method.

2.7.2. Mean Field in the Rijke Tube. The hotter gas above the heater rises, inducing a draft in the tube. In steady flow there is an abrupt rise, in the limit a discontinuity, of temperature across the heater. Continuity of mass flow requires[28]

$$\overline{\rho}_L \overline{u}_L S_c = \overline{\rho}_U \overline{u}_U S_c \tag{2.134}$$

where S_c is the cross-section area. Subscripts $(\quad)_L$ and $(\quad)_U$ denote values in the lower and upper regions of the tube; and $\overline{(\quad)}$ stands for average value.

We assume that the average flow is uniform above and below the heater, and that the perfect gas law holds with the gas constant having the same value throughout, $p = \rho RT$. In this low speed flow the pressure is approximately uniform except for a negligible change across the heater due to viscous effects (drag and

[28]Strictly, careful derivation of this relation gives $\overline{\rho u} S_c = constant$. We assume $\overline{\rho u} = \overline{\rho}\ \overline{u}$; see discussion of the equations for the average flow in Chapter 3.

heat transfer). Hence certainly as a good first approximation, we have the simple relation connecting the density and temperature ratios across the heating grid

$$\frac{\overline{\rho}_L}{\overline{\rho}_U} = \frac{\overline{T}_L}{\overline{T}_U} > 1 \tag{2.135}$$

2.7.3. Acoustic Field in the Rijke Tube. The simplest representation of the acoustic field is based on the assumptions that the mean flow has negligible effects on the unsteady field; and that viscous losses at the lateral walls may be ignored. Then the classical acoustic conservation equations for one-dimensional motions apply:

$$\textit{Mass} \qquad \frac{\partial \rho'}{\partial t} + \frac{\partial \rho'}{\partial x}(\overline{\rho} u') = 0 \tag{2.136}$$

$$\textit{Momentum} \qquad \overline{\rho}\frac{\partial u'}{\partial t} + \frac{\partial p'}{\partial x} = 0 \tag{2.137}$$

$$\textit{Pressure (Energy)} \qquad \frac{\partial p'}{\partial t} + \gamma \overline{p}\frac{\partial u'}{\partial x} = (\gamma - 1)\,\dot{Q}'\delta(x - \ell_g) \tag{2.138}$$

The effect of the heater is represented by the fluctuation $\dot{Q}'$ of heat exchanged between the grid and the flow, assumed to occur in the infinitesimally thin plane at $x = \ell_g$. These familiar equations are derived in a more general context in Chapters 3–5; see Sections 3.3 and 5.1.

The idea now is to solve (2.136)–(2.138) separately in the regions upstream and downstream of the heater. Because $\dot{Q}' = 0$ outside the heater, the solutions represent freely traveling waves. Then the field in the tube will be found by applying suitable boundary conditions at the ends, and matching conditions at the heater.

The required matching conditions are obtained by integrating the conservation equations over a small region containing the heating grid, Figure 2.71, $(\ell_g - \delta) < x < (\ell_g + \delta)$ and then letting $\delta \to 0$.

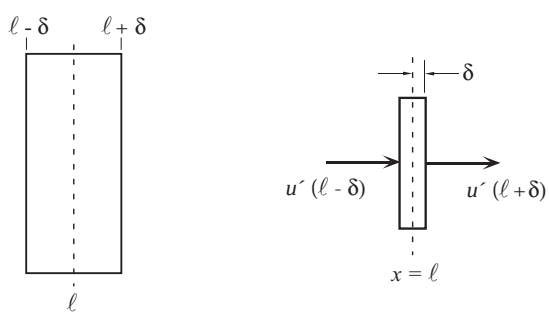

FIGURE 2.71. Region of integration for obtaining matching conditions.

Applying the procedure to the differential equation (2.136) for conservation of mass gives

$$\int_{\ell_g-\delta}^{\ell_g+\delta} \frac{\partial \rho'}{\partial t} dx + \int_{\ell_g-\delta}^{\ell_g+\delta} \frac{\partial}{\partial x}(\overline{\rho} u') dx = 0$$

so for small δ,

$$(\overline{\rho} u')_{\ell_g+\delta} - (\overline{\rho} u')_{\ell_g-\delta} = 0$$

For $\delta \to 0$ we have

$$\overline{\rho}_U u'_{\ell_g+} = \overline{\rho}_L u'_{\ell_g-} \tag{2.139}$$

This result is the formal statement that the acoustic mass flux is constant through the heater.

Similarly, the momentum equation (2.137) leads to continuity of the acoustic pressure,

$$p'_{\ell+} = p'_{\ell-} \tag{2.140}$$

Integration of the energy equation (2.138) across the heater introduces the influence of the unsteady heat addition:

$$\int_{\ell_g-\delta}^{\ell_g+\delta} \frac{\partial p'}{\partial t} dx + \int_{\ell_g-\delta}^{\ell_g+\delta} \gamma \overline{p} \frac{\partial u'}{\partial x} dx = (\gamma - 1) \int_{\ell_g-\delta}^{\ell_g+\delta} \dot{Q}'_g \delta(x - \ell) dx$$

For $\delta \to 0$:

$$\gamma \overline{p} \left(u'_{\ell_g+} - u'_{\ell_g-} \right) = (\gamma - 1) \dot{Q}'_g$$

so the discontinuity of the velocity fluctuation is

$$u'_{\ell_g+} = u'_{\ell_g-} + (\gamma - 1) \frac{\dot{Q}'_g}{\gamma \overline{p}} \tag{2.141}$$

Combination of (2.139) and (2.141) gives

$$u'_{\ell_g-} = \frac{1}{\frac{\overline{\rho}_L}{\overline{\rho}_U} - 1} (\gamma - 1) \frac{\dot{Q}'_g}{\gamma \overline{p}} \; ; \quad u'_{\ell_g+} = \frac{\overline{\rho}_L / \overline{\rho}_U}{\frac{\overline{\rho}_L}{\overline{\rho}_U} - 1} (\gamma - 1) \frac{\dot{Q}'_g}{\gamma \overline{p}} \tag{2.142)a,b}$$

There is only one source of energy for the acoustic field in this form of the problem, the heating grid. We will ignore all losses at the ends and lateral boundary of the tube. Depending on the heat transfer between the grid and unsteady motions of the gas, a small amplitude disturbance may grow or decay. That is, we are really concerned at this point with stability of waves in the tube. We examine the matter in two ways: by finding the wave field in the tube subject to appropriate boundary conditions and the matching conditions just derived; and with a method based on spatial averaging. In practice, the chief difference between the two approaches is that the second approach gives the desired result for stability without requiring knowledge of the actual acoustic field.

2.7.4. Acoustic Field and Stability by Matching Waves. The method used in this section has often been applied to problems involving planar waves. Several examples have appeared in the literature of combustion-driven oscillations, e.g., Dowling 1995; Candel 1992, 2001. Here we have only to use the matching conditions derived above to join representations of standing waves on the two sides of the heater. In the regions between the heater and the ends, the linearized momentum and energy equations are

$$\begin{aligned} \overline{p} \frac{\partial u'}{\partial t} + \frac{\partial p'}{\partial x} &= 0 \\ \frac{\partial p'}{\partial t} + \gamma \overline{p} \frac{\partial u'}{\partial x} &= 0 \end{aligned} \tag{2.143)a,b}$$

The wave equation for the pressure is formed by differentiating (2.123)b with respect to time and replacing $\partial u'/\partial t$ by (2.123)a.

For $\overline{p}$, $\overline{\rho}$ constant and $\overline{a}^2 = \gamma \overline{p} / \overline{\rho}$, the result is

$$\frac{\partial^2 p'}{\partial t^2} - \overline{a}^2 \frac{\partial^2 p'}{\partial x^2} = 0 \tag{2.144}$$

Solutions of the form $p' \sim e^{\lambda t} e^{\chi x}$ are easily found, appropriate combinations then form representations of standing waves. We ignore radiation of acoustic energy from the ends of the tube, a condition that is enforced by requiring that the pressure fluctuations vanish:

$$\begin{aligned} p'(0;t) &= 0 \\ p'(L;t) &= 0 \end{aligned} \tag{2.145)a,b}$$

It is convenient to use the complex form for the time dependence; a solution to (2.144) for the lower part of the tube, satisfying (2.125)a is

$$p'_L(x;t) = P_L e^{-i\Omega t} \sin(k_L x) \quad (0 \le x < L) \tag{2.146}$$

where Ω is the complex frequency and k_L is the complex wavenumber:

$$\begin{aligned} \Omega &= \omega + i\alpha \\ k_L &= \Omega/\overline{a}_L = \frac{\omega}{\overline{a}_L} + i\frac{\alpha}{\overline{a}_L} \end{aligned} \tag{2.147}$$

As defined here, α is positive for an unstable wave.

The acoustic momentum equation (2.123)a is satisfied, with (2.146) for the pressure, if the corresponding velocity fluctuation is

$$u'_L(x;t) = -i\frac{P_L}{\overline{\rho}_L \overline{a}_L} e^{-i\Omega t} \cos(k_L x) \qquad (0 \le x < \ell_g) \tag{2.148}$$

Similarly, the solutions in the upper part[29] of the tube are

$$\begin{aligned} p'_U(x;t) &= P_U e^{-i\Omega t} \sin k_U(L-x) \\ u'_U(x;t) &= i\frac{P_U}{\overline{\rho}_U \overline{a}_U} e^{-i\Omega t} \cos k_U(L-x) \end{aligned} \qquad (\ell_g < x \le L) \tag{2.149)a,b}$$

With these solutions, application of the conditions (2.140) for continuity of acoustic pressure and (2.141) for the discontinuity of velocity fluctuation gives the two equations relating the unknown amplitudes P_L and P_U:

$$\begin{aligned} P_L \sin(k_L \ell_g) &= P_U \sin k_U(L-\ell_g) \\ P_U \cos k_U(L-\ell_g) &= -P_L \left(\frac{\overline{\rho}_U \overline{a}_U}{\overline{\rho}_L \overline{a}_L}\right) \cos(k_L \ell_g) - i\left(\frac{\overline{\rho}_U \overline{a}_U}{\gamma \overline{p}}\right)(\gamma-1)\dot{Q}'_g e^{i\Omega t} \end{aligned} \tag{2.150)a,b}$$

The heat exchanged between the grid and the flow likely depends on both the pressure and velocity, but in the absence of experimental and theoretical results, it is reasonable simply to assume that $\dot{Q}'_g$ is proportional to the velocity fluctuation with a time lag. But what velocity fluctuation? As an approximation, we assume that the average value across the heater is a reasonable choice, so

$$\dot{Q}'_g = \frac{Q_u}{2}\left[u'_L\left(\ell_g; t-\tau_u\right) + u'_U\left(\ell_g; t-\tau_u\right)\right] \tag{2.151}$$

Substitution in (2.145)b and rearrangement leads to

$$-\xi P_L \cos(k_L \ell_g) = P_U \cos k_U(L-\ell_g) \tag{2.152}$$

[29]Note that there is a sign change in $u'L$ because x is replaced by $L-x$. Also, the complex frequency Ω has the same value throughout the tube because we assume 'steady' waves—'steady' except for slow growth or decay.

where

$$\xi = \frac{\overline{\rho}_U \overline{a}_U}{\overline{\rho}_L \overline{a}_L} \frac{1 + \frac{(\gamma-1)Q_u}{2\gamma\overline{p}} e^{i\Omega\tau_u}}{1 - \frac{(\gamma-1)Q_u}{2\gamma\overline{p}} e^{i\Omega\tau_u}} \tag{2.153}$$

Division of (2.145)a by (2.152) gives the transcendental equation for the complex eigenvalue Ω (recall $k_L = \Omega/\overline{a}_L$ and $k_U = \Omega/\overline{a}_U$):

$$\xi \tan(k_L \ell_g) = -\tan k_U (L - \ell_g) \tag{2.154}$$

The last equation can only be solved numerically in general, but for the case of weak heating, an instructive result is readily obtained by expansion about the limit of no heating. When $Q_0 = 0$ so the gas properties are uniform, $\xi = 1$; after expansion of (2.154) the dependence of ℓ_g drops out and we recover the classical condition setting the wavenumbers in an open-open straight tube:

$$\sin kL = 0$$

and

$$kL = 0, \pi, 2\pi, \cdots \ell\pi \tag{2.155}$$

When weak heating is assumed, the wavenumbers differ slightly from (2.155); for the first mode ($\ell = 1$) set[30]

$$k_L = k_U \approx \frac{1}{L}(\pi + \delta) \tag{2.156}$$

and the problem comes down to determining δ. Then to first order in δ,

$$\begin{aligned} \tan(k_L \ell_g) &= \tan(\pi + \delta)\frac{\ell_g}{L} \\ \tan k_L (L - \ell_g) &= \tan(\pi + \delta)\left(1 - \frac{\ell_g}{L}\right) \end{aligned} \tag{2.157)a,b}$$

It is sufficient for the purposes here to consider the special case $\ell_g/L = 1/4$, when the heating grid is one-quarter of the tube length from the inlet. Experimentally it is well-known that the first mode is excited when the heater is in the lower half of the tube. With $\ell_g/L = 1/4$, substitution of (2.157)a,b in (2.154) gives

$$\xi \tan\frac{1}{4}(\pi + \delta) = -\tan\frac{3}{4}(\pi + \delta) \tag{2.158}$$

where ξ differs from unity by an amount of the order of δ. If we assume $\frac{\overline{\rho}_U \overline{a}_U}{\overline{\rho}_L \overline{a}_L} = 1 + \epsilon$ and set

$$\Delta = \frac{\gamma - 1}{2\overline{p}} Q_u e^{i\Omega\tau_u} \tag{2.159}$$

Then ξ (2.153) becomes

$$\xi = (1 + \epsilon)\frac{1 + \Delta}{1 - \Delta} \cong 1 + (\epsilon + 2\Delta)$$

to first order in small quantities. Also to first order in δ,

$$\begin{aligned} \tan\frac{1}{4}(\pi + \delta) &\cong \frac{1 + \frac{\delta}{4}}{1 - \frac{\delta}{4}} \cong 1 + \frac{\delta}{2} \\ \tan\frac{3}{4}(\pi + \delta) &\cong \frac{1 - \frac{3}{4}}{-1 - \frac{3}{4}} \cong -\left(1 - \frac{3}{2}\delta\right) \end{aligned}$$

[30] We ignore the small increase in the speed of sound in the flow through the grid. This affects the frequency slightly and even less the growth or decay constant (time averaging part of the wavenumber).

Substitution of these approximations in (2.158) leads to

$$1 + (\epsilon + 2\Delta) = \frac{1 - \frac{3}{2}\delta}{-1 - \frac{\delta}{2}} \approx 1 - 2\delta$$

and

$$\delta = -\frac{\epsilon}{2} - \Delta = -\left(\frac{\epsilon}{2} + \frac{\gamma - 1}{2\overline{p}} Q_u \cos \Omega\tau_u\right) - i\frac{\gamma - 1}{2\overline{p}} Q_u \sin \Omega\tau_u \tag{2.160}$$

Now by definition, the complex wavenumber and frequency are related by

$$k = \frac{\Omega}{\overline{a}} = \frac{\omega}{\overline{a}} - i\frac{\alpha}{\overline{a}} = \frac{1}{L}(\pi + \delta) \ ,$$

the second equality following from (2.156). Hence, with (2.160) we find

$$\omega = \pi\frac{\overline{a}}{L} - \frac{1}{2}\left(\epsilon + \frac{\gamma - 1}{\overline{p}} Q_u \cos \Omega\tau_u\right) \ ; \quad \alpha = \frac{\overline{a}}{L}\frac{\gamma - 1}{2\overline{p}} Q_u \sin \Omega\tau_u$$

But since α is first order in small quantities we must replace Ω, by the unperturbed classical frequency, $\omega \approx \pi\frac{\overline{a}}{L}$, so the first order approximations to the frequency and growth constant are

$$\begin{aligned} \omega &= \pi\frac{\overline{a}}{L} - \frac{1}{2}\left[\left(\frac{\overline{\rho}_U}{\overline{\rho}_L}\frac{\overline{a}_U}{\overline{a}_L} - 1\right) + \frac{\gamma - 1}{\overline{p}} Q_u \cos\left(\pi\frac{\overline{a}}{L}\tau_u\right)\right] \\ \alpha &= \frac{\overline{a}}{L}\frac{\gamma - 1}{2\overline{p}} Q_u \sin\left(\pi\frac{\overline{a}}{L}\tau_u\right) \end{aligned} \tag{2.161)a,b}$$

Because the growth constant α must be positive for the mode to be unstable, we have the simple criterion for instability that the time lag τ_u must be in the range

$$0 < \tau_u < \frac{L}{\overline{a}} \tag{2.162}$$

The period of the fundamental mode is $2\pi/\omega_1 = 2\pi/\overline{a}k = 2L/\overline{a}$. Hence the condition (2.162) requires that for unstable oscillations the heat addition should not lag the velocity oscillation by more than one-half period. Similar results can be obtained for higher modes. For excitation of oscillations, there is also a restriction on the location of the heater, not easily found with the analysis given here. Both restrictions on the temporal and spatial properties of the heater are readily obtained with the method based on spatial averaging.

2.7.5. Stability Analyzed by a Method of Spatial Averaging. The generic character of the mechanism examined in the preceding section is better shown with a special case of the analytical framework developed in Chapters 3 and 4. We use the same example, but initially without the restriction to energy addition at an infinitesimally thin grid. Hence the speed of sound must be treated as a function of position in the tube. However, the mean pressure is constant and uniform, and formation of the wave equation as in the steps leading to (2.144) now gives

$$\frac{\partial^2 p'}{\partial t^2} - \frac{\partial}{\partial x}\left(\overline{a}^2\frac{\partial p'}{\partial x}\right) = \frac{R}{C_v}\frac{\partial \dot{Q}'}{\partial t}$$

which we write in the form appropriate for small changes in the speed of sound,

$$\frac{\partial^2 p'}{\partial t^2} - \overline{a}_0^2\frac{\partial^2 p'}{\partial x^2} = \frac{R}{C_v}\frac{\partial \dot{Q}'}{\partial t} - \frac{\partial p'}{\partial x}\frac{d\delta\overline{a}^2}{dx} \tag{2.163}$$

where $\overline{a}^2 = \overline{a}_0^2 + \delta\overline{a}^2$, $\overline{a}_0^2$ being constant,

$$h = \frac{R}{C_v}\frac{\partial \dot{Q}'}{\partial t} - \frac{\partial p'}{\partial x}\frac{d\delta\overline{a}^2}{dx} \tag{2.164}$$

The boundary conditions set at the ends of the tube are

$$\begin{aligned} p'(0;t) &= 0 \\ p'(L;t) &= 0 \end{aligned} \tag{2.165)a,b}$$

We assume always the classical acoustic problem for motions with no perturbations. Here the definition of the unperturbed problem is clear: $\dot{Q}'$ and $d\overline{a}^2/dx$ vanish. Since we are normally interested in determining what effects the perturbations have on the known classical behavior, we concentrate on analyzing the difference between the actual and classical problems. The idea is to construct the spatially averaged weighted difference in the following way.

Let p_1' denote the pressure in the fundamental mode of classical motion satisfying the homogeneous wave equation and the same boundary conditions as for the actual problem:

$$\frac{\partial^2 p_1}{\partial t^2} - \overline{a}_0^2 \frac{\partial^2 p_1}{\partial x^2} = 0 \tag{2.166}$$

$$\begin{aligned} p_1(0;t) &= 0 \\ p_1(L;t) &= 0 \end{aligned} \tag{2.167)a,b}$$

Multiply (2.163) by p_1, (2.158) by p', subtract the results and integrate over the volume of the tube to give

$$\int_0^L \left[p_1 \frac{\partial^2 p'}{\partial t^2} - p' \frac{\partial^2 p_1}{\partial t^2} \right] S_c dx - \overline{a}_0^2 \int_0^L \left[p_1 \frac{\partial^2 p'}{\partial x^2} - p' \frac{\partial^2 p_1}{\partial x^2} \right] S_c dx = \int_0^L h S_c dx \tag{2.168}$$

Integrate the second integral by parts and substitute the boundary conditions (2.165)a,b and (2.167)a,b to find

$$\begin{aligned} \int_0^L \left[p_1 \frac{\partial^2 p'}{\partial x^2} - p' \frac{\partial^2 p_1}{\partial x^2} \right] S_c dx &= \int_0^L \left[p_1 \frac{\partial p'}{\partial x} - p' \frac{\partial p_1}{\partial x} \right] S_c dx \\ &\quad - \int_0^L \left[\frac{\partial p_1}{\partial x} \frac{\partial p'}{\partial x} - \frac{\partial p'}{\partial x} \frac{\partial p_1}{\partial x} \right] S_c dx \\ &\quad \left[p_1 \frac{\partial p'}{\partial x} - p' \frac{\partial p_1}{\partial x} \right] S_c dx - 0 \\ &= 0 \end{aligned}$$

From earlier results we take $p_1' = P_1 \sin \omega_1 t \sin k_1 x$, so in the first integral of (2.168),

$$\frac{\partial^2 p_1}{\partial t^2} = -\omega_1^2 p_1$$

where $\omega_1 = \overline{a}_0 k_1$. We assume that the spatial dependence of the motion is not much affected by the heat addition,[31] but the amplitude $\eta_1(t)$ varies in time, in a manner to be determined; thus for the actual oscillation we assume the form

$$p' = \overline{p} \eta_1(t) \sin k_1 x \tag{2.169}$$

[31] This is a key step clarified in Chapter 4.

Substituting p_1 and p' in the first integral of (2.168) we have

$$\int_0^L \left[p_1 \frac{\partial^2 p'}{\partial t^2} - p' \frac{\partial^2 p_1}{\partial t^2}\right] S_c dx = \int_0^L \left[P_1 \sin\omega_1 t \sin k_1 x \left(\overline{p}\ddot{\eta}_1 \sin k_1 x - \omega_1^2 \overline{p}\eta_1 \sin k_1 x\right)\right] S_c dx$$

$$= P_1 \overline{p} \sin\omega_1 t \left(\ddot{\eta}_1 + \omega_1^2 \eta_1\right) S_c \int_0^L \sin^2 k_1 x dx$$

Inserting these results in (2.163) leads to

$$\frac{d^2\eta_1}{dt^2} + \omega_1^2 \eta_1 = \frac{1}{\overline{p}E_1^2} \int_0^L h \sin k_1 x dx \tag{2.170}$$

and

$$E_1^2 = \int_0^L \sin^2 k_1 x dx = \frac{L}{2} \tag{2.171}$$

With h given by (2.164), equation (2.170) becomes

$$\frac{d^2\eta_1}{dt^2} + \omega_1^2 \eta_1 = \frac{2(R/C_v)}{\overline{p}L} \int_0^L \sin k_1 x \frac{\partial \dot{Q}'}{dt} dx - \frac{2}{\overline{p}L} \int_0^L \frac{\partial p'}{\partial x} \frac{d\delta\overline{a}^2}{dx} dx \tag{2.172}$$

To simplify the calculations we will ignore the change $\delta\overline{a}^2$ in the speed of sound, and for comparison with the results found in the preceding section, we specialize (2.172) to the case of a thin heating region. For some further generality we assume that the fluctuations of heat addition depend on both the local velocity and pressure fluctuations. Hence we add a term to the representation (2.151) to give

$$\dot{Q} = \left\{\frac{Q_u}{2}\left[u'_L(\ell_g; t-\tau_u) + u'_U(\ell_g; t-\tau_u)\right] + Q_p p'(\ell_g; t-\tau_u)\right\} \delta(x-\ell_g) \tag{2.173}$$

It is a great advantage of the method based on spatial averaging that in the right-hand side of (2.172) we can use, as a first approximation,[32] the unperturbed classical forms for the pressure and velocity fields. Thus the discontinuity in the velocity fluctuation at the grid is ignored and (2.173) becomes

$$\dot{Q}' = \left\{Q_u u'(\ell_g; t-\tau_u) + Q_p p'(\ell_g; t-\tau_p)\right\} \delta(x-\ell_g) \tag{2.174}$$

The unperturbed form for p' is (2.169); the corresponding form for u' is

$$u' \approx \frac{\dot{\eta}_1}{\gamma k_1} \cos k_1 x \tag{2.175}$$

This formula is justified as the zeroth order approximation for the velocity fluctuation because together (2.169) and (2.175) satisfy the unperturbed acoustic momentum equation (2.137) providing $k_1^2 = \omega_1^2/\overline{a}^2$ and (as zeroth approximation) η_1 satisfies the wave equation without perturbations; substitution in (2.137) gives

$$\overline{\rho}\frac{\partial}{\partial t}\left(\frac{\dot{\eta}_1}{\gamma k_1} \cos k_1 x\right) + \frac{\partial}{\partial t}(\overline{p}\eta_1 \sin k_1 x) = 0$$

This equation leads to

$$\frac{d^2\eta_1}{dt^2} + \omega_1^2 \eta_1 = 0 \tag{2.176}$$

where $\omega_1^2 = \overline{a}^2 k_1^2$.

[32] The matter of correct systematic approximations, an iterative procedure, is discussed in Chapter 4.

Substitution of (2.162) and (2.175) in (2.174) gives the formula for $\dot{Q}'$ to be used in (2.172):

$$\dot{Q}' = \left\{ \frac{Q_u}{\gamma k_1} \cos k_1 \ell_g \frac{d}{dt} \eta_1(t-\tau_u) + Q_p \overline{p} \sin k_1 x \eta_1(t-\tau_p) \right\} \delta(x-\ell_g) \tag{2.177}$$

Then

$$\frac{\partial \dot{Q}'}{\partial t} = \left\{ -\frac{Q_u \omega_1^2}{\gamma k_1} \cos(k_1 \ell_g) \eta_1(t-\tau_u) + Q_p \overline{p} \sin k_1 x \frac{d}{dt} \eta_1(t-\tau_p) \right\} \delta(x-\ell_g) \tag{2.178}$$

where we have used (2.176) as an approximation in the first term.

Finally, use (2.177) in (2.172) and rearrange the result to give

$$\frac{d^2\eta_1}{dt^2} - 2\left[Q_p \frac{R/C_v}{L} \sin^2 k_1 \ell_g \right] \frac{d}{dt} \eta_1(t-\tau_p) + \omega_1^2 \left[\eta_1(t) + Q_u \frac{R/C_v}{\gamma \overline{p} L k_1} \sin 2k_1 \ell_g \eta_1(t-\tau_u) \right] = 0 \tag{2.179}$$

This equation represents the behavior of a linear oscillator with time delays associated with internal feedback. To determine stability, we assume that the amplitude η_1 is a sinusoid with slowly growing or decaying amplitude:

$$\eta_1(t) = Ce^{-i\Omega t} \tag{2.180}$$

where C is constant and the complex frequency is

$$\Omega = \omega + i\alpha \tag{2.181}$$

For instability, α must be positive with the sign convention chosen here. Both α and the difference between the actual (ω) and unperturbed (ω_1) frequencies are small: $|\alpha| \ll \omega_1$ and $|\omega - \omega_1| \ll \omega_1$. Substitute (2.180) in (2.179) to find

$$-\Omega^2 - 2A(-i\Omega)e^{i\Omega\tau_p} + \omega_1^2(1 + Be^{i\Omega\tau_u}) = 0 \tag{2.182}$$

where

$$\begin{aligned} A &= Q_p \frac{R/C_v}{L} \sin^2 k_1 \ell_g \\ B &= Q_u \frac{R/C_v}{\gamma \overline{p} L k_1} \sin 2k_1 \ell_g \end{aligned} \tag{2.183)a,b}$$

Expanded to show the real and imaginary parts, (2.182) is

$$[-\omega^2 + \omega_1^2(1 + B\cos\omega_1\tau_u) - 2A\omega_1 \sin\omega_1\tau_p] + i[-2\alpha\omega_1 = 2A\omega_1\cos\omega_1\tau_p + \omega_1^2 B \sin\omega_1\tau_u] = 0$$

where second order quantities have been ignored.[33] The brackets must vanish separately and we have the approximations for the frequency and growth (or decay) constant.

$$\begin{aligned} \frac{\omega}{\omega_1} &= 1 - \frac{A}{\omega_1} \sin\omega_1\tau_p + \frac{1}{2} B \cos\omega_1\tau_u \\ \frac{\alpha}{\omega_1} &= \frac{A}{\omega_1} \cos\omega_1\tau_p + \frac{1}{2} B \sin\omega_1\tau_u \end{aligned}$$

With (2.183)a,b, these formulas are

$$\begin{aligned} \frac{\omega}{\omega_1} &= 1 - Q_p \left[\frac{R/C_v}{\omega_1 L} \sin^2 k_1 \ell_g \right] \sin\omega_1\tau_p + Q_u \left[\frac{R/C_v}{2\gamma \overline{p} L k_1} \sin 2k_1 \ell_g \right] \cos\omega_1\tau_u \\ \frac{\alpha}{\omega_1} &= Q_p \left[\frac{R/C_v}{\omega_1 L} \sin^2 k_1 \ell_g \right] \cos\omega_1\tau_p + Q_u \left[\frac{R/C_v}{2\gamma \overline{p} L k_1} \sin 2k_1 \ell_g \right] \sin\omega_1\tau_u \end{aligned} \tag{2.184)a,b}$$

The conditions for instabilities immediately follow from (2.184)b as the conditions under which $\alpha/\omega > 0$. For 'velocity coupling', heat addition dependent on velocity fluctuations, the conditions are: $0 < \omega_1\tau_u < \pi$

[33] The perturbations represented by A and B are small, of first order, as are $|\alpha|$ and $|\omega - \omega_1|$.

and $0 < 2k_1\ell_g < \pi$; and for 'pressure coupling', the single condition must be satisfied: $-\pi/2 < \omega_1\tau_p < \pi/2$. Hence with $\omega_1 = \pi\frac{\overline{a}}{L}$, we have the conditions for the first mode to be unstable:

$$\textit{Pressure Coupling}: \qquad -\frac{\tau_1}{4} < \tau_p < \frac{\tau_1}{4} \tag{2.185}$$

$$\textit{Velocity Coupling}: \qquad \begin{aligned} 0 < \tau_p &< \frac{\tau_1}{2} \\ 0 < \ell_g &< \frac{L}{2} \end{aligned} \tag{2.186}$$

where $\tau_1 = 1/f_1 = 2L/\overline{a}$ is the period of the fundamental mode. There is no restriction on the location of the heater because the pressure fluctuations is in-phase at all points along the tube. The velocity fluctuation suffers a π phase change at the center, so the velocity fluctuations in the upper and lower halves are π out-of-phase.

We are now able to answer two of the three questions posed at the end of Section 2.7.1. To question (i), the answer is that the frequencies are closely those of the classical acoustic modes and hence are determined mainly by the length of the tube and the temperatures distribution axially. According to the calculations just completed, the position of the grid matters because it selects the phase between the acoustic pressure and velocity fluctuations. That conclusion, which answers question (ii), is certainly contained in the results of the method based on matching waves, but is difficult to extract. With the method based on spatial averaging, the conclusion is immediate.

It is particularly to be noted that observations have established that for a Rijke tube excited either by an electrical grid or by a sample of heated gauge, the first mode is excited only if the source of heating is in the lower half of the tube. Hence the results (2.186) demonstrates what is intuitively evident, that convective heat transfer dependent on velocity fluctuations is most probably the basic mechanism. That is likely also true for a tube driven unstable by a flame, but the observational results are too limited to make a definite statement.

2.7.6. Nonlinear Behavior due to Rectification. It seems that the observed dependence of the oscillations on vertical orientation of the Rijke tube is probably due to the need for a draft, an average flow through the tube (question (iii), Section 2.7.1). In this section we use the method of spatial averaging to demonstrate that assertion, but without quantitative results for the amplitudes of oscillation. The starting point is the simplified oscillator equation (2.172) for the first mode and include only the heat source on the right-hand side

$$\frac{d^2\eta_1}{dt^2} + \omega_1^2\eta_1 = 2\frac{R/C_v}{\overline{p}L}\int_0^L \sin k_1 x \frac{\partial \dot{Q}'}{\partial t} dx \tag{2.187}$$

Other than the somewhat vague requirement of 'smallness', no restrictions have been placed on $\dot{Q}'$. In particular, it need not be linear. Two sorts of elementary nonlinear behavior are likely found in practice: rectification, and saturation. The latter refers to an upper limit to the amount or rate of energy supplied to the wave system by whatever processes dominate the mechanism. We will return to some aspects of saturation later in the context of the control and limit cycles. Here we consider rectification associated with convective heat transfer as the only nonlinear process present.[34]

Convective heat transfer depends mainly on the relative speed of the flow past the surface and less so in the direction. For example, for flow normal to a wire, Figure 2.72(a), the rate of heat transfer should be the same in the two cases. On the other hand, a preferred flow direction for maximum heat transfer rate may be

[34] In particular we ignore the significant effects of nonlinear gasdynamics, covered in Chapter 7.

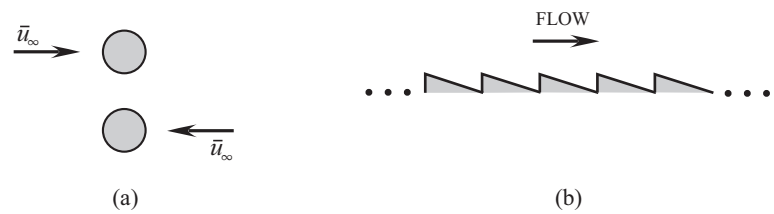

FIGURE 2.72. (a) Illustrating the independence of heat transfer on flow direction; (b) illustrating possible dependence of heat transfer on flow direction due to microscopic properties of the surface.

caused by microscopic characteristics of the surface, one case being shown in Figure 2.72(b). We ignore that type of behavior and assume that the heat transfer depends only on the magnitude of the relative velocity,

$$\dot{Q} = f(|\overline{u}|) \tag{2.188}$$

We also assume for application to the Rijke tube that the flow is always parallel to the axis, having both mean and fluctuating components; the total and average rates are then

$$\dot{Q} = f(|\overline{u} + u'|); \quad \overline{\dot{Q}} = f(|\overline{u}|) \tag{2.189}$$

Hence the fluctuation is

$$\dot{Q}' = f(|\overline{u} + u'|) - f(|\overline{u}u|) \tag{2.190}$$

The simplest possibility, sufficient for the reasoning here, is that $\dot{Q}$ is proportional to $|\overline{u}|$, i.e. $f(|\overline{u}|) = K|\overline{u}|$, and (2.190) becomes

$$\dot{Q}' = K\left\{|\overline{u} + u'| - |\overline{u}|\right\} = K|\overline{u}|\left\{\left|1 + \frac{u'}{\overline{u}}\right| - 1\right\} \tag{2.191}$$

This formula contains three sorts of behavior illustrated in Figure 2.73. To interpret the meanings of Figure 2.73, we assume that the fluctuations of heat transfer is given by (2.191). Hence $\dot{Q}'$ is proportional to the values lying in the heavy lines with lower sketches of the three parts. For small values of the fluctuation, $|u'|/|\overline{u}| < 1$, the heat transfer fluctuates entirely at the frequency of the imposed velocity fluctuation, Part (a). As $|u'|/|\overline{u}|$ increases and is greater than unity, rectification occurs and there are components of heat transfer at other frequencies, including a steady (DC) value, as Part (b) shows. Finally, if there is no average velocity, rectification is complete, as Part (c) indicates, and there is no oscillation of heat transfer at the frequency of the imposed oscillatory flow. The behavior just described seems to offer a likely explanation for the third observation and question (iii) listed at the end of Section 2.7.1. If an operating Rijke tube is tilted from the vertical, the amplitude of the oscillation is reduced, finally disappearing before the tube is horizontal. That is also why an electrically drive tube, conveniently mounted horizontally, must be equipped with a system for forcing air through the tube. It is an important advantage of such an arrangement that one has control over the flow rate (Matveev and Culick, 2002).

2.7.7. A Simple Analysis of the Flame-Driven Rijke Tube. Many laboratory devices for studying thermoacoustic instabilities and their control are essentially straight ducts or tubes with one end closed to permit injection of liquid or gaseous reactions. Combustion takes place downstream, usually anchored by some sort of flameholder. The simplest approximation to the energy addition by combustion is a flat flame (a 'flame sheet') perpendicular to the axis, as sketched in Figure 2.74. A configuration of this type is effectively a Rijke tube closed at one end. Hence stability of the system can be investigated with analysis that is chiefly a paraphrase of that covered in Sections 2.7.4 to 2.7.5. First we use the method based on spatial averaging,

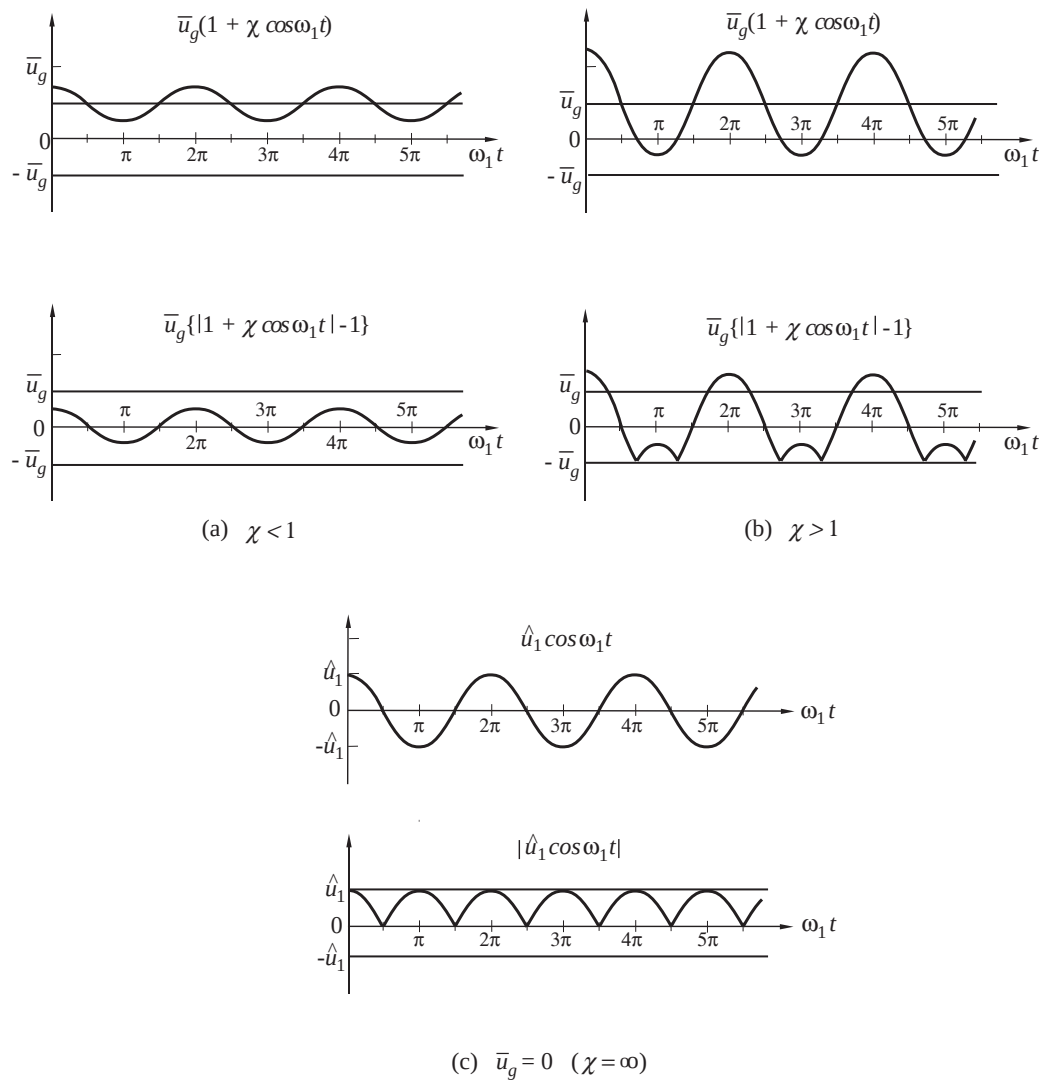

FIGURE 2.73. Three sorts of nonlinear behavior due to rectification distinguished by the relative values of the mean and fluctuating components of velocity: graphs of $\dot{Q}'/K$, eq. (2.191), with $\chi = \hat{u}/\bar{u}$.

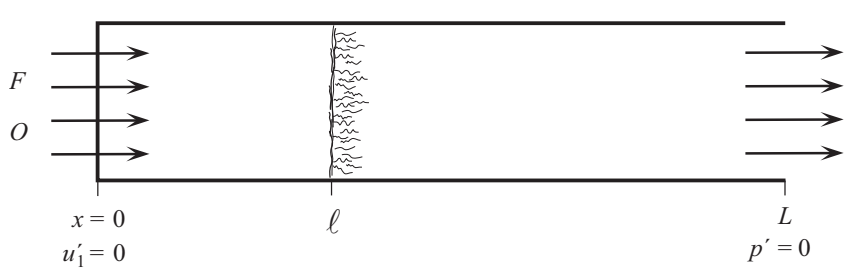

FIGURE 2.74. A basic flame-driven Rijke tube.

beginning again with the oscillator equation (2.170) with only the heat addition accounted for:

$$\frac{d^2\eta_1}{dt^2} + \omega_1^2\eta_1 = \frac{R/C_v}{\overline{p}E_1^2}\int_0^L p_1\frac{\partial\dot{Q}'}{\partial t}dx \tag{2.192}$$

The modal function p_1 must now be chosen to satisfy the boundary condition of zero velocity normal to the entrance plane at $x = 0$; for the fundamental mode:

$$p_1' = P_1 \sin\omega_1 t \cos k_1 x = p_1 \sin\omega_1 t$$

and

$$k_1 = \frac{\pi}{2L} \tag{2.193)a,b}$$

Note that the wavelength, $\lambda_1 = 2\pi/k_1 = 4L$ and the tube is a 'quarter-wave tube'. The corresponding value of the mode shape for the acoustic velocity is

$$u_1' = -\frac{P_1}{\overline{\rho a}}\cos\omega_1 t \sin k_1 x \tag{2.194}$$

With p_1 given by (2.149), $E_1^2 = L/2$ and the oscillator equation is

$$\frac{d^2\eta_1}{dt^2} + \omega_1^2\eta_1 = 2\frac{R/C_v}{\overline{p}L}\int_0^L \cos k_1 x\frac{\partial\dot{Q}'}{\partial t}dx \tag{2.195}$$

It is commonly assumed that the fluctuation of energy addition from an infinitesimally thin flat flame is proportional to the velocity fluctuation, with time lag τ_u:

$$\dot{Q}' = Q_0 u'(\ell; t-\tau_u)\delta(x-\ell) \tag{2.196}$$

The question again arises: what velocity should be used? Following reasoning in Section 2.7.5, we ignore the spatial discontinuity due to the heat addition and assume the relation (2.175) for u', but with the current mode shape $\sin k_1 x$:

$$\begin{aligned} u'(x; t-\tau_u) &= \frac{P_1}{\gamma k_1^2}\frac{d}{dt}\eta(t-\tau_u)\frac{d}{dx}(\cos k_1 x) \\ &= \frac{P_1}{\gamma k_1}\dot{\eta}_1(t-\tau_u)\sin k_1 x \end{aligned} \tag{2.197}$$

The fluctuation of heat addition is

$$\dot{Q}' = -\frac{P_1}{\gamma k_1}\dot{\eta}_1(t-\tau_u)\sin k_1 x\delta(x-\ell) \tag{2.198}$$

which gives to first order in small quantities:

$$\begin{aligned} \frac{\partial\dot{Q}'}{\partial t} &= \frac{P_1}{\gamma k_1}\ddot{\eta}(t-\tau_u)\sin k_1 x \\ &= \frac{P_1 Q_0}{\gamma k_1}\omega_1^2\eta_1(t-\tau_u)\sin k_1 x \end{aligned} \tag{2.199}$$

Substitution in the oscillator equation (2.194) gives

$$\frac{d^2\eta_1}{dt^2} + \omega_1^2\eta_1 = \kappa\eta_1(t-\tau_u) \tag{2.200}$$

with

$$\kappa = \frac{R}{C_v}\frac{P_1 Q_0}{\gamma\overline{p}Lk_1}\omega_1^2\sin 2k_1\ell \tag{2.201}$$

Now assume solution of the form

$$\eta_1 = Ne^{\alpha t}e^{-i\omega t} = Ne^{-i\omega t} \; ; \quad \Omega = \omega + i\alpha \tag{2.202}$$

Substitution in (2.200) leads to the complex algebraic equation for α and ω:

$$\left[-\omega^2 + \omega_1^2 - \kappa \cos \omega_1 \tau_u\right] + i\left[-2\alpha\omega + \kappa \sin \omega_1 \tau_u\right] \tag{2.203}$$

where again we ignore quantities of higher than first order. The real and imaginary parts of (2.203) must vanish, giving to first order:

$$\begin{aligned} \frac{\omega}{\omega_1} &= 1 - \frac{1}{2}\kappa \cos \omega_1 \tau_u \\ \frac{\alpha}{\omega_1} &= -\frac{\kappa}{2\omega_1^2} \sin \omega_1 \tau_u \end{aligned} \tag{2.204)a,b}$$

Since $\alpha > 0$ for an instability, and with κ given by (2.201), the fundamental mode is unstable if

$$\sin 2k_1 \ell \sin \omega_1 \tau_u < 0 \tag{2.205}$$

which is satisfied if

$$\begin{aligned} &\text{(a)} \quad \sin \omega_1 \tau_u < 0 \quad \text{and} \quad \sin 2k_1 \ell > 0 \\ \text{or} \quad &\text{(b)} \quad \sin \omega_1 \tau_u > 0 \quad \text{and} \quad \sin 2k_1 \ell < 0 \end{aligned}$$

In the first case,

$$\begin{aligned} &\frac{\pi}{2} < \omega_1 \tau_u < \frac{3\pi}{2} \\ \text{and} \qquad &-\frac{\pi}{2} < 2k_1 \ell < \frac{\pi}{2} \end{aligned}$$

With $k_1 = \pi/2L$ and $\omega_1 = 2\pi f_1 = 2\pi/\tau$ these two inequalities become ($\frac{\ell}{L} < 0$ is excluded):

$$\begin{aligned} \frac{\tau_1}{4} < \tau_u &< \frac{3}{4}\tau_1 \\ 0 < \frac{\ell}{L} &< \frac{1}{2} \end{aligned} \tag{2.206}$$

In the second case (b) above,

$$\begin{aligned} -\frac{\pi}{2} < \omega_1 \tau_u &< \frac{\pi}{2} \\ \frac{\pi}{2} < 2k_1 \ell &< \frac{3\pi}{2} \end{aligned}$$

which become

$$\begin{aligned} -\frac{\tau_1}{4} < \tau_u &< \frac{\tau_1}{4} \\ \frac{1}{2} < \frac{\ell}{L} &< 1 \end{aligned} \tag{2.207}$$

Together, the two cases offer the ranges for the time delay and flame location

$$\begin{aligned} -\frac{\tau_1}{4} < \tau_u &< \frac{3\tau_1}{4} \\ 0 < \frac{\ell}{L} &< 1 \end{aligned} \tag{2.208)a,b}$$

The differences between these results for the flame-driven Rijke tube and (2.185) and (2.186) for the electrically-heated case arise entirely because the mode shapes of the fundamental modes differ (a quarter-wave in the present case and a half-wave for the electrically-driven tube).

Solution by matching waves in the manner of Section 2.7.4 produces similar results, but as in that calculation, the restriction on the location of the heating zone, (2.208)b, cannot be obtained (Poinsot and

Veynante 2001; Candel *et al.* 2001). The analyses covered here have shown, even for these simple cases, the ease with which the method based on spatial averaging can be applied. Moreover, matching waves is successful only for problems of longitudinal motions. The analytical framework based on spatial averaging is not only applicable to combustors of any shape, but accommodates any form of reactants—solid, liquid, or gaseous.